VEGF-Dependent Mechanisms Controlling Osteoblast Differentiation and Bone Formation During Bone Repair

VEGF-dependent Mechanisms Controlling Osteoblast Differentiation and Bone Formation during Bone Repair

A dissertation presented

by

Kai Hu

to

The Department of Biological Sciences in Dental Medicine

in partial fulfillments of the requirements

for the degree of

Doctor of Philosophy

in the subject of

Biological Sciences in Dental Medicine

Harvard University

Cambridge, Massachusetts

May, 2015

Dissertation Advisor: Dr. Bjorn R. Olsen Kai Hu

VEGF-dependent Mechanisms Controlling Osteoblast Differentiation and Bone Formation during Bone Repair

Abstract

Osteoblast-derived vascular endothelial growth factor (VEGF) is important for bone development and postnatal bone homeostasis. Several studies have demonstrated that VEGF affects bone repair and regeneration; however, the cellular mechanisms by which it works are not fully understood. In this study, we investigated the functions of osteoblast-derived VEGF in healing of a cortical bone defect. In addition, how VEGF signaling modulates BMP2 functions during bone healing was also examined.

To define the roles of osteoblast-derived VEGF in bone repair, a mouse tibial monocortical defect model was used. The effects of deleting *Vegfa or Vefgr2* in osteoblast precursors and their descendants on the bone repair process were analyzed at various time points after surgery. To study how VEGF modulates the osteogenic activity of BMP2, BMP2, with or without the soluble VEGFR (sFlt1, VEGF decoy receptor), was delivered to the cortical defects in *VE-cadherin-cre;tdTomato* mice.

The results indicate that osteoblast-derived VEGF is important at various stages during healing of the cortical defect. In the inflammation phase, osteoblast-derived VEGF controls neutrophil release into the circulation and macrophage-related angiogenic responses. VEGF is required, at optimal levels, for angiogenesis-osteogenesis coupling in

areas where repair occurs by intramembranous ossification (IO). In this role, VEGF likely functions as a paracrine factor since deletion of *Vegfr2* in osteoblast precursors and their progeny enhances osteoblastic maturation and mineralization. Furthermore, osteoblast- and hypertrophic chondrocyte-derived VEGF stimulates recruitment of blood vessels and osteoclasts, and promotes cartilage resorption at the repair site during the periosteal endochondral ossification stage. Finally, osteoblast-derived VEGF stimulates osteoclast formation in the final remodeling phase of the repair process. Our data also indicate that skeletal stem cells at different locations respond differently to BMP2, and that the osteogenic activity of BMP2 is modulated by extracellular VEGF. In the cortical defect, delivery of recombinant BMP2 inhibits intramembranous bone formation in the intramedullary space while it enhances endochondral bone formation in the injured periosteum. Inhibition of extracellular VEGF by sFlt1 reverses the inhibitory effects of BMP2 on intramembranous ossification-mediated bone repair.

These findings add to the understanding of VEGF functions and provide a basis for clinical strategies to improve bone regeneration and treat cases of compromised bone healing.

Table of Contents

ACKNOWLEDGMENTS

First and foremost, I would like to thank my mentor, Dr. Bjorn Olsen for his irreplaceable guidance and support during the whole course of my graduate study. He taught me the essentials required for a successful scientist, and allowed me freedom to pursue various projects. I feel fortunate to study under his guidance. Thanks him for leading me to enjoy the beauty of science, where I could have the opportunity to appreciate the magnificence and gorgeousness of the nature from the microscopic histology world. Without his constant guidance and support, this work wouldn't have been possible.

I would like to specially thank the chair of my dissertation committee, Dr. Beate Lanske, who was also the chairman of my dissertation advisory committee and preliminary qualification examination committee, for her broad knowledge and invaluable advice. She always encourages me to overcome the difficulties, and whenever needed, she provides insightful advice and help. All her efforts and dedication ensured my project went smoothly.

Since the beginning of my project, my dissertation advisory committee members, Drs. Louis Gerstenfeld, and Giuseppe Intini generously provided me precious advice and continuous support. Their constructive criticisms and guidance made my project more broad and sound. Thanks sincerely for all they have done.

I would like to thank Drs. Francesca Gori, Antonios Aliprantis and Ernest Reichenberger for taking time to serve on my examination committee. Their scientific questions, constructive criticisms and their help with the data interpretation and figure preparation have better shaped my dissertation.

I would also like to thank all the past and current members of Dr. Olsen's lab.

Particularly I am grateful to Agnes Berendsen, Tatiana Besschetnova, and Wei Huang, for their kind help and support. I would like to thank Dawn DeCosta, Jim Mcbride, Yulia Pittel, Deborah Milstein and Leanne Jacobellis for their help whenever I needed. I am also grateful to my fellow graduate students in Biological Sciences in Dental Medicine, for providing great friendship and encouragement.

Many people outside the lab have helped me during my graduate studies as well. I would like to thank Drs. Henry Kronenberg, Jun Guo and Minlin Liu at Endocrinology Department in Massachusetts General Hospital, for teaching me the principles and techniques in skeletal biology. Thanks to Drs. Yefu Li, Lin Xu and Roland Baron for their help and advice. I thank Drs. Louis Gerstenfeld and Jason Pittman in Boston University School of Medicine for showing me the procedure of distraction osteogenesis, and thank Dr. Jill Helms at Stanford University School of Medicine for sharing some protocols for histology staining.

Specifically, I would like to thank my parents for their unconditioned understanding and love. They always think from my point and sacrifice for my behalf. The Ph.D training is a like long journey. I feel lucky to have my beloved wife, Na Tian, who was also in the graduate study to accompany me in this journey. She is always caring and supportive. We share every moment of happiness and sadness together, making the unforgettable journey full of love and beauty.

List of Figures

List of Abbreviations

ALP	Alkaline phosphatase
BCP	Biphasic calcium phosphate
bFGF	Basic fibroblast growth factor, also known as FGF2
BMPs	Bone morphogenetic proteins
BMP2	Bone morphogenetic protein 2
BMP4	Bone morphogenetic protein 4
BMP7	Bone morphogenetic protein 7
BMSCs	Bone marrow-derived stem cells
BSP	Bone sialoprotein
BW	Body weight
CXCL12	C-X-C motif chemokine 12, also known as SDF-1
CXCR4	C-X-C motif chemokine receptor type 4
DAPI	4',6-diamidino-2-phenylindole
DOX	Doxycycline
ECM	Extracellular matrix
EDTA	Ethylenediaminetetraacetic acid
EGR-3	Early growth response protein 3
EndMT	Endothelial to mesenchymal transition
EO	Endochondral ossification
ERK1/2	Extracellular signal-regulated kinases 1/2
FAK	Focal adhesion kinase

FBS	Fetal bovine serum
FGF	Fibroblast growth factor
FGFR	Fibroblast growth factor receptor
FOP	Fibrodysplasia ossificans progressiva
FSP-1	Fibroblast-specific protein 1
GBR	Guided bone regeneration
GFP	Green fluorescent protein
GTP	Guanosine-5'-triphosphate
HIF-1α	Hypoxia-inducible factor 1-alpha
Id1	Inhibitor of DNA binding 1
IGF	Insulin growth factor
IL-1	Interleukin-1
IL-6	Interleukin-6
IL-8	Interleukin-8
IO	Intramembranous ossification
MAPK	Mitogen-activated protein kinase
MDSCs	Muscle-derived stem cells
MEK	Mitogen-activated protein kinase kinase
M-CSF	Macrophage colony-stimulating factor
MMP13	Matrix metalloproteinase 13
MMP9	Matrix metalloproteinase 9
MSCs	Mesenchymal stem cells

MT1-MMP	Membrane-type 1 Matrix Metalloproteinase
NR4A2	Nuclear receptor subfamily 4, group A, member 2
OCN	Osteocalcin
OCT	Optimal cutting temperature
P38	P38 mitogen-activated protein kinases
PAI-1	Plasminogen activator inhibitor-1
PDGF	Platelet-derived growth factor
PDGFR	Platelet-derived growth factor receptor
PI3K	Phosphoinositide 3-kinase
PIGF	Placental Growth Factor
PKC	Protein Kinase C
PLC-γ	Phospholipase C-γ
PLGA	Poly(lactic-co-glycolic acid)
PO	Periosteum
POC	Primary ossification center
rBMP2	Recombinant BMP2
SCPP	Strontium-doped calcium polyphosphate
TGF-β1	Transforming growth factor beta1
TRAP	Tartrate-resistant acid phosphatase
TRE	Tetracycline response element
TUNEL	Terminal deoxynucleotidyl transferase dUTP nick end labeling

VEGF	Vascular endothelial growth factor
VEGFR1	Vascular endothelial growth factor receptor 1, also known as Flt1
VEGFR2	Vascular endothelial growth factor receptor 2, also known as Flk1
VHL	von Hippel-Lindau tumor suppressor

Chapter I

General Introduction

The role of vascular endothelial growth factor in bone repair and regeneration

Unlike many other organs, human bones heal in response to injury or surgical treatments. Bone repair is a process that utilizes endogenous regenerative potential to restore original bone structure without increasing bone volume. Although sharing certain similarities with bone repair, bone regeneration is a complex, well-orchestrated regenerative process, usually involving external elements to promote formation of new mineralized tissues, and leads to an increase of bone volume (Ai-Aql et al., 2008). Generally, bone repair is a rapid and efficient process. However, the process is compromised in certain pathological situations. This is demonstrated by the delayed union or nonunion in about 10% patients with bone fracture, and unhealed large bone defects (Gomez-Barrena et al., 2015). Certain bone regeneration procedures, such as bone grafting, reconstruction of large bone defects in the craniofacial region and distraction osteogenesis, sometimes fail in patients. Possible causes of such failure include, but are not limited to, impaired blood supply, damage of periosteum, reduced number of osteoprogenitor cells with age or osteoporosis, inadequate immobilization, and infection of the injury site (Bishop et al., 2012). The cellular mechanisms of these defective repair and impaired regeneration processes are not fully understood, making improvement of current therapies difficult.

Blood vessels and bone cells communicate closely to ensure that the cells maintain physical proximity and functional codependency (Clarkin and Gerstenfeld, 2013). As one of the most important regulators of vascular development and

angiogenesis (Coultas et al., 2005; Hoeben et al., 2004), VEGF also plays critical roles in skeletal development (Gerber et al., 1999; Maes et al., 2010; Zelzer et al., 2002). Postnatal bone repair and regeneration recapitulates some of these normal developmental process (Ai-Aql et al., 2008; Ferguson et al., 1999), including intramembranous and endochondral ossification, but they also exhibits additional features, such as recruitment of inflammatory cells and decreased numbers of stem cells (Bruder et al., 1994; Simon et al., 2002). VEGF has previously been reported to participate in several stages of bone repair and regeneration, however, most studies primarily examined the consequences for bone repair when VEGF levels were manipulated at local injury sites or systemically. Evidence related to the detailed mechanisms by which cells generate VEGF and how cells respond to VEGF is lacking. Here we review VEGF-based strategies for improvement of bone repair and regeneration. We summarize available data and speculate on the potential roles of VEGF.

VEGF family, receptors and signaling

VEGF belongs to a family of homodimeric proteins consisting of at least 6 members: VEGF-A, VEGF-B, VEGF-C, VEGF-D, VEGF-E and PIGF (Cross et al., 2003; Ferrara et al., 2003). VEGF-A, the most abundant form, plays important roles in proliferation, migration and activation of endothelial cells as well as in promotion of permeability and fenestration of blood vessels (Ferrara et al., 2003). VEGF-C and -D are important for lymphangiogenesis (Sleeman, 2006; Yonemura et al., 2005); VEGF-B has a role in embryonic angiogenesis (Claesson-Welsh, 2008) and PIGF is critical for pathological angiogenesis (Carmeliet et al., 2001).

VEGF-A was discovered first and is usually referred to as VEGF. Depending on alternative splicing, VEGF mRNA is translated into four major isoforms in humans, including VEGF121, VEGF165, VEGF189 and VEGF206 (Conn et al., 1990; Pepper et al., 1994), and three isoforms in mice including VEGF120, VEGF164, and VEGF188 (Ferrara and DavisSmyth, 1997). VEGF121/120 can diffuse freely, whereas VEGF189/188 and 206 are almost sequestered in the extracellular matrix (ECM). VEGF165/164, the most abundant VEGF isoform, is mostly bound to ECM (Phillips et al., 1994), and this isoform is usually used to explore VEGF functions in animal models of bone healing and *in vitro* experiments.

VEGF receptors include VEGFR1, VEGFR2, VEGFR3, Neuropilin1 and Neuropilin 2 (Neufeld et al., 1999). Their ligand preferences and signaling pathways are illustrated in Figure 1. VEGFR2 is the main VEGF receptor and is mostly expressed in endothelial cells to mediate angiogenesis and vasculogenesis, as well as promotion of vessel permeability in response to VEGF (Ferrara et al., 2003). Although VEGFR1 was the firstly discovered VEGF receptor, its functions are still debated. In addition to binding to VEGF-A, VEGFR1 also binds to VEGF-B and PIGF, but not to VEGFR2 (Olofsson et al., 1998; Park et al., 1994). In addition to endothelial cells, VEGFR1 is also found in other cell types (Hattori et al., 2002), adding complexity to VEGFR1-mediated signaling. VEGFR1 is expressed as both soluble and membrane-bound forms, depending on alternative splicing, but exhibits a minimal kinase activity. Decreased VEGFR1 expression in infantile hemangioma leads to constitutive VEGFR2 activation and abnormal angiogenesis, indicating that membranous-bound and soluble form of VEGFR1 function as decoy receptors of VEGF (Ferrara et al., 2003; Jinnin et al., 2008). In

contrast, other studies showed that VEGFR1 is capable of transducing a mitogenic signal in a similar way as VEGFR2 in certain circumstances (Maru et al., 1998). For example, monocyte migration in response to VEGF depends on the tyrosine kinase domain of VEGFR1 (Barleon et al., 1996). VEGFR3 mainly binds to VEGF-C and VEGF-D in lymphatic endothelial cells, and plays an important role in regulation of lymphangiogenesis (Joukov et al., 1996; Makinen et al., 2001). Upon binding to ligands, VEGF receptors undergo dimerization. This results in phosphorylation of certain tyrosine residues, and this mediates downstream mitogenic, chemotactic and pro-survival signals. The PLC-γ-PKC-ERK1/2 pathway is responsible for the pro-proliferative effects (Takahashi et al., 1999). Cytoskeletal reorganization and cell migration is promoted through p38 in MAPK and FAK pathway (Abedi and Zachary, 1997; Lamalice et al., 2004). In addition, activation of PI3K by VEGF leads to activation of Akt, induction of endothelial nitric oxide and small GTP-binding protein Rac, and this results in pro-survival, vascular permeability and cell migration effects (Fulton et al., 1999; Olsson et al., 2006).

Figure 1

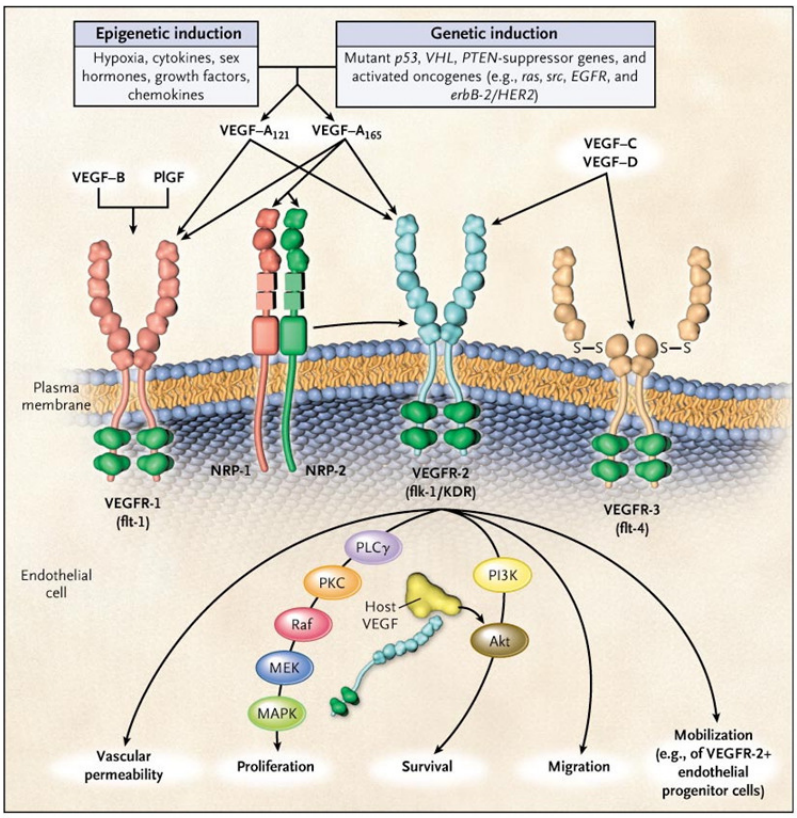

Figure 1. **VEGF receptors and their downstream pathways.** The diffusible isoforms of VEGF, including VEGF121 and VEGF165, signal through VEGFR2, the major VEGF signaling receptor for angiogenesis. The binding of VEGF to VEGFR2 leads to a cascade of different signaling pathways. Binding of ligands causes dimerization of the receptor, followed by intracellular activation of the PLCγ– PKC–Raf kinase–MEK–MAPK pathway and subsequent initiation of DNA synthesis and cell growth, whereas activation of PI3K–Akt pathway leads to increased endothelial-cell survival. Activation of Src can lead to actin cytoskeletal changes and induction of cell migration. (Figure and illustration from Kerbel RS. *N Engl J Med* 2008; 358:2039-2049)

VEGF regulating factors and genes regulated by VEGF

VEGF is regulated by many factors, including growth factors, hormones, transcription factors and mechanical stimuli. Hypoxia is considered a major driver of VEGF expression, especially in tumor tissues and bones (Krock et al., 2011; Wang et al., 2007). The transcription factor, hypoxic inducing factor-1 (HIF-1α), is greatly up-regulated under low oxygen tension in tumor cells or osteoblasts, and this promotes transcriptions of various angiogenic factors, including VEGF (Spector et al., 2001; Steinbrech et al., 2000). Under normal aerobic conditions, HIF-1α is hydroxylated and targeted for proteasomal degradation by the von Hippel-Lindau (VHL) tumor suppressor (Maxwell et al., 1999). Deletion of HIF-1α in osteoblasts causes reduction of VEGF expression, leading to interruption of both angiogenesis and osteogenesis, while deletion of VHL in osteoblasts increases both expression of HIF-1α and VEGF, leading to the promotion of bone formation and angiogenesis (Wang et al., 2007). In addition to HIF-1α, VEGF is also regulated by the transcription factor, osterix, expressed in osteoblastic lineage cells to regulate their differentiation (Tang et al., 2012). Certain hormones, including estrogen and parathyroid hormone, regulate VEGF levels as well. VEGF plasma levels are decreased in women after menopause (Senel et al., 2013), and animal experiments demonstrate decreased VEGF levels in ovariectomized mice (Ding et al., 2011). Several growth factors that play critical roles in bone development and postnatal bone repair also regulate VEGF expression, particularly in osteoblastic cells. These factors include, but are not limited to, members of the TGF-β superfamily, such as TGF-β1, TGF-β2, BMP2, BMP4 and BMP7 (Deckers et al., 2000; Yeh and Lee, 1999), insulin-like growth factor (Goad et al., 1996) and FGF2 (Saadeh et al., 2000).

Inflammatory factors, such as prostaglandin E1 and E2, IL-1, IL-6 and IL-8, which are increased during the inflammation phase of bone repair, also induce VEGF expression (Harada et al., 1994; Jung et al., 2001; Tzeng et al., 2013). Mechanical strain is another regulator of VEGF expression. Under mechanical stress, osteoblasts release VEGF and this VEGF stimulates biological responses (Nakai et al., 2009; Thi et al., 2010). All these VEGF regulatory factors play critical roles in bone development and homeostasis, suggesting that modulation of VEGF levels in osteoblasts may provide a basis for strategies aimed at controlling bone repair and regeneration.

VEGF signaling shares downstream signaling pathways with other growth factors, such as EGF and PDGF. Therefore, profiles of genes that are regulated by VEGF signaling overlap with those of genes regulated by other growth factors, especially those of common downstream pathways of receptor tyrosine kinases, like RAS-Raf-ERK1/2 and PI3K-Akt. Currently, the list of genes that are specifically regulated by VEGF signaling is incomplete. Schweighofer *et al.* characterized the genes in HUVECs induced by VEGF, EGF and IL-1, and found that NR4A2 and EGR-3 were selectively regulated by VEGF (Schweighofer et al., 2009). Other studies demonstrated that NR4A and EGR-3 are essential mediators of VEGF-induced endothelial activation and angiogenesis (Liu et al., 2003; Liu et al., 2008). The profiles of genes that are regulated by VEGF signaling in other cell types, such as mesenchymal progenitor cells or osteoblasts, are not fully characterized.

Cellular mechanisms during bone repair and regeneration

Bone repair represents the endogenous healing capability of human bones. Facture healing, the most common form of bone repair, is characterized by several overlapping stages, namely, an inflammation phase, soft callus phase, cartilage turnover (replacement by bony callus) and bone remodeling phase (Marsell and Einhorn, 2011). After fracture or many other forms of bone injury, a hematoma is formed in the injury sites due to disruption of blood vessels. In the first couple of days, neutrophils are recruited to the hematoma and phagocytose tissue debris and microorganisms. This is followed by influx of macrophages to remove the dead neutrophils, promote angiogenic responses and initiate the repair cascade. With invasion of blood vessels, mesenchymal progenitor cells migrate to the injury site, particularly to the intramedullary region or fracture gap, where they proliferate and differentiate to either osteoblasts or chondrocytes. Depending on the stability of facture fixation and supply of blood vessels, endochondral or intramembranous ossification occurs at the facture sites. Instability or lack of blood supply may lead to endochondral bone formation during the repair, while a stable facture or fracture rich in vasculature facilitates intramembranous ossification (Dimitriou et al., 2005). In addition, a third type of ossification called 'transchondroid bone formation' has been proposed in a model of distraction osteogenesis. During transchondroid ossification, chondrocyte-like cells induced by mechanical strains form chondroid bone, which is gradually transformed to bone (Choi et al., 2002; Yasui et al., 1997). In endochondral ossification, the cartilage is gradually resorbed and replaced by bony callus consisting of woven bone. In both intramembranous and endochondral sites, the newly formed woven bones is gradually remodeled to lamellar bone. The human body can restore small bone defects and repairs bone fractures that are not severe, but it hardly

heals large bone defects without intervention. Distraction osteogenesis is a good example of mechanical strain-induced bone regeneration procedures where mechanical forces elicit biological response by cells. In addition, exogenous bone either in the form of autograft, allograft, xenografts, bone substitutes or bone forming cells can be transplanted or added to the injury sites when relatively large amounts of bone are needed.

The role of VEGF in the inflammation phase during bone repair

The hematoma after bone trauma and the subsequent inflammatory response initiate bone repair. VEGF plays a critical role in this process and is concentrated in the hematoma after bone injury. It has been reported that VEGF concentrations in hematoma can be 15-fold higher than in plasma, although VEGF levels in plasma already increased significantly compared with healthy controls (Street et al., 2000). The hypoxia in the hematoma greatly induces VEGF expression in surrounding bone cells or recruited inflammatory cells. In addition, the fibrin matrix in hematoma could be a reservoir of VEGF (Street et al., 2000). Shortly after injury, the number of neutrophils in the peripheral circulation increases as neutrophil retention in the bone marrow is reduced by inflammatory stimuli (Eash et al., 2010). Neutrophils are recruited to the hematoma to help remove bone debris and microbial pathogens. VEGF has been reported to induce neutrophil chemotaxis and increase sinusoid permeability in the bone marrow (Ancelin et al., 2004; Lim et al., 2014). Therefore, it is possible that osteoblast-derived VEGF may facilitate the entry of neutrophils into the circulation. Following neutrophil infiltration, macrophages and other inflammatory cells are recruited to the injury sites. This results in a release of cytokines, such as TNF-α, IL-1α, and IL-1β (Ukai et al., 2003). These

cytokines activate endothelial cells and promote revascularization at the injury sites. They are also efficient inducers of VEGF in inflammatory and osteoblastic cells. VEGF is a chemotactic factor for macrophage/monocytes (Barleon et al., 1996; Leek et al., 2000). Considering that macrophages release angiogenic factors (Sunderkotter et al., 1991; Wu et al., 2013), the pro-angiogenic effect of VEGF may be mediated by macrophages in addition to direct targeting of endothelial cells. In the resolution phase of inflammation, macrophages are recruited to phagocytose dead or aging neutrophils. Subsequent uptake of apoptotic neutrophils causes a switch of macrophage phenotype from activated M1 to reparative M2 macrophages. This stimulates macrophages to release mediators, such as TGF-β1, which can suppress the pro-inflammation response and initiate the repair process (Brancato and Albina, 2011).

The role of VEGF in endochondral bone ossification during bone repair

The mechanism of endochondral ossification during bone repair recapitulates the key processes of endochondral bone formation during development, including cartilage formation, vascular invasion, osteoclastogenesis and cartilage removal. VEGF was previously shown to play important roles in bone development and growth (Figure 2). VEGF generated by osteoblast precursors in the perichondrium and hypertrophic chondrocytes induces osteoblastic cells to migrate into the primary ossification center together with blood vessels and osteoclasts (Maes et al., 2010; Zelzer et al., 2002). In addition to stimulating skeletal vascularization, VEGF is also a critical factor for epiphyseal chondrocyte survival (Zelzer et al., 2004).

Cartilage formation is the early step in endochondral ossification (EO). Large amounts of cartilage are observed in unstable bone fractures, and moderate amounts of cartilage are also observed in the injured periosteum of stable fracture models. Skeletal stem cells from the bone marrow, periosteum and surrounding muscles can differentiate into either chondrocytes or osteoblasts. It has been suggested that VEGF regulates the differentiation of skeletal stem cells. Inhibition of VEGF signaling in early skeletal progenitors facilitates the fate of determination from osteogenic to chondrogenic cells (Chan et al., 2015). In addition, soluble Flt1 gene therapy was shown to improve BMP4-induced chondrogenenic differentiation of muscle-derived stem cells (MDSCs) *in vitro* and promote articular cartilage repair *in vivo*. (Kubo et al., 2009; Matsumoto et al., 2009), further suggesting that VEGF inhibition, when combined with BMPs, might be a therapeutic strategy for regeneration of cartilage when needed.

Figure 2

A

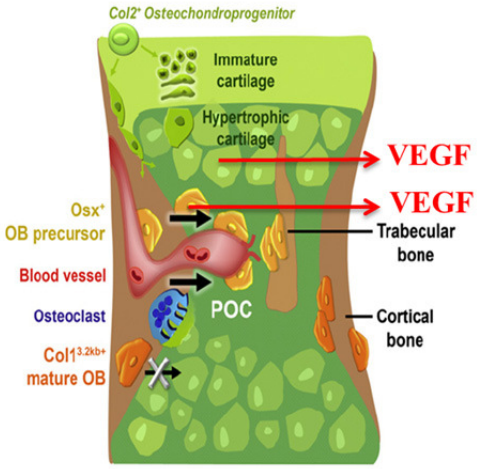
Col2+ Osteochondroprogenitor
Immature cartilage
Hypertrophic cartilage
VEGF
VEGF
Osx+ OB precursor
Trabecular bone
Blood vessel
POC
Osteoclast
Cortical bone
Col1 3.2kb+ mature OB

B

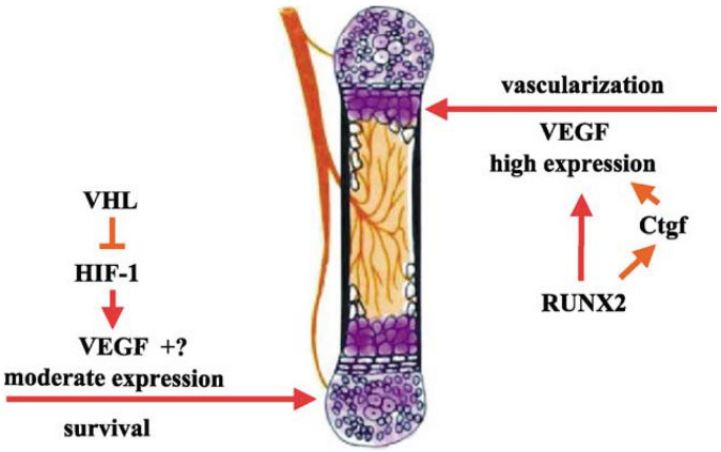
vascularization
VEGF
high expression
Ctgf
RUNX2
VHL
HIF-1
VEGF +?
moderate expression
survival

Figure 2 (continued). **Diagram indicating major functions of VEGF during endochondral ossification. (A)** Schematic outline of the events during the initial invasion of the cartilaginous bone model and the formation of the primary ossification center (POC). Col2-expressing osteochondroprogenitors (green) give rise to cells in the central growth cartilage and to cells at the periphery with osteoblastic fates. The first committed osteoblast lineage cells appear in the perichondrium surrounding the mid-diaphyseal hypertrophic cartilage. Early cells of the lineage, represented by the Osx-expressing osteoblast precursors (yellow), produce VEGF, and this VEGF stimulates the differentiation of the precursor cells. These cells move into the developing POC together with vascular endothelial cells (red) and osteoclasts (blue), and populate it as stromal cells, pericytes, or osteoblasts. (Figure and illustration adapted from Maes C *et al.* Dev Cell 2010; 19(2): 329–344). **(B)** In hypertrophic chondrocytes, high-level expression of VEGF, controlled by the transcription factor Runx2, is essential for vascularization of cartilage in the primary ossification center and continued capillary sprouting under the growth plates as the bone grows. In epiphyseal chondrocytes, a moderate level of VEGF expression, controlled by HIF-1 and VHL, is necessary for chondrocyte survival. (Figure and illustration adapted from Zelzer E *et al. Curr Top Dev Biol* 2005;65: 169–87).

During bone development, VEGF is a critical factor for the survival of epiphyseal chondrocytes. Maes *et al*. observed cell death in chondrocytes within epiphyseal regions of long bones from $VEGF^{188/188}$ mice (mice only expressing the VEGF 188 isoform) (Maes et al., 2004). In mice with *Vegfa* deleted in Col2-positive chondrocytes, massive chondrocyte death was observed in the central epiphyseal/growth plate region of developing skeletal elements (Zelzer et al., 2004). The effect of VEGF on chondrocyte survival appears to depend on the chondrocyte differentiation stage. Although VEGF promotes chondrocyte survival in areas lacking blood vessels at the early stage of endochondral ossification, it also induces cell death in hypertrophic chondrocytes when VEGF levels are greatly elevated. The apoptosis of hypertrophic chondrocytes promoted by VEGF may be indirectly mediated by vascular invasion, as increased oxygen tension with invasion of blood vessels decreases the level of HIF-1α, which in turn leads to increased cell death (Pfander et al., 2006). Systemic administration of sFlt1 delays chondrocyte death. This results in increased numbers of hypertrophic chondrocytes and thus expansion of the growth plate (Gerber et al., 1999). In addition, inhibition of VEGF leads to reduced apoptosis of articular chondrocyte and improvement of articular cartilage in a mouse model of osteoarthritis (Matsumoto et al., 2008), consistent with the idea that VEGF may be a detrimental factor in the progression of osteoarthritis.

In the later stages of endochondral ossification during bone development and repair, chondrocytes in the cartilaginous template stop proliferating, enlarge to hypertrophic chondrocytes, and synthesize collagen type X. Hypertrophic chondrocytes express osterix, a strong inducer of VEGF expression (Tang et al., 2012), and produce high levels of VEGF (Carlevaro et al., 2000; Zelzer et al., 2001). VEGF stimulates vessel

invasion and recruitment of chondroclasts into the hypertrophic cartilage (Carlevaro et al., 2000; Zelzer and Olsen, 2005). In a model of BMP4-induced ectopic ossification, VEGF enhanced angiogenic responses, cartilage resorption and its replacement by bone (Peng et al., 2002). In a murine femoral fracture model, inhibition of VEGF signaling by Flt1, delayed cartilage turnover, disrupted conversion of soft cartilaginous callus to a hard bony callus, and impaired fracture healing (Street et al., 2002). These data are consistent with the delayed endochondral bone formation observed in $VEGF^{120/120}$ mice (mice expressing only the VEGF120 isoform) and mice treated with sFlt1 during bone development (Gerber et al., 1999; Zelzer et al., 2002).

Osteoclasts (chondroclasts) are multi-nucleated terminal differentiated cells derived from monocytes/macrophages. During development, hypertrophic chondrocyte-derived VEGF binds to VEGFR1 in monocytes to promote their migration and differentiation to osteoclasts (Aldridge et al., 2005; Barleon et al., 1997). VEGF also binds to VEGFR2 in osteoclasts and promotes their survival through PI3K/Art signaling (Yang et al., 2008). *In vivo* and *in vitro* evidence show that VEGF can substitute for M-CSF to promote osteoclast differentiation and bone resorption (Kodama et al., 1991; Niida et al., 1999). In addition, VEGF also enhances the bone resorbing activity of osteoclasts (Nakagawa et al., 2000). Therefore, during endochondral ossification, VEGF from hypertrophic chondrocytes are critical for the invasion of osteoclasts to the cartilaginous template and replace it by bone. The enhanced osteoclast function by VEGF on during bone development could also be observed in postnatal bone repair, and thus the potential influence of osteoclast mediated bone resorption should be considered when using VEGF as a therapeutic strategy to promote bone repair and regeneration.

Coupling of angiogenesis and osteogenesis by VEGF

Unlike endochondral ossification, where blood vessels prevent the formation of cartilage, intramembranous bone formation relies on the coupling of angiogenesis and osteogenesis. VEGF has an essential role in this communication, since both vascular and skeletal morphogenesis is interdependent (shown as Figure 3). Under stimulation of hypoxia during inflammation, osteoblasts release factors including VEGF, through HIF-1α pathway. This activates endothelial cells, and promotes vessel permeability (Wang et al., 2007). The increased vasculogenesis and angiogenesis bring bone-forming progenitors as well as nutrition, oxygen and minerals necessary for mineralization. In addition, osteogenic factors, such as BMP2, released from blood vessels, promote osteoblast differentiation and mineralization (Matsubara et al., 2012). As a positive feedback, maturating osteoblasts also generate certain angiogenic factors, including PDGF and VEGF.

Figure 3

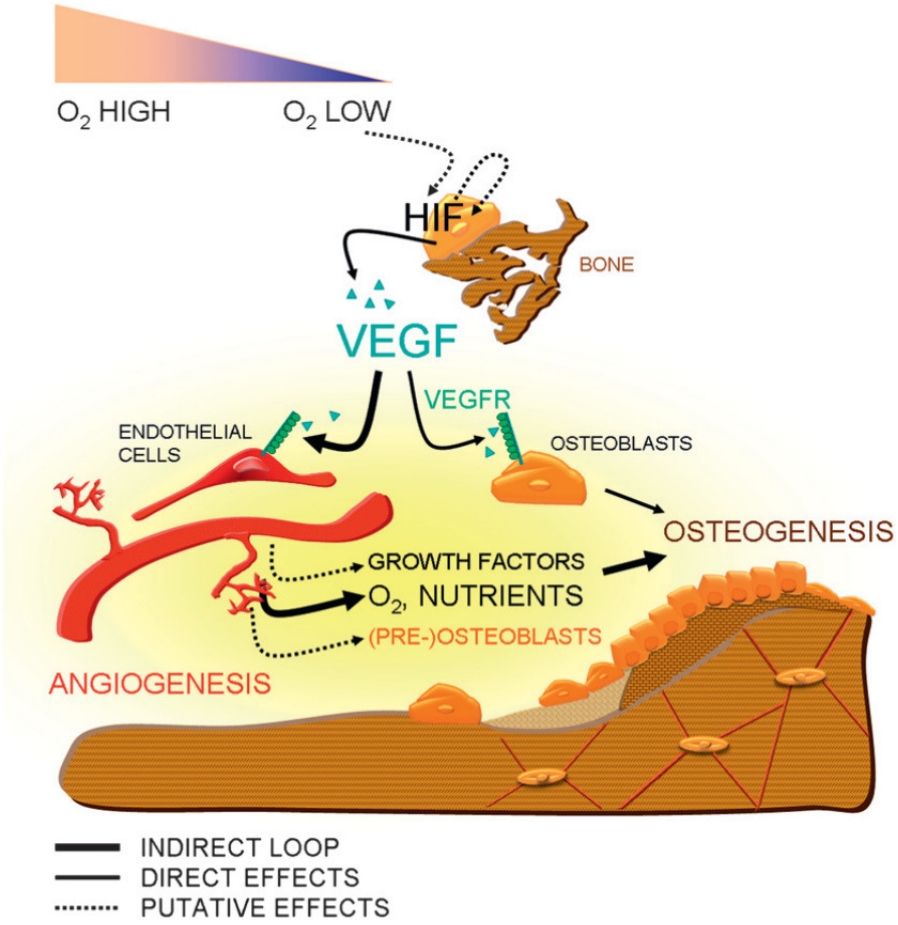
O_2 HIGH
O_2 LOW
HIF
BONE
VEGF
VEGFR
ENDOTHELIAL CELLS
OSTEOBLASTS
OSTEOGENESIS
GROWTH FACTORS
O_2, NUTRIENTS
(PRE-)OSTEOBLASTS
ANGIOGENESIS
INDIRECT LOOP
DIRECT EFFECTS
PUTATIVE EFFECTS

Figure 3 (continued). **Regulation of osteogenesis-angiogenesis coupling by HIF and VEGF.** Mature osteoblasts located on the bone surface express HIFs and respond to HIF activation. In addition to cell-autonomous effects of HIF on osteogenesis, HIF stabilization in mature osteoblasts also increases accumulation of VEGF. VEGF can act through its receptors on endothelial cells to induce angiogenesis, thereby increasing the supply of oxygen and nutrients required for osteogenesis. Increased vascularization may also lead to influx of skeletal stem cells and/or (pre)osteoblasts and to elevated levels of endothelium-derived osteogenic growth factors or anabolic signals. In addition, VEGF can affect osteogenesis through direct interactions with receptors on osteoblasts. Altogether, the HIF–VEGF pathway is critically important in coupling the processes of angiogenesis and osteogenesis (Figure adapted from Schipani E *et al. J Bone Miner Res* 2009;24:1347–1353).

The role of VEGF in bone healing mediated by intramembranous ossification

Intramembranous bone formation during bone repair has been suggested to depend on VEGF signaling. Blocking extracellular VEGF by sFlt1 decreased blood vessel formation and bone regeneration in a tibial cortical bone defect model, while administration of exogenous VEGF increased formation of mineralized bone within the bone defects in the same model (Street et al., 2002). However, consequences of exogenous VEGF application in various models of bone repair exhibited a certain extent of variation. Exogenous VEGF successfully enhanced bone healing and regeneration in several bone repair models where endogenous VEGF levels were decreased (Behr et al., 2010; Kawao et al., 2013), but failed to improve bone repair in certain studies using ex vivo gene therapy or recombinant VEGF (Kaipel et al., 2012; Peng et al., 2002; Schonmeyr et al., 2010). In contrast to repair of large bone defects, it is possible that only small amount VEGF were needed for healing of small bone defects. Exogenous VEGF may not help to regenerate bone when endogenous VEGF levels are adequate, and excess VEGF may even have detrimental effects on regeneration. Too much VEGF may recruit excess numbers of osteoclasts, resulting in resorption of newly formed bone, since VEGF regulates the differentiation and migration of osteoclasts (Henriksen et al., 2003; Nakagawa et al., 2000). In addition, excess VEGF inhibits the function of pericytes through VEGFR2 mediated inhibition of PDGFR (Greenberg et al., 2008), a molecule required for pericyte maturation, and this leads to formation of immature blood vessels and interruption of angiogenesis-osteogenesis coupling. A good example of this was the unexpected increase of mature vessels in tumors of patients treated with anti-VEGF

therapy (Benjamin et al., 1998; Bergers et al., 2003), demonstrating the complexity of VEGF functions in pathology and therapeutic strategies.

VEGF signaling in osteoblastic cells

Osteoblast-derived VEGF usually acts in a paracrine manner on adjacent endothelial cells via binding to VEGF receptors to regulate endothelial migration, proliferation and vessel permeability. In addition to endothelial cells, VEGF receptors are also expressed and functional in other cells types, including pericytes and osteoclasts (Greenberg et al., 2008; Yang et al., 2008). However, expression of VEGF receptors in osteoblasts is quite variable, particularly in mice, making paracrine/autocrine effects of osteoblast-derived VEGF on osteoblasts difficult to study. In murine osteoblastic MC3T3 cells, VEGF was shown to promote levels of alkaline phosphatase and osteocalcin (Jaasma et al., 2007). However, other studies also showed that primary murine mesenchymal progenitors and osteoblasts failed to respond to exogenous VEGF (Liu et al., 2012). Mice with deletion of *Vegfr1* or *Vegfr2* in osteoblastic cells exhibit reduced bone density two weeks after birth. In addition, reduced number of osteoprogenitor cells was observed in the bone marrow of these mice (Liu et al., 2012), indicating that both VEGFR1 and VEGFR2 in osteoblastic cells are important for postnatal bone formation. However, to what extent such autocrine effects of osteoblast-derived VEGF are important during postnatal bone healing is not clear.

In addition to the secreted VEGF, cells also generate intracellular (intracrine) VEGF, which is not secreted but participate in transcriptional regulation and in cell survival. This phenomenon was first reported in the case of VEGF signaling for the

survival of hematopoietic and endothelial cells (Gerber et al., 2002; Lee et al., 2007). In early osteoblast precursors, intracellular VEGF also plays a role in the control of osteoblast and adipocyte differentiation (Liu et al., 2012). Recombinant VEGF can be used to restore extracellular VEGF levels but do not affect intracrine VEGF. If intracellular VEGF in osteoblasts is also important for the osteoblast maturation and mineralization during bone repair, it may explain why exogenous VEGF failed to improve bone repair in some cases. Should this turn out to be the case, modified cell-permeable VEGF, fused to a nuclear localization signal, may enhance intracellular levels of VEGF, and promote bone repair and regeneration when application of traditional recombinant VEGF fails.

The role of VEGF in bone remodeling

In the remodeling phase of bone repair, replacement of woven bone by lamellar bone requires coupling of osteoclast mediated bone resorption and osteoblast mediated bone formation. VEGF influences the function of both types of bone cells, and normal VEGF levels are necessary for maintaining normal bone remodeling. Several osteogenic factors, such as TGF-β1, IGF, PDGF-BB, are released from bone matrix or pre-osteoclasts during the process of bone resorption (Crane and Cao, 2014; Tang et al., 2009; Xie et al., 2014). These factors induce neo-angiogenesis, which is required for angiogenesis, and coordination of bone formation. VEGF binds VEGFR1 in osteoclasts and regulates their differentiation and activation. Therefore, reduction of VEGF in bone remodeling may decrease the angiogenic and osteogenic signals indirectly through inhibition of bone resorption. In a mouse femur facture model, inhibition of VEGF by

sFlt1 caused reduced callus volume at various stages of repair, including bone remodeling, while treatment with exogenous VEGF increased vascularity and mineral density in the calcified callus (Street et al., 2002). These data indicate that recruitment of osteoclasts by VEGF may be necessary to maintain normal bone remodeling.

The role of VEGF in distraction osteogenesis

Unlike bone repair, bone regeneration is a process in which a relative large amount of new bone is formed in response to the external elements, such as mechanical force, exogenous bony tissues or bone forming cells. Bone regeneration is widely used in treatment of non-union fractures, craniofacial reconstructions, segmental bone defects after tumor resection, augmentation of jaw bones, lengthening of long bone, promotion of implant, and bone grating. Distraction osteogenesis and bone grafting, represent the use of mechanical forces to induce bone formation and the addition of exogenous bony tissues to help form new bone. As bone grafting is very much like bone repair, we will here only discuss the role of VEGF in distraction osteogenesis.

Distraction osteogenesis (DO) is a surgical procedure used to treat limb length discrepancies, bone deformities and bone loss. It is widely used in orthopedics and oral and maxillofacial surgery. The process of DO involves slow and steady distraction of an osteotomy gap after a period of latency. VEGF expression during active distraction is primarily located to the maturing osteoblasts at the primary mineralization front (Choi et al., 2002), indicating that the main recourse of VEGF at distraction sites is the osteoblast lineage cells.

As a key regulator of angiogenesis-osteogenesis coupling, VEGF has multiple roles during DO. First, it is released from osteoblastic cells in response to mechanical forces and regulates osteoblast differentiation and mineralization in an autocrine mechanism (Thi et al., 2007; Thi et al., 2010). Second, the induced VEGF from osteoblastic cells binds receptors on adjacent endothelial cells, enhancing neo-angiogenesis and promoting the release of osteogenic factors, such as BMP2 and BMP4, from blood vessels (Schipani et al., 2009). Disruption of VEGFR1 and VEGFR2 using neutralizing antibodies reduced the angiogenic response and bone regeneration in a mouse distraction osteogenesis model (Jacobsen et al., 2008), highlighting the importance of VEGF signaling-mediated angiogenesis. Third, in addition to the autocrine and paracrine effects, intracrine VEGF within osteoblastic cells may play a role of stimulating osteoblast differentiation and mineralization, since exogenous VEGF or antagonists failed to affect the differentiation of early osteoblastic lineage cells (Eckardt et al., 2003; Liu et al., 2012),

Strategies to promote bone repair and regeneration

Skeletal stem cells, cytokine, growth factors, hormones, and bone matrix scaffolds are currently the components of strategies to stimulate tissue regeneration. As a grow factor, VEGF interacts with other factors, such BMPs and PDGF, regulates stem cell functions, and exhibits various activities in different extracellular matrices or engineered scaffolds. Understanding the biology of VEGF from the perspective of its interactions with stem cells in the context of extracellular matrices, may be of help in developing novel techniques for modulating VEGF activity to promote bone regeneration.

The extracellular matrix or matrix-like engineered scaffolds can serve as a reservoirs for VEGF. Different properties of different scaffolds influence the loading capability, speed of release, and activities of VEGF. VEGF delivered to the distraction gap through a mini-osmotic pump in a rabbit distraction osteogenesis model failed to improve blood flow and bone mineral content (Eckardt et al., 2003). In this case, no scaffold was used to trap VEGF at the injury sites, and thus VEGF was possibly disseminated to adjacent tissues or was metabolized within a relative short period of the time after delivery. Similarly, by using the guided bone regeneration (GBR) technique to repair critical-sized defects in rats, Kaigler *et al.* found that a bolus of VEGF delivered to the defects without a scaffold failed to improve vasculogenesis and bone formation, while a bolus of VEGF loaded in hydrogels that released VEGF at a relatively slow speed, successfully enhanced both angiogenesis and osteogenesis (Kaigler et al., 2013). These studies indicates that an optimal scaffold loaded with VEGF may significantly influence the outcome of bone repair. Loading of VEGF in a heparin cross-linked demineralized bone matrix improved vasculogenesis when implanted subcutaneously (Chen et al., 2010). Porous strontium-doped calcium polyphosphate (SCPP) scaffolds have been proposed to promote the secretion of VEGF from human osteoblast-like MG63 cells. These scaffolds together with mesenchymal stem cells (MSCs) improved bone regeneration in a rabbit segmental bony defects model (Cu et al., 2013). The release kinetics of VEGF is also important for the effects of biomaterial on vascularization and bone formation. Several studies showed that sustained release of VEGF increased the efficiency of bone regeneration. Scaffolds with the capability to release VEGF slowly include biomimetic poly (lactide-co-glycolide) (PLGA) scaffolds, cylindrical chitosan

sponges, a biomimetic bone matrix modified with heparin, and biphasic calcium phosphate (BCP) ceramics. These scaffolds could produce prolonged bioavailability of VEGF.

Skeletal stem cells are heterogeneous cell populations that may be found in cancellous bone, perisinusoidal niche in bone marrow, endosteum, periosteum, and skeletal muscle. Under certain conditions, these cells can further differentiate to multiple cell types, such as osteoblasts, chondrocytes, adipocytes and myoblasts. VEGF participates in the regulation of such cells. VEGF from bone marrow mesenchymal progenitors is important for the lineage fate determination between osteoblasts and adipocytes. Reducing VEGF levels in these cells causes adipogenic differentiation at the expense of osteogenic differentiation. (Liu et al., 2012). Osteochondroprogenitors are present in the periosteum, located in the cambium layer, and can differentiate to osteoblasts or chondrocytes. VEGF levels in the periosteum control the lineage choice during periosteal responses after injury. Inhibition of VEGF by sFlt1was found to enhance the BMP2 induced cartilage formation (Peng et al., 2005), indicating that VEGF may act as a negative regulator of chondrogenesis. This is consistent with the findings that inhibition of VEGF signaling by sFlt1 promoted chondrogenesis of transplanted fetal skeletal tissues at the expense of osteogenesis (Chan et al., 2015).

Many growth factors, in addition to VEGF, such as PDGF and BMPs, have been widely used in animal models of bone repair and regeneration. They share similar downstream signal transduction pathways and a better understanding of their interactions may help to refine strategies based on the use of recombinant proteins to promote bone regeneration.

BMPs and VEGF have frequently been used together in many studies of bone regeneration. However, the results have been quite variable. VEGF promotes BMP2 induced ectopic bone formation, and accelerates resorption of cartilage and its replacement by bone, while VEGF blocker, sFlt1, inhibits BMP2 induced ectopic bone formation, but promotes cartilage formation and delays the resorption of cartilages (Peng et al., 2005). In a critical-sized defect model, muscle-derived stem cells in combination with overexpression of VEGF failed to heal the defect (Peng et al., 2002). When cells were co-transfected with vectors encoding VEGF and BMP2, a lower ratio of VEGF to BMP2 (1:5) induced greater bone regeneration than BMP2 alone (Peng et al., 2005) while a higher ratio (5:1) failed to promote bone healing. Similarly, only a low ratio of VEGF to BMP4 (1:5) promoted bone regeneration in a critical-sized defect, while high ratios (5:1) inhibited bone regeneration (Peng et al., 2002). This is consistent with the finding that co-expression of VEGF and BMP4 in muscle derived stem cells reduces their bone forming potential (Li et al., 2009).

Except for indirect effects on osteoclast recruitment, the inhibitory effects of VEGF on bone regeneration may also be attributed to direct effects of VEGF on osteoblasts. VEGF has been shown to retard the terminal differentiation of osteoblasts by up-regulation of Id1 (Song et al., 2011). In endothelial cells, VEGF strongly inhibits TGF-β1 stimulation of PAI-1 production and activation of smad2/3(Yamauchi et al., 2004). VEGF also inhibits the mesenchymal transition of endothelial cells induced by BMP4 through the Smad2/3 pathway (Medici et al., 2010). Although evidence that the inhibitory effects of VEGF on downstream signaling of TGF-β family members, including BMPs, is lacking in the case of osteoblasts, such an effect, if it occurred, could

explain, at least in part, why too much VEGF has antagonistic effects on osteoblast activity particularly in the presence of BMPs.

PDGF is another important factor for bone regeneration (Caplan and Correa, 2011). Platelet rich plasma containing PDGF has been widely studied in various bone regenerative procedures (Albanese et al., 2013). VEGF prevents maturation of pericytes through a VEGFR2 mediated inhibition of PDGFR. This leads to formation of immature blood vessels (Greenberg et al., 2008). Since osteoblasts and pericytes are derived from same mesenchymal progenitors, the inhibitory effects by VEGF on PDGF-receptor activation by VEGF may occur in osteoblasts as well. Recombinant VEGF-A competitively blocks PDGF-dependent activation of PDGFR and its signaling effects in several cell types (Pennock and Kazlauskas, 2012). Structural similarities between PDGF-B and VEGF-A (Muller et al., 1997), also suggest that VEGF-A may bind to PDGFRs on mesenchymal stem cells (Ball et al., 2007). However, whether such binding would enhance or inhibit PDGFR-mediated downstream signaling pathways and cellular responses in osteoblast lineage cells is unclear.

Summary and future directions

Osteoblastic cells represent a major source of VEGF in the bone environment. Mice with reduced levels of VEGF in osteoblastic cells display an osteoporotic phenotype (Liu et al., 2012). It was reported that VEGF levels in osteolineage cells including mesenchymal progenitor cells are decreased with age or in some anabolic

disorders (Costa et al., 2009; Wilson et al., 2010), and this reduction may be related to Thus, supplement of proper amount of VEGF to normal level specifically in osteoblasts may prevent or treat age-related osteoporosis or defective bone healing. Since osteoblasts are very metabolically active, certain drugs that efficiently up-regulated VEGF in osteoblasts, such as stains (Maeda et al., 2003; Tsartsalis et al., 2012), might become the potential strategy.

The relationship between growth factors, bone forming progenitor cells and scaffolds are important components in bone regeneration, and the current studies of VEGF functions may provide the basis for novel strategies using VEGF modulation to improve bone regeneration. Such strategies may be based on the following considerations: 1) Scaffolds with slow release of physiological levels of VEGF are needed and application of exogenous VEGF should be carefully considered, particularly when evidence for reduced levels of VEGF is lacking. 2) The paracrine, autocrine and intracrine effects of VEGF on bone forming stem cells or progenitors add to the complexity of VEGF applications. VEGFR2 modulation and the use of cell-permeable VEGF may be considered in certain scenarios. 3) The combination of VEGF with other growth factors, such BMPs, PDGF, and TGF-β, should be carefully considered, based on the knowledge that VEGF may potentially inhibit downstream signaling of BMPs/TGF-β, and compete with PDGF-BB for binding to PDFGRs. These interactions may vary depending on repair region, such as bone marrow vs. periosteum, or type of repair mechanism, such as intramembranous ossification vs. endochondral ossification.

Overall Hypothesis

VEGF, synthesized from osteoblast lineage cells, regulates osteoblast differentiation and bone formation during bone repair.

Study Aims

Aim 1: To study the role of osteoblast-derived VEGF in bone repair

Aim 2: To study the roles of VEGF receptor 2 in osteoblast lineage cells during cortical defect healing

Aim 3: To study the modulation of VEGF on osteogenic activity of BMP2 during cortical defect healing

Chapter II

Osteoblast-derived VEGF regulates osteoblast differentiation and bone formation during bone repair

Introduction

Bone repair following injury is usually a rapid and efficient process. However, it can be compromised in certain clinical circumstances. For example, delayed union or nonunion of bone fragments occurs in about 5-10% of patients with bone fracture (Gomez-Barrena et al., 2015), and bone regenerative procedures sometimes fail. Possible causes include impaired blood supply, reduced numbers of osteoprogenitor cells, damaged periosteum and infection, but the underlying mechanisms are often not fully understood (Bishop et al., 2012). Thus, in-depth studies of cellular and molecular mechanisms of bone healing are required for further improvement of procedures aimed at stimulating bone regeneration.

As one of the most important cytokines/growth factors for regulation of vascular development and postnatal angiogenesis (Coultas et al., 2005; Hoeben et al., 2004), VEGF also plays critical roles in bone repair and regeneration since angiogenesis and osteogenesis are highly coupled (Gerber et al., 1999; Zelzer et al., 2004). Both endochondral and intramembranous bone formation was found to depend on VEGF signaling in previous studies using various bone repair models. At bone repair sites, VEGF promotes recruitment of osteochondroprogenitors cells, induces cartilage formation, and stimulates cartilage resorption and its replacement by bone (Peng et al., 2002; Tarkka et al., 2003), while inhibition of VEGF by sFlt1, which is a soluble VEGF decoy receptor, impaired bone healing by disrupting conversion of the cartilaginous callus to bony callus (Street et al., 2002). Blocking receptors for VEGF, VEGFR1 and VEGFR2, with neutralizing antibodies decreased blood vessel formation and bone

regeneration(Jacobsen et al., 2008), while administration of exogenous VEGF increased formation of mineralized bone within bone defects (Behr et al., 2010; Emad et al., 2006; Street et al., 2002).

These studies demonstrated that consequences of bone repair can be affected by the manipulation of VEGF levels, but the mechanisms by which different cell types generate and respond to VEGF in repair situations have not been studied in detail. Osteoblast lineage cells along with chondrocytes are considered important sources of VEGF in bone environment (Wang et al., 1996; Zelzer and Olsen, 2005). During bone development, VEGF generated by osteoblast precursors in the perichondrium of cartilage models of future bones, stimulates osteoblast differentiation (Maes et al., 2010; Zelzer et al., 2002), and VEGF produced by hypertrophic chondrocytes serves as a chemotactic factor for migration of these osteoblasts into primary ossification centers together with vascular endothelial cells and osteoclasts (Gerber et al., 1999; Zelzer et al., 2004). During postnatal bone homeostasis, paracrine VEGF from osteoblasts, which acts on adjacent endothelial cells to mediate mitogenic and angiogenic effects, plays an important role in maintaining vasculature integrity and bone mass (Liu et al., 2012; Wang et al., 2007). These VEGF also promotes migration and maturation of osteoclasts to control the balance of bone remodeling (Liu et al., 2012; Nakagawa et al., 2000; Niida et al., 1999). In addition, the intracrine VEGF in osteoblasts regulates the balance of osteoblast and adipocyte differentiation, and disruption of this balance lead to osteoporosis (Liu et al., 2012).

The reduced VEGF was observed in many cell types including mesenchymal progenitors with aging (Efimenko et al., 2011; Jiang et al., 2008; Pola et al., 2004; Swift

et al., 1999; Wilson et al., 2010), and this reduction in osteolineage cells may be related to the decreased bone mass and vasculature possibly leading to osteoporosis (Costa et al., 2009; Liu et al., 2012; Maharaj and D'Amore, 2007). Thus pharmaceutical strategies to target VEGF in bone environment may be used to prevent osteoporosis related defective bone healing and promote bone regeneration. However, currently to what extent osteoblast-derived VEGF recapitulate their functions in bone development and how they contribute to bone repair is unclear. To address this lack of understanding, we used tibial monocortical defects to study bone repair in mice with conditional deletion of *Vegfa* or *Vefgr2* in Osterix (Osx)-expressing osteoblast precursors, and revealed that during bone healing, osteoblast-derived VEGF acts as a pro-inflammatory, angiogenic, and osteogenic growth factor, which regulates osteoblastic activity by stimulating cross-talk between endothelial cells, osteoblastic and hematopoietic cells.

Materials and Methods

Mouse Strains

Osx-GFP::Cre (Rodda and McMahon, 2006), *VE-cadherin-cre* (Alva et al., 2006) and *CAG-loxP-stop-loxP-ZsGreen* (Ai6), *CAG-loxP-stop-loxP tdTomato* (Ai14) mouse lines were purchased from Jackson Laboratory. *Vegfa* floxed and *Flk-1(Vegfr2)* floxed mice were provided by Genentech. To generate $Vegfa^{fl/fl}$*;Osx-cre* mice, hemizygous *Osx-cre* transgenic mice were crossed with $Vegfa^{fl/fl}$ mice to produce heterozygous $Vegfa^{fl/+}$ offspring carrying a *Cre* allele. These mice were then crossed with $Vegfa^{fl/fl}$ mice generating the following three genotypes: $Vegfa^{fl/fl}$*;Osx-cre* (*Vegfa CKO* mice), $Vegfa^{fl/+}$*;Osx-cre* and $Vegfa^{fl/fl}$. In studies of the consequence of postnatal deletion of *Vegfa*, cre expression in Osx-cre mice carrying a tetracycline responsive element (TRE; tetO) was suppressed by feeding the pregnant mice and their progeny with water containing 2mg/ml doxycycline. The efficiency of *Osx-cre*–mediated inactivation of *Vegfa* was assessed by previous studies showing that *Vegfa* transcripts in extracts of bones from *Vegfa* CKO mice were reduced by about 70% compared with those from controls (Liu et al., 2012). To allow better tracing of osteoblastic cells, ZsGreen (ZsG), a *Cre* activating fluorescent reporter, was introduced into *Osx-cre,* $Vegfa^{fl/+}$*;Osx-cre* and $Vegfa^{fl/fl}$*;Osx-cre* mice. $Vegfa^{fl/fl}$*;VE-cadherin-cre* and $Flk1^{fl/fl}$*;Osx-cre* mice were generated using a similar strategy.

Tibial monocortical defect model

The tibial cortical defect used as a simplified stable facture model, was described previously (Kim et al., 2007; Minear et al., 2010a; Minear et al., 2010b). Skeletal mature

mice (9-12 weeks old male) were used for all studies. Mice were placed under general anesthesia by intraperitoneal injection of 100 mg/kg ketamine and 10 mg/kg xylazine. The lateral aspect of right tibia was exposed and carefully cleared of overlying soft tissues while preserving the periosteum. A monocortical osseous hole (0.8 mm diameter) was created on the anterior surface of the tibia crest using a round burr attached to a dental drill. Irrigation with saline was used to remove bone dust and fragments. The soft tissue wound was closed by suturing the muscle and skin layers separately with 5-0 absorbable gut suture (Reli). After surgery, mice received subcutaneous injection of 0.05-0.1mg/kg buprenorphine for analgesia.

Delivery of recombinant VEGF

Absorbable collagen hemostatic sponges (Avitene) were cut to the dimensions of the injured region. Sponges were soaked in 1 μl of human recombinant VEGF (R&D System) with concentration of 1 or 0.1 μg/μl for 30 min at 4 Cº. After the injury was made, the loaded sponge was inserted into the defects, followed by a single stitch of the cut muscle flap to over the wound.

μCT analysis

Tibiae were isolated, fixed overnight in 10% neutral buffered formalin, and kept in 70% ethanol until analyzed using a μCT 35 system (Scanco Medical) with a spatial resolution of 7μm. Sagittal images of injured tibiae were used to perform three-dimensional (3-D) histomorphometric analysis. We defined the region of interest to cover the hole region between the interrupted cortical bone ends, injured bone marrow, and periosteal callus outside the hole, separately. The remained old bone fragments during drilling were excluded from the region of interest. Then we used a total of 96-100

consecutive images (about 0.672-0.7mm in length) to present most of the injured region and periosteal callus for 3-D reconstruction and analysis. 3-D structural parameters analyzed included: total tissue volume (TV), trabecular bone volume per tissue volume (BV/TV), trabecular number (Tb.N), trabecular thickness (Tb.Th) and trabecular separation (Tb.Sp).

Histology and histomorphorphometry

Fixed samples were decalcified in 0.5 M EDTA (pH 8.0) for 14 days and embedded in paraffin or optimal cutting temperature (OCT) compound (Tissue-TEK). 8μm longitudinal sections using the hole region as landmark were cut, and stained for H&E, aniline blue, movat pentachrome, safranin O or tartrate resistant acid phosphatase (TRAP). The comparisons between *Vegfa* CKO and control mice were mainly covering the hole region between the interrupted cortical bone ends and the adjacent areas, visible in the same sections, while most staining in the wounded bone marrow was not quantified because histological details in longitudinal sections of bone marrow cannot be guaranteed to be in the same horizontal plane as those of the hole region.

6-8 tissue sections for each mouse stained with aniline blue were used to determine the amount of newly formed osseous tissues. Each section was photographed and analyzed in a method described previously (Minear et al., 2010a). The digital images were imported into Adobe Photoshop CS5 (Adobe System Inc). We choose a rectangular region of interest which covered the hole region and encompassed about 10^6 pixels. The number of aniline blue-stained pixels was determined using magic wand tool. The percent of collagen in the hole region was calculated as the aniline blue positive pixels/10^6 pixels. The mineralization/collagen ratio could be further calculated as BV/TV

(μCT) divided by the percent of aniline blue stained area. For quantifying the cartilage, periosteal area about 2mm distal to the defects was chosen, and Safranin-O positive area was calculated using magic wand tool.

Immunofluorescence and Immunohistochemistry

Immunostaining was performed using a standard protocol. We incubated sections with primary antibody to neutrophil marker NIMP-R14 (1:100, Santa Cruz), macrophage marker F4/80 (1:100, AbD Serotek), CD31 (1:50, BD Biosciences), CD45 (1:100, BD Biosciences), Osterix (1:100, Abcam or 1:50, Santa Cruz), Bone sialoprotein (BSP, 1:50, Santa Cruz), Osteocalcin (OCN, 1:50, Santa Cruz), Alkaline phosphatase (ALP,1:50, Santa Cruz), VEGF (1:50, Santa Cruz), or Biotin conjugated lectin (1:100, Vector Lab), BMP2 (1:100, Abcam), FSP1 (1:100, Abcam) overnight at 4ºC. For immunohistochemistry, a horse radish peroxidase-streptavidin system (ABC) was subsequent to detect the immunoactivity, followed by counterstaining with hematoxylin. For immunofluorescence, secondary antibodies conjugated with fluorescence (1:200, Life Technologies) were added, and slides were incubated at room temperature for 90 min while avoid light. Sections were then stained with or without DAPI and coverslipped as above. For quantification of BSP, OCN, VEGF and ALP level, photographs including fields within the hole region were taken from 40X objective of confocal microscopy (Nikon A14), and were analyzed in Image J. Blood vessel (microvessel) density was calculated based on anti-CD31 staining. Single CD31 immunoreactive endothelial cells, or endothelial cell clusters separate from other microvessels, were counted as individual vessels. The total number of blood vessels in a specific field divided by total area was considered as blood vessel density. For BrdU staining, mice were injected with biotin

conjugated BrdU (20mg/kg body wight, i.p., Sigma-Aldrich) three hours prior to euthanasia. A commercial BrdU staining kit (Life Technologies) was used to staining the proliferative cells. For TUNEL staining, dead cells were detected using in situ cell death detection kit, TMR Red (Roche) as described in manufacturer's instructions.

Isolation of osteoblastic cells from mouse long bones

Isolation and culture of primary osteoblasts from tibia and femur of 8- to 12-week-old mice were as described (Bakker and Klein-Nulend, 2012). Bone marrow cells were flushed out, and cleaned diaphysis were cut into small pieces and incubated in 1 mg/ml collagenase II (Life Technologies) at 37°C for one hour with constant shaking. The bone pieces were cultured in DMEM containing 15% FBS (Hyclone) and 100μg/ml ascorbic acid (sigma-Aldrich) until cells migrating from the bone chips became confluent.

Isolation of bone marrow stromal cells

Bone marrow cells from tibia and femur of 8- to 12-week-old mice were flushed out and cultured in α-MEM containing 10% FBS. The primary cells were kept undisturbed until day 4 when half of medium was changed. Then we change medium every other day until day14. Cells were digested, passaged and maintained in complete culture medium. These adhered cells from bone marrow were considered as bone marrow stromal cells (BMSCs). Cells in the passage 1-2 were used for differentiation assay and passage 2-4 for migration and proliferation assay.

Adenoviral infection

Adenoviruses were purchased from Vector BioLab. We cultured the isolated BMSCs in 12-well plates with a-MEM medium containing 10% FBS for 48 hours before

they reached confluence, and then infected them with adenoviral-cre or adenoviral–green fluorescent protein (GFP) (2×10^7 plaque-forming units adenovirus per well) for 48 hours, and continue the culture in differentiation medium.

In vitro osteoblastic differentiation and mineralization assay

BMSCs and osteoblastic cells were seeded in 12-well plates containing complete culture medium. Upon reaching 70-80% confluency, cells with or without adenovirus treatment were switched to osteogenic medium (10% FBS, 10mM β-glycerophosphate, and 50μg/mL ascorbic acid with 100nM dexamethasone). Culture medium was replaced every 2 days. Von Kossa and Alizarin Red staining was used to measure mineralization after 21 days of culture.

CCK8 cell proliferation assay

4,000 BMSCs were seeded in each well of 96-well plate. The next day, cells were given αMEM medium with 10% FBS or 2% FBS containing vehicle, 10-40ng/ml recombinant VEGF (R&D) and/or 2-40ng/ml recombinant PDGF-BB (R&D). After two days of additional culture, 10μl cell counting kit 8 (Sigma-Aldrich) was added to each well and incubated for 3 hours. Absorbance at 450 nm, representing relative cell numbers, was measured using a microplate reader.

In vitro wound closure assay

Confluent monolayers of BMSCs (passage 2-4) were scratched with a yellow pipette tip to create an about 1000μm wide cell-free wound. Wounded monolayers were incubated for 24 h and photographed at time 0 and at 24 h. The average rate of wound

closure was calculated as the difference between the starting width and the width at any incubation time/incubated time.

Complete blood analysis

Mice were placed under general anesthesia, and peripheral blood was collected from the heart. About 20 µl of blood samples were analyzed by Hemavet 950 Chemistry Analyzer (Drew Scientific Inc.).

Statistics

The data are presented as mean ± standard error using unpaired 2-tailed Student's *t*-test. Spearman's correlation coefficient was used to measure the dependency of two variables. *P* values less than 0.05 were considered significant.

Study approval

All animal experiments were approved by the Harvard Medical Area Standing Committee on Animals and in accordance with the U.S. Public Health Service Policy on Humane Care and Use of Laboratory Animals.

Results

Osteoblast-derived VEGF stimulates macrophage-related angiogenesis and promotes infiltration of regenerative cells during the inflammatory phase

Histology of a tibial cortical bone defect in wild type mice at various time points after surgery (see Methods) is shown in Figure 4. Post-surgery days (PSD) 1-3 were considered the inflammation phase. At PSD3, VEGF levels and blood vessels in the hole region of *Vegfa*$^{fl/fl}$*;Osx-cre* (*Vegfa* CKO) mice decreased by 76.1% and 64.4%, respectively, compared with *Vegfa*$^{fl/fl}$ littermates (Figure 5A, B). In *Vegfa* CKO mice, the number of F4/80-positive macrophages was reduced by 74.5% and 57.4% in hole region and adjacent marrow space, respectively (Figure 5C). Strong correlation between the density of blood vessels and macrophage numbers indicated that blood vessel invasion is associated with macrophage recruitment (Figure 5D). Only a few CD45-positive cells were recruited into the defects, indicating that lymphocytes were not among the major recruited inflammatory cell types at this stage (Figure 6A). The number of osterix-positive osteoblastic precursors was lower in defects of *Vegfa* CKO mice than of *Vegfa*$^{fl/fl}$ mice, but this reduction was proportional to the decrease in total cell numbers (Figure 6B). We analyzed percentages of different cellular components in the hole region, and found that only the number of macrophages and endothelial cells were lower in *Vegfa* CKO than in control mice (Figure 6C). This underscores the importance of angiogenesis and macrophage recruitment for the infiltration of other cell types into the injured region. In addition, *in vitro* wound closure experiments using BMSCs from *Vegfa* CKO and control mice, showed that migration of *Vegfa* CKO cells was reduced (Figure 6D),

providing a potential mechanism for the decreased cell infiltration to repair sites in *Vegfa* CKO mice.

Figure 4

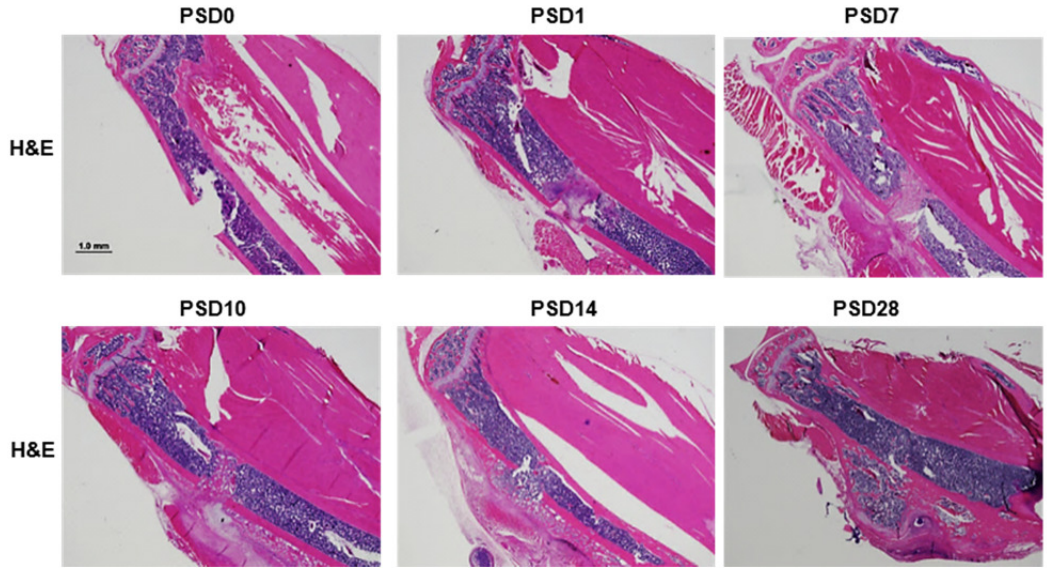

Figure 4. **Representative images of histological details for the injury tibiae at various time points after surgery**. Scale bar: 1mm.

Figure 5

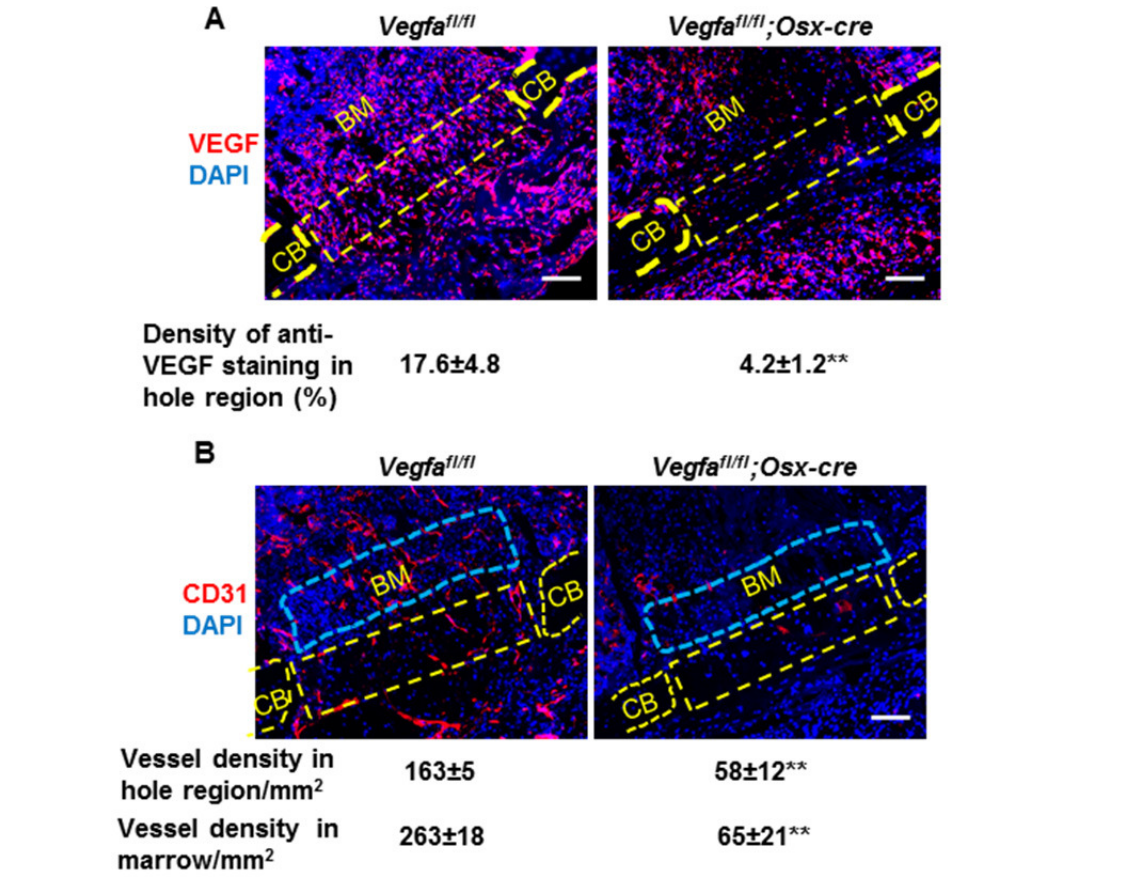
A
Vegfa fl/fl
Vegfa fl/fl;Osx-cre
VEGF
DAPI
BM
CB
Density of anti-VEGF staining in hole region (%)
17.6±4.8
4.2±1.2**
B
Vegfa fl/fl
Vegfa fl/fl;Osx-cre
CD31
DAPI
Vessel density in hole region/mm2
163±5
58±12**
Vessel density in marrow/mm2
263±18
65±21**
C
Vegfa fl/fl
Vegfa fl/fl;Osx-cre
F4/80
Macrophage density in hole region /mm2
321±46
82±19*
Macrophage density in adjacent BM region/mm2
336±69
143±26**
D
R2 =0.877
P < 0.001
Blood vessel density in hole region (/mm2)
Macrophage density in hole region (/mm2)

Figure 5 (continued). **Osteoblast-derived VEGF stimulates macrophage-related angiogenesis at PSD3 and promotes migration of bone marrow cells *in vitro*. (A)** High density (17.6 ± 4.8%) of anti-VEGF staining in rectangular hole region of *Vegfa*$^{fl/fl}$ mice compared with *Vegfa*$^{fl/fl}$*;Osx-cre* mice (4.2 ± 1.2%). N=5-6. **(B)** High density of blood vessels (as determined by anti-CD31staining) in hole region (163 ± 5/mm^2) and adjacent rectangular marrow region (263 ± 18/mm^2) of *Vegfa*$^{fl/fl}$ mice as compared with *Vegfa*$^{fl/fl}$*;Osx-cre* mice (58 ± 12 and 65 ± 21/mm^2). N= 4-7. **(C)** High density of F4/80-positive macrophages in hole region and adjacent rectangular marrow region of *Vegfa*$^{fl/fl}$ mice compared with *Vegfa*$^{fl/fl}$*;Osx-cre* mice. N=5-6. **(D)** High correlation between blood vessel and macrophage densities in hole region. Scale bars: 100μm (A, B), 200μm (C). Yellow stippled rectangles: hole regions (A, B, C); blue stippled rectangles: bone marrow regions (B, C). CB: cortical bone. *, *P<0.01*; **, *P<0.05*.

Figure 6

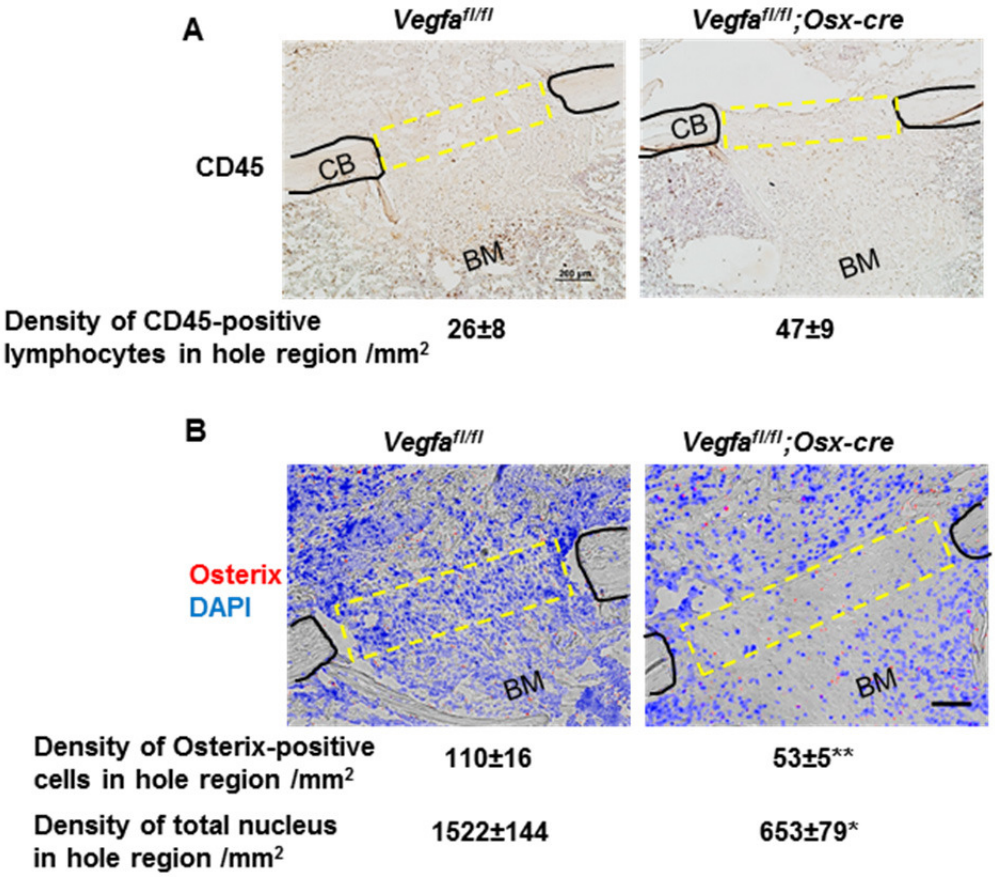
A
Vegfa fl/fl
Vegfa fl/fl;Osx-cre
CD45
CB
BM
CB
BM
Density of CD45-positive lymphocytes in hole region /mm2
26±8
47±9
B
Vegfa fl/fl
Vegfa fl/fl;Osx-cre
Osterix
DAPI
BM
BM
Density of Osterix-positive cells in hole region /mm2
110±16
53±5**
Density of total nucleus in hole region /mm2
1522±144
653±79*

Figure 6 (continued)

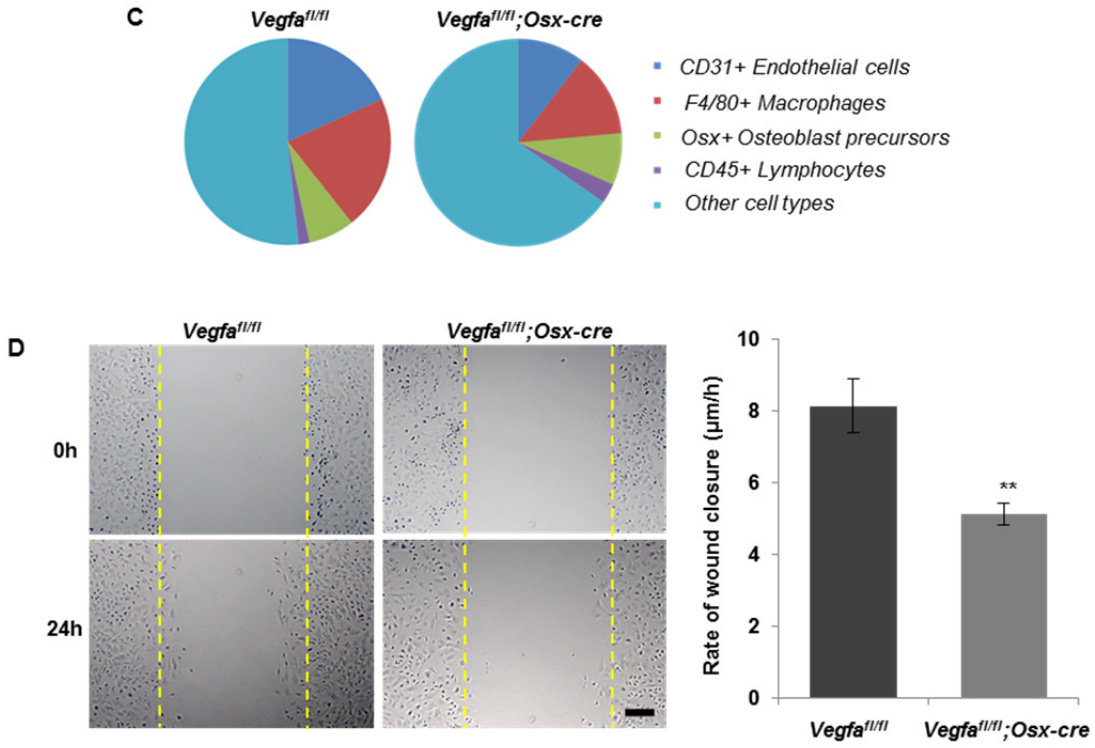

Figure 6 (continued). **Osteoblast-derived VEGF promotes infiltration of regenerative cells at PSD3. (A)** No difference of CD45-positive lymphocyte density in hole region of *Vegfa* $^{fl/fl}$*;Osx-cre* and *Vegfa* $^{fl/fl}$ mice. N=4-6. **(B)** Low density of osterix-positive osteoblast precursor cells and total cells, represented approximately by numbers of total nucleus, in the hole region of *Vegfa* $^{fl/fl}$*;Osx-cre* compared with *Vegfa* $^{fl/fl}$ mice. N=5-6. **(C)** Percentage of different cell types in the hole region in *Vegfa* $^{fl/fl}$*;Osx-cre* and *Vegfa* $^{fl/fl}$ mice. **(D)** In vitro wound closure assay. Stippled lines indicate the edges of the wound at time 0. Based on three independent experiments, the rate of wound closure was higher with cells from *Vegfa* $^{fl/fl}$ mice than with *Vegfa* $^{fl/fl}$; Osx-cre cells. Scale bar: 100μm (B), 200μm (A, D). Yellow stippled rectangles: hole region (A, B). CB: cortical bone. *, *P<0.01*; **, *P<0.05*.

Hematopoiesis is not altered but neutrophil release after injury is impaired in mice with reduced VEGF in osteoblastic cells

Osteoblasts regulate functions of some hematopoietic lineages in the bone marrow (Eash et al., 2010; Rankin et al., 2012; Wu et al., 2008). To determine whether loss of osteoblast-derived VEGF affects hematopoiesis, complete blood analysis using peripheral blood collected from mice before and 24 hours after surgery was applied. The number of most blood cells was not significantly different between *Vegfa* CKO and *Vegfa*$^{fl/fl}$ mice before surgery, with most parameters in the normal range (Figure 7A). However, 24 hours after surgery, the number of neutrophils was increased in both *Vegfa* CKO and controls compared with the number before surgery, indicating a release of neutrophils into the circulation during the acute inflammatory phase (Figure 7A). In *Vegfa*$^{fl/fl}$ mice, the number of neutrophils increased 3.0-fold after surgery, with a 3.5-fold increase in the percentage of neutrophils among total white blood cells. However, in *Vegfa* CKO mice, only 1.6 and 1.2-fold increases were observed (Figure 7B, C), indicating that the neutrophil release after injury may be regulated by osteoblast-derived VEGF. Since neutrophils are recruited to local injury sites, NIMP-R14 staining was used to display neutrophil infiltration. The number of NIMP-R14 positive neutrophils in the hole region of *Vegfa* CKO mice was lower than that of controls at PSD1, but statistical difference was lacking (Figure 7D). In addition, only few macrophages were observed in the defects of both *Vegfa*$^{fl/fl}$ and *Vegfa* CKO mice (Figure 7E), indicating that influx of macrophages comes after the massive infiltration of neutrophils into the hematoma at PSD1.

Increased cell proliferation but decreased collagen accumulation after injury in mice with reduced VEGF in osteoblastic cells

Following the inflammation phage, mesenchymal progenitor cells migrate into the wound site, proliferate and differentiate into bone forming osteoblasts. At PSD5, aniline blue staining showed 93.2% less collagen accumulation in the hole region of *Vegfa* CKO mice than in controls (Figure 8A), indicating a significant delay of osteoinduction. However, BrdU incorporation into cells showed 2.4-fold increase in the hole region of *Vegfa* CKO mice compared with control mice (Figure 8B). This enhanced proliferation was associated with an increase in cell numbers from PSD3 to PSD7 in *Vegfa* CKO compared with control mice (4.5 fold vs. 1.8 fold, Figure 8C). *In vitro* assays showed that recombinant VEGF inhibited while PDGF-BB greatly induced proliferation of BMSCs (Figure 8D-F). VEGF also inhibited the enhanced proliferation induced by PDGF-BB (Figure 8F). These results may explain, at least in part, the increased proliferation rates at the repair site when VEGF levels were reduced.

Figure 7

A

	$Vegfa^{fl/fl}$	*Vegfa CKO*	$Vegfa^{fl/fl}$	*Vegfa CKO*	Normal range
WBC (K/μL)	3.6 ± 0.3	3.5 ± 0.8	3.5 ± 0.4	4.3 ± 0.4	1.8-10.7
NE (K/μL)	0.4 ± 0.1	0.6 ± 0.1	1.2 ± 0.1*	0.9 ± 0.1*	0.1-2.4
LY (K/μL)	3.1 ± 0.3	2.9 ± 0.7	2.2 ± 0.3	3.3 ± 0.3	0.9-9.3
NE %	11.1 ± 1.6	17.8 ± 2.7	34.5 ± 3.1*	20.3 ± 1.2	6.6-38.9
LY %	85.4 ± 2.1	79.1 ± 2.8	61.1 ± 3.5*	76.7 ± 1.6	55.8-91.6
RBC (M/μL)	8.9 ± 0.4	8.7 ± 0.7	9.0 ±0.4	8.8 ± 0.4	6.4-9.4
Hb (g/dL)	10.9 ± 0.4	11.1 ± 0.9	11.5 ± 0.4	10.8 ± 0.4	11.0-15.1
HCT %	44.9 ± 2.4	43.4 ± 3.0	44.6±2.2	43.7 ± 2.5	35.1-45.4
PLT (K/μL)	589.3 ± 45	417.3 ± 76.5	581.5 ± 36.6	578.9 ± 22.1	592-2972

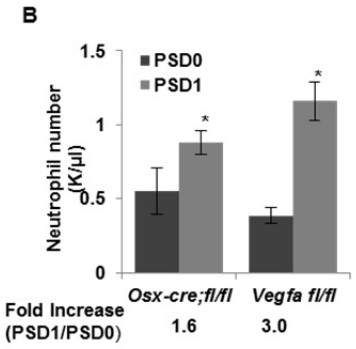

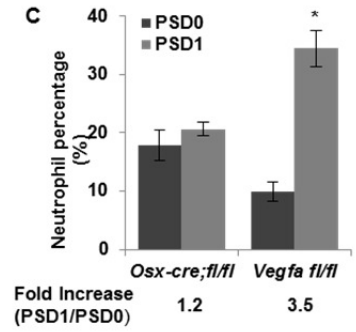

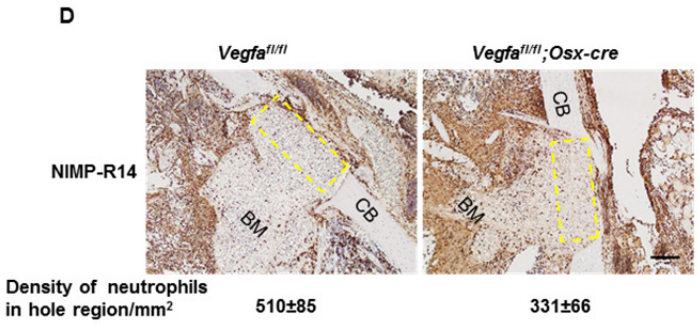

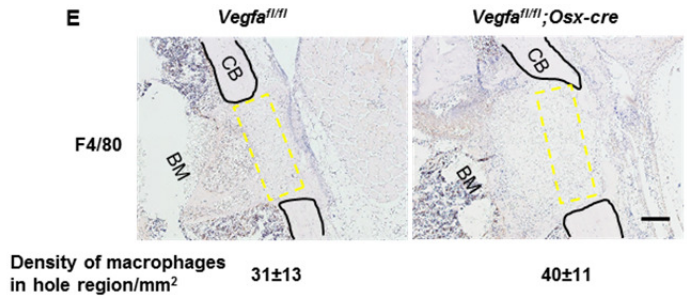

Figure 7 (continued). **Decrease of neutrophil release after injury in *Vegfa$^{fl/fl}$; Osx-cre* mice during inflammation. (A)** Complete analysis of peripheral blood from mice before and 24 hours after surgery. N=6-7. **(B, C)** Fold increase of average neutrophil numbers (B) and average percentage of neutrophil among white blood cells (C) in peripheral blood before and 24 hours after surgery. N=7. **(D, E)** Similar density of NIMP-R14 positive neutrophils (D) and F4/80-positive macrophages (E) in hole region of *Vegfa$^{fl/fl}$;Osx-cre* and *Vegfa$^{fl/fl}$* mice. N=4-7. Scale bar: 200μm (D, E). Yellow stippled rectangles: hole region. CB: cortical bone. *, *P<0.01*; **, *P<0.05*. *, *PSD1 vs. PSD0.*

Figure 8

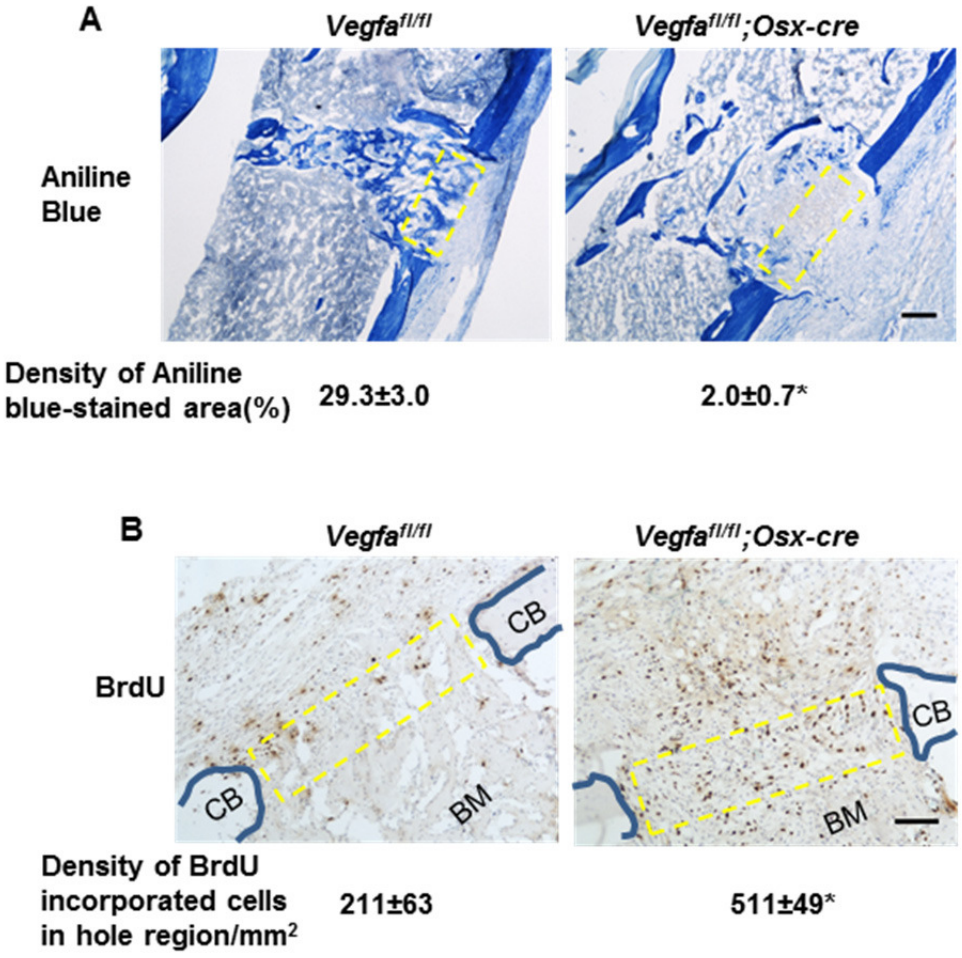
A
Vegfa fl/fl
Vegfa fl/fl;Osx-cre
Aniline Blue
Density of Aniline blue-stained area(%)
29.3±3.0
2.0±0.7*
B
Vegfa fl/fl
Vegfa fl/fl;Osx-cre
BrdU
CB
CB
BM
CB
BM
Density of BrdU incorporated cells in hole region/mm2
211±63
511±49*

Figure 8 (continued)

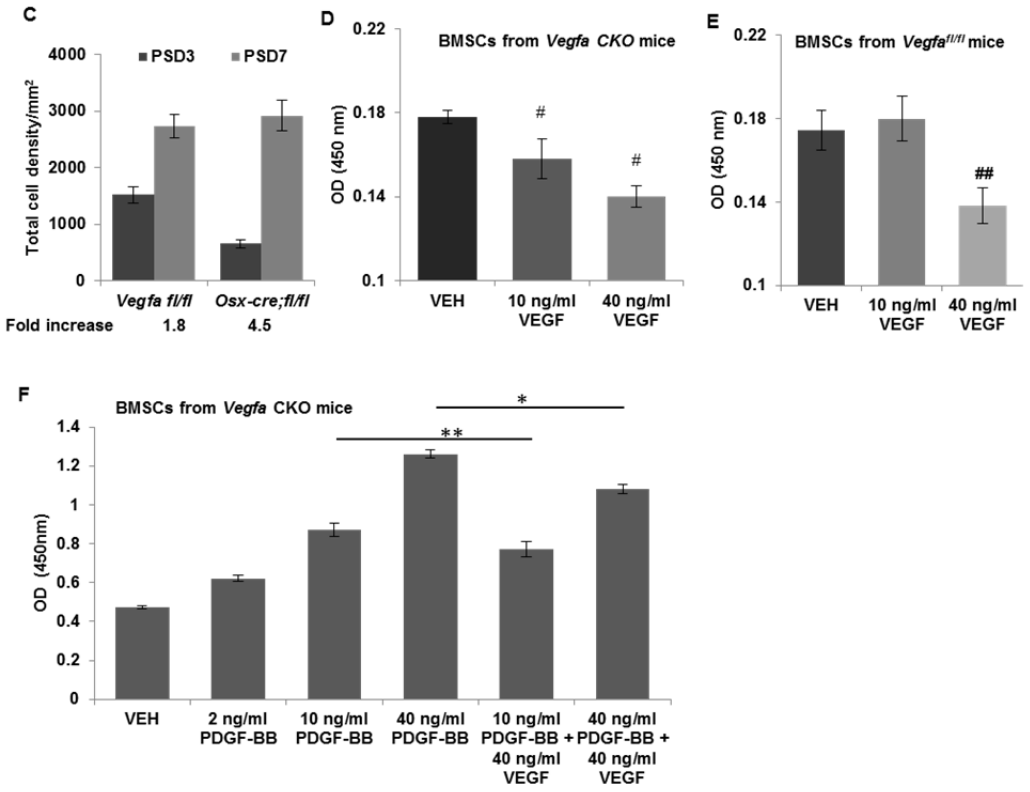

Figure 8 (continued). **Increased cell proliferation but decreased collagen accumulation in *Vegfa$^{fl/fl}$;Osx-cre* mice at PSD5**. **(A)** Reduced density of aniline blue-stained areas in hole region of *Vegfa$^{fl/fl}$;Osx-cre* mice compared with *Vegfa$^{fl/fl}$* mice. N=4-5. Scale bar: 200μm. **(B)** Increased density of BrdU incorporated cells in hole region of *Vegfa$^{fl/fl}$;Osx-cre* mice compared with *Vegfa$^{fl/fl}$* mice. N=3-4. Scale bar: 100μm. **(C)** Fold increase in total cell density in hole region of *Vegfa$^{fl/fl}$;Osx-cre* and *Vegfa$^{fl/fl}$* mice from PSD3 to PSD7. **(D-F)** Proliferation of BMSCs cultured in medium for 48 hour monitored by CCK8. OD_{450nm} represents relative cell number. At least 4 wells were used for each group and data are representative of three independent experiments. Yellow stippled rectangles: hole region. CB: cortical bone. *, $^{\#}$, *P<0.01*; **, $^{\#\#}$ *P<0.05*. $^{\#}$ *vs. VEH* (D, E)

Delayed intramembranous bone formation in defects in mice with reduced VEGF in osteoblastic cells

Absence of safranin O-stained cartilage in the injured region indicated that newly formed trabecular bone at PSD7 represents intramembranous ossification (IO), while the presence of cartilage in the periosteum close to the injury hole suggests the occurrence of endochondral bone formation (Figure 9). μCT was used to quantify the newly formed bone in the defect at this stage. Lateral views of the 3-D reconstruction of injured tibia showed less mineralized tissue in defects of *Vegfa*$^{fl/fl}$*;Osx-cre* mice than of controls (Figure 10A). In *Vegfa* CKO mice, trabecular bone volume was decreased in the hole region as well as in the wounded marrow, and this reduction was dependent on the extent of *Vegfa* reduction (Figure 10B, C). In addition, the mineralized bone in defects of *Vegfa* CKO mice showed an increase in trabecular separation and a decrease in trabecular number; however, trabecular thickness was not significantly altered (Figure 10D-H). Collagen accumulation, as revealed by aniline blue (Figure 10I, J) and movat pentachrome staining (Figure 10L), was decreased while the amount of fibrous tissue was increased in the defects of *Vegfa*$^{fl/fl}$*;Osx-cre* mice, suggesting a decrease of collagen containing osteoid. Decreased mineralization/collagen ratio in *Vegfa* CKO mice further indicated a delay in osteoid mineralization (Figure 10K). In addition, BMSCs and osteoblasts from *Vegfa*$^{fl/fl}$*;Osx-cre* mice exhibited reduced mineralization in culture when compared with cells from *Vegfa*$^{fl/fl}$ mice (Figure 10M, N). BMSCs from *Vegfa*$^{fl/fl}$ mice also showed decreased mineralization in culture following treatment with Cre-adenovirus compared with GFP-adenovirus (Figure 10O). Based on these data, we conclude that loss

of VEGF in osteoblastic lineage cells results in a mineralization defect during bone repair.

Figure 9

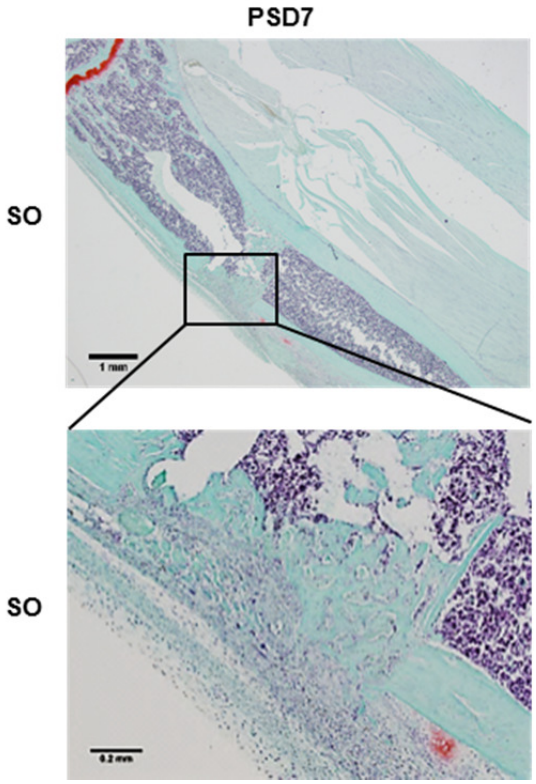

Figure 9. **Intramembranous bone formation in the hole region and endochondral bone formation in the injured periosteum during cortical defect healing.** Safranin O-stained sections in wild type mice showing that the absence of SO-positive cartilage in hole region while existence of cartilage in injured periosteum. Scale bar: 200μm.

Figure 10

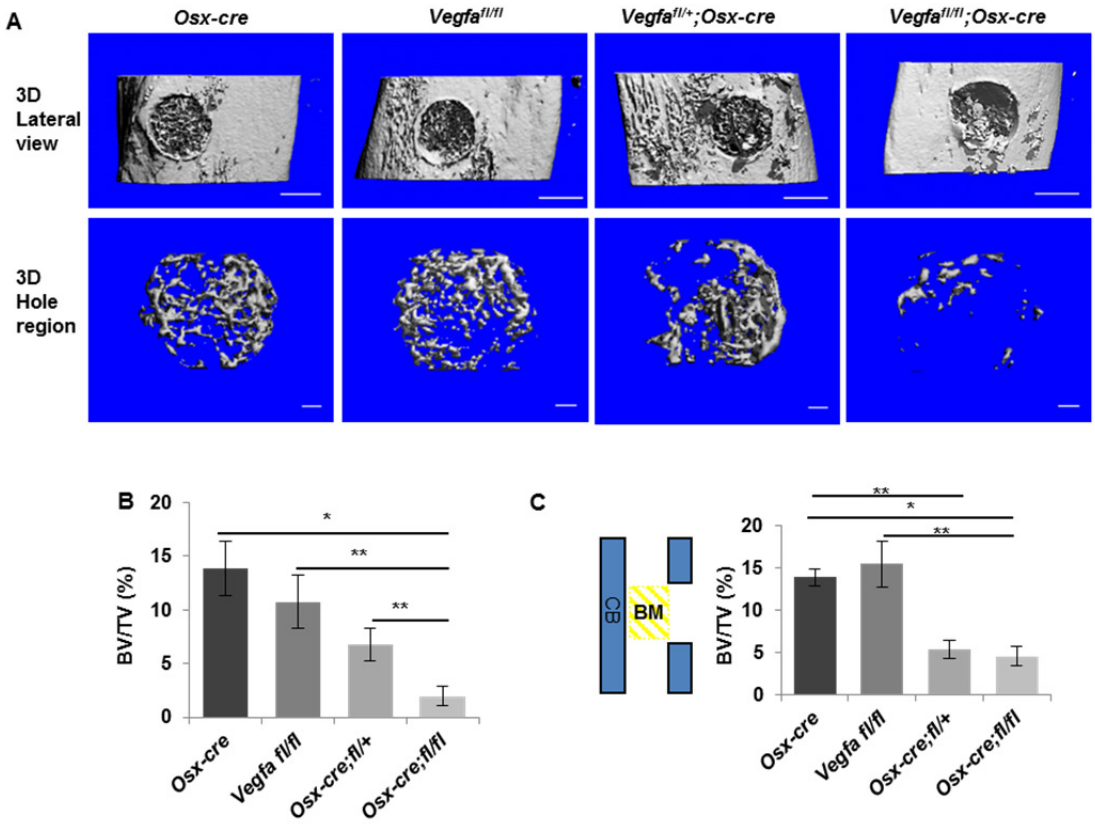
A
Osx-cre
Vegfa fl/fl
Vegfa fl/+;Osx-cre
Vegfa fl/fl;Osx-cre
3D Lateral view
3D Hole region
B
BV/TV (%)
20
15
10
5
0
*
**
**
Osx-cre
Vegfa fl/fl
Osx-cre;fl/+
Osx-cre;fl/fl
C
CB
BM
**
*
**
BV/TV (%)
20
15
10
5
0
Osx-cre
Vegfa fl/fl
Osx-cre;fl/+
Osx-cre;fl/fl

Figure 10 (continued)

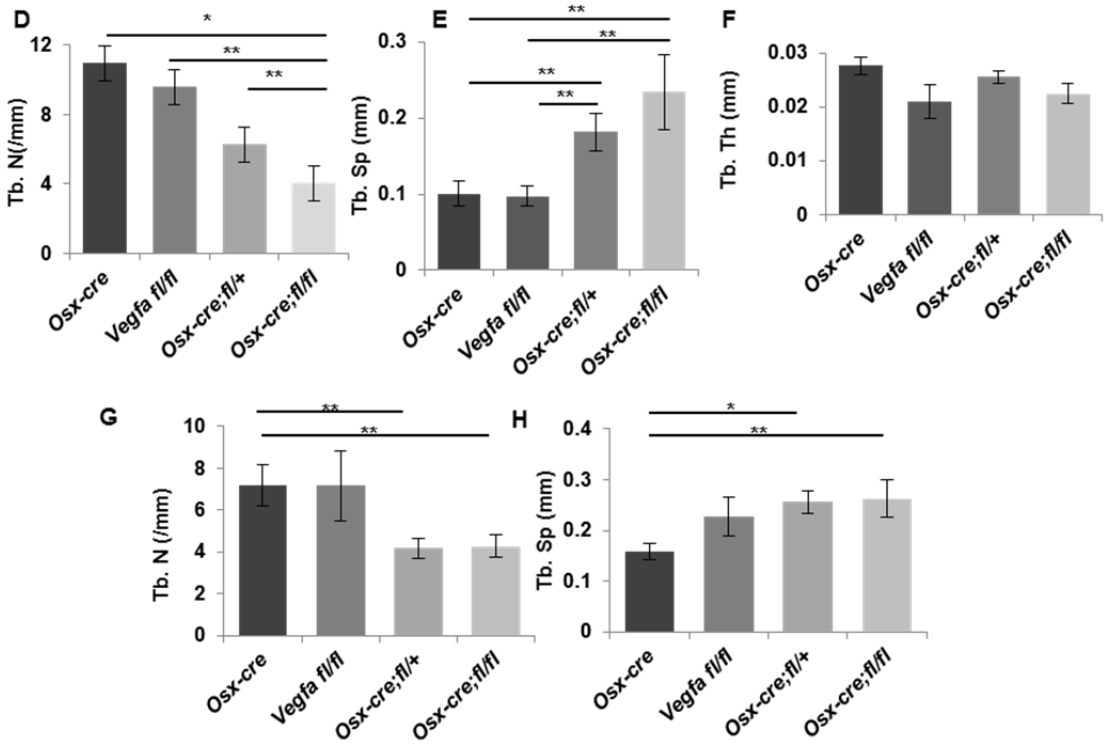

Figure 10 (continued)

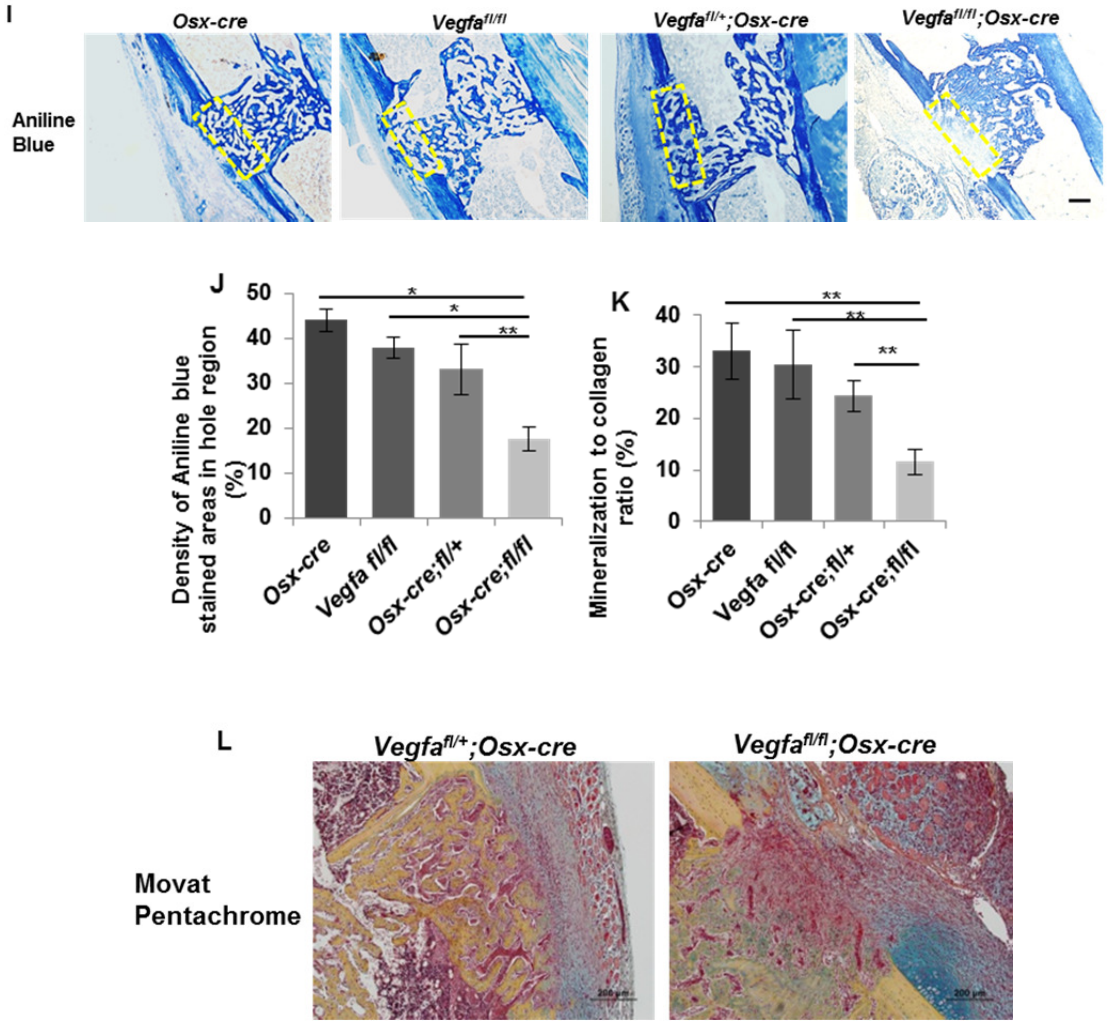

Figure 10 (continued)

Figure 10 (continued). **Impaired intramembranous bone formation in defects of *Vegfa$^{fl/fl}$;Osx-cre* mice at PSD7. (A)** 3D-reconstruction of the injured tibia from lateral views (top panel, scale bar: 500μm) and mineralized bone formed in hole region (Lower panel, scale bar: 100μm) by μCT. **(B, D-F)** μCT analysis of the mineralized bone formed in hole region. N=6. **(C, G, H)** μCT analysis of the mineralized bone formed in the wounded marrow (yellow area). CB: cortical bone. N=6. **(I)** Aniline blue staining showing reduced collagen accumulation in hole region of *Vegfa$^{fl/fl}$;Osx-cre* mice. Density of aniline blue stained area was calculated in hole region indicated by yellow frame. Scale bar: 200μm. **(J)** Low density of aniline blue-stained area in hole region of *Vegfa$^{fl/fl}$;Osx-cre* mice. N=8-11. **(K)** Decrease of mineralization to collagen ratio (BV/TV divided density of aniline blue stained area in hole region) in *Vegfa$^{fl/fl}$;Osx-cre* mice. N=5-6. **(L)** Movat pentachrome staining showing histological details in hole region. Collagen fibers are stained as yellow and muscle or fibrous tissues are stained as red. Scale bar: 200μm. **(M, N)** Alizarin red or Von Kossa staining of BMSCs (M) and osteoblasts (N) after 21 days of culture in mineralization medium. **(O)** Alizarin red and Von Kossa staining of BMSCs (from *Vegfa$^{fl/f}$* mice), treated with GFP or Cre adenovirus and followed by 21 days of culture in mineralization medium. The data were representative for three independent experiments (M-O) *, $P<0.01$; **, $P<0.05$.

Osteoblastic lineage cells are the main generators of VEGF at the bone repair site

A cre-activated reporter, ZsGreen (ZsG), was used to trace Osx-expressing osteoblast precursor cells and their progeny. The majority of VEGF staining was localized in ZsG-positive cells (Figure 11), indicating that osteolineage cells are important generators of VEGF. Compared with *Osx-cre;ZsG* mice, VEGF levels and numbers of ZsG+ cells expressing VEGF were decreased in *Vegfa$^{fl/fl}$;Osx-cre;ZsG* mice by 60.6% and 67.0%, respectively (Figure 11). This indicates that VEGF was successfully deleted from osteoblastic cells. *VE-cadherin-cre;tdTomato* mice were used to trace endothelial lineage cells. In the injury region of *VE-cadherin-cre;tdTomato* mice, only a few tdTomato-positive cells expressed VEGF at PSD7, while moderate levels of VEGF was observed in tdTomato-positive cells of the metaphyseal vasculature (Figure 12A, B). To further examine the roles of endothelial cell-derived VEGF in healing of bone defects, cortical defects were made in *Vegfa$^{fl/fl}$;VE-cadherin-cre* mice and their littermate controls. μCT of samples harvested at PSD7 showed that the volume of newly formed bone in the hole region and wounded marrow was practically the same in *Vegfa$^{fl/fl}$;VE-cadherin-cre, Vegfa$^{fl/+}$;VE-cadherin-cre, and Vegfa$^{fl/fl}$* mice (Figure 12C, D), indicating that VEGF produced by other cell types may compensate for the reduction of VEGF in endothelial cells.

Osteoblast-derived VEGF stimulates angiogenesis and osteoblast differentiation at cortical bone repair site

Total number of bone forming cells, represented by ZsG-positive cells, was not significantly different in defects of *Vegfa*$^{fl/fl}$*;Osx-cre;ZsG* mice compared with littermate controls at PSD7 (Figure 13A). The number of FSP1-positive fibroblasts showed a 2.7-times increase in defects of *Vegfa*$^{fl/fl}$*;Osx-cre;ZsG* mice compared with controls (Figure 13B), consistent with the increase in fibrous tissue as indicated by movat pentachrome staining. Co-staining for FSP1 in ZsG-positive cells was more frequently observed in *Vegfa*$^{fl/fl}$*;Osx-cre;ZsG* mice than in *Osx-cre;ZsG* mice (18.3±3 % Vs. 4.8±1.8 %, Figure 13B), suggesting that a higher percentage of osteolineage cells differentiate into fibroblasts when VEGF levels are reduced. Levels of bone sialoprotein (BSP) and osteocalcin (OCN), markers of osteoblasts at their middle and mature stages of differentiation respectively, were greatly decreased in the hole region of *Vegfa*$^{fl/fl}$*;Osx-cre;ZsG* compared with *Osx-cre;ZsG* mice (Figure 13C, D). The number of blood vessels was also reduced in both hole region and adjacent extracortical area of *Vegfa*$^{fl/fl}$*;Osx-cre;ZsG* mice (Figure 13E, F). Correlation of blood vessel areas with BSP/OCN levels indicated an association between angiogenesis and osteoblast differentiation (Figure 13G, H). The lack of significant differences in the numbers of BrdU-, TUNEL- and TRAP-positive cells between the different genotypes (Figure 13I-K), suggested that the delayed repair in *Vegfa* CKO mice at PSD7 is unlikely to be caused by alterations in cell proliferation, cell death or osteoclast infiltration.

Figure 11

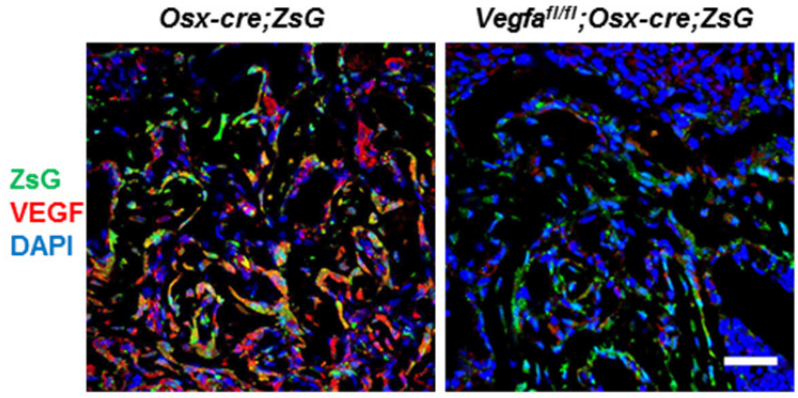

Density of anti-VEGF stained areas (%)	15.5±2.1	6.1±1.8**
VEGF expressing ZsG+ cells/ total ZsG+ cells (%)	51.5±8.3	17±5.2**

Figure 11. **Osteoblastic cells are main generator of VEGF in bone repair, and VEGF levels in osteoblasts are reduced in defects of *Vegfa CKO* mice.** Low density of anti-VEGF staining (6.1±1.8%) and percent of VEGF expressing ZsG+ osteolineage cells shown as yellow (17±5.2%) in hole region of *Osx-cre;ZsG* mice compared with *Vegfa$^{fl/fl}$;Osx-cre;ZsG* mice (15.5±2.1and 51.5±8.3%, respectively). Scale bar: 50 μm. N=4-6. **, *P<0.05. vs. Osx-cre;ZsG.*

Figure 12

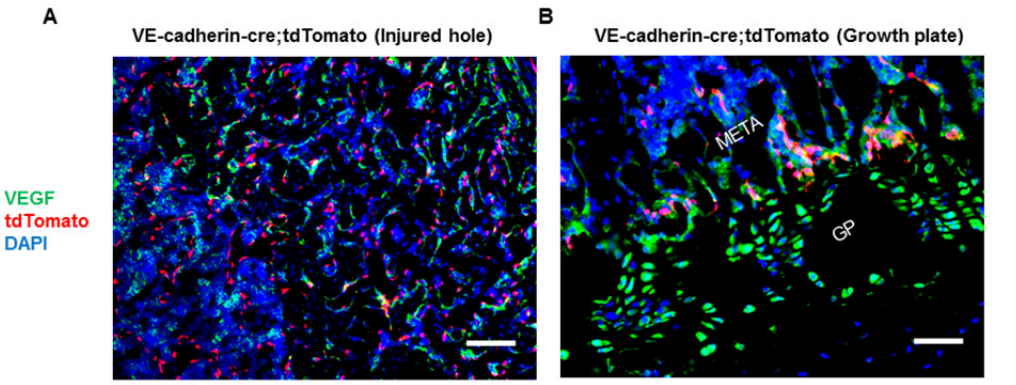

C

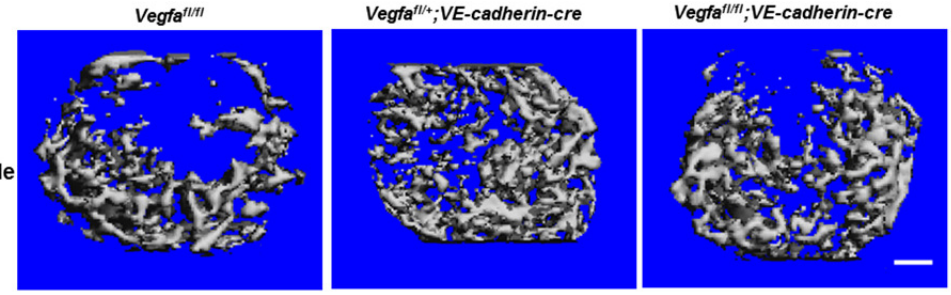

	Vegfa$^{fl/fl}$	*Vegfa*$^{fl/+}$;*VE-cadherin-cre*	*Vegfa*$^{fl/fl}$;*VE-cadherin-cre*
BV (mm^3)	0.015±0.0042	0.013±0.0039	0.0173±0.002
BV/TV (%)	10.74±2.47	11.05±2.99	15.33±1.51
TB.N (/mm)	9.58±1.54	8.47±1.7	11.35±1.42
TB.TH (/mm)	0.021±0.0031	0.026±0.002	0.027±0.0005
TB.SP (/mm)	0.098±0.013	0.14±0.038	0.095±0.012

D

μCT parameter of newly formed bone in marrow space at PSD7

	Vegfa$^{fl/fl}$	*Vegfa*$^{fl/+}$;*VE-cadherin-cre*	*Vegfa*$^{fl/fl}$;*VE-cadherin-cre*
BV (mm^3)	0.057±0.013	0.079±0.014	0.089±0.013
BV/TV (%)	13.82±2.74	17.6±3.37	21.05±2.75
TB.N (/mm)	7.16±1.65	9.37±2.7	10.7±2.67
TB.TH (mm)	0.029±0.002	0.030±0.0006	0.030±0.001
TB.SP (mm)	0.23±0.038	0.15±0.049	0.13±0.032

Figure 12 (continued). **Deletion of *Vegfa* in endothelial cells does not influence bone repair. (A)** Minority of anti-VEGF staining localizes in tdTomato-positive endothelial in defects of *VE-cadherin;tdTomato* mice at PSD7. **(B)** Some tdTomato-positive endothelial cells in the metaphyseal vasculature express VEGF. GP: growth plate. META: metaphysis. **(C, D)** μCT analysis of mineralized bone formed in the hole region (C) and wounded BM (D) from mice at PSD7. N=5-6. Scale bar: 100μm (A, C); 50μm (B).

Figure 13

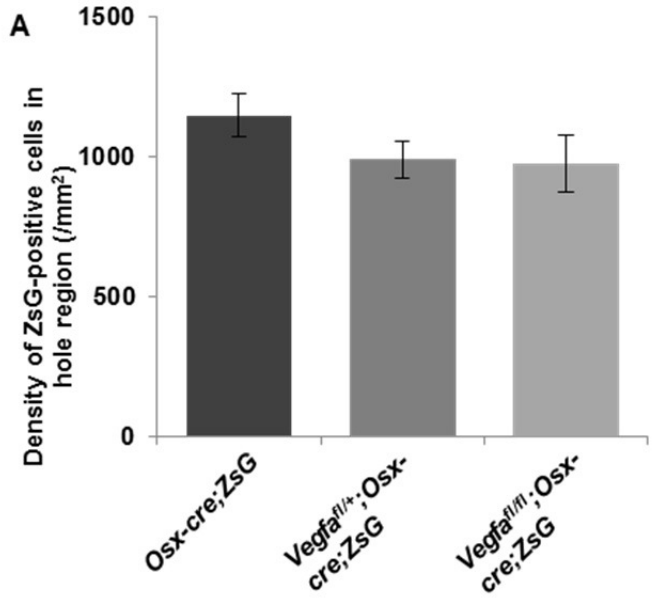

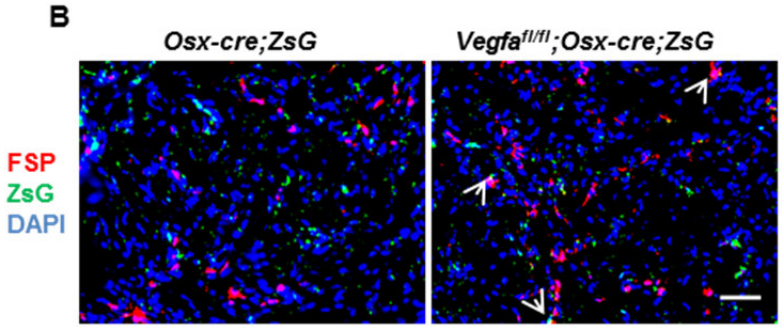

Fibroblast density in hole region /mm²	189±34	392±37*
FSP expressing ZsG+ cells/ total ZsG+ cells (%)	4.8±1.8	18.3±3*

Figure 13 (continued)

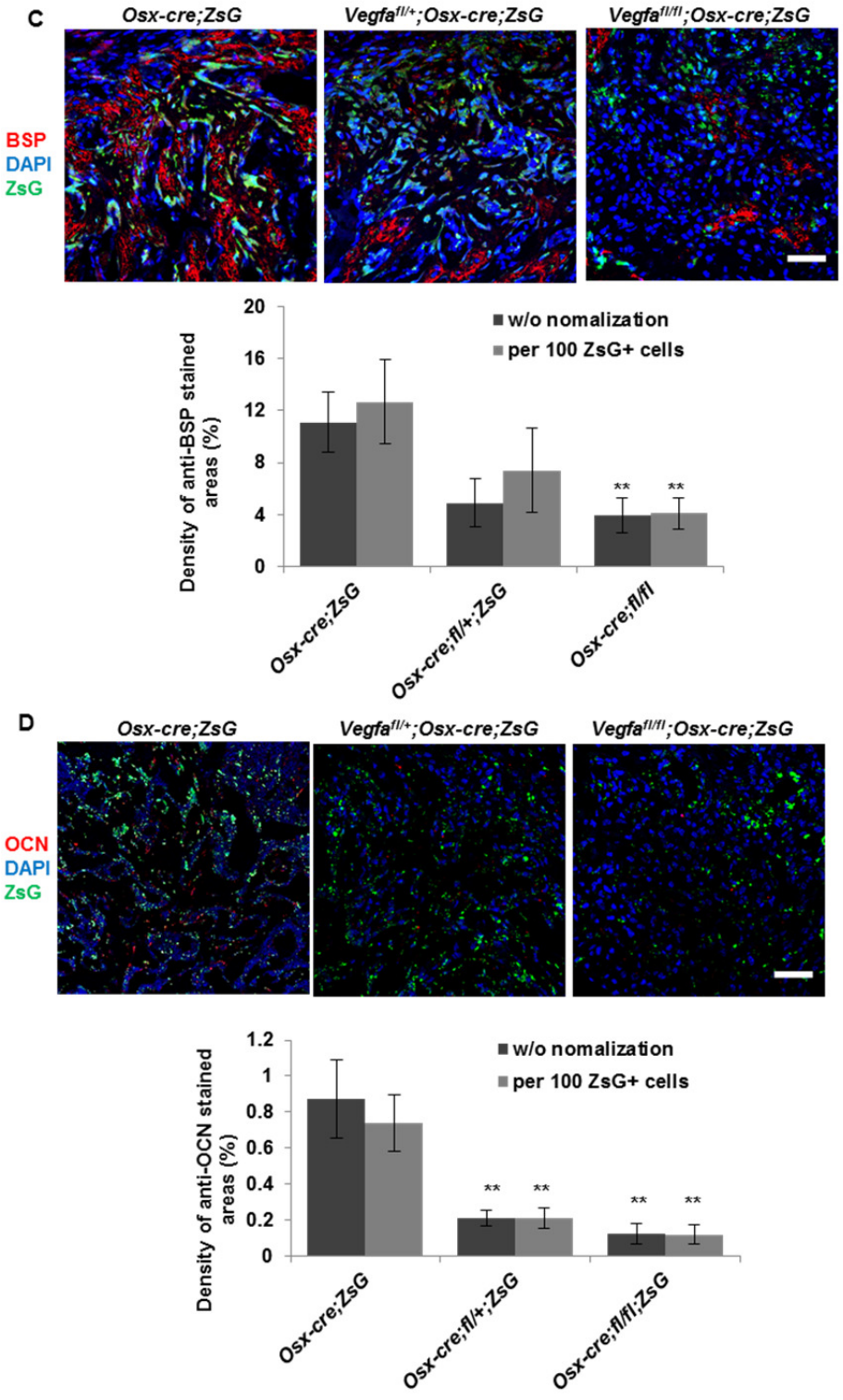

Figure 13 (continued)

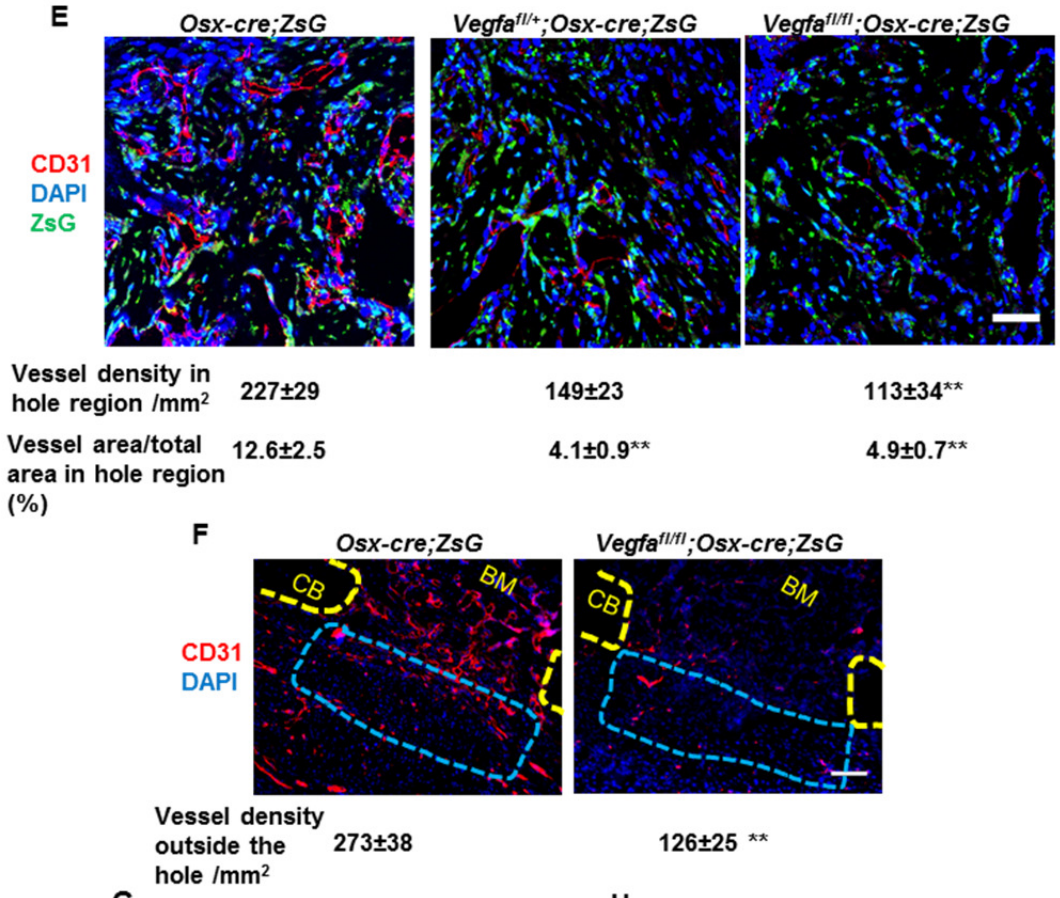

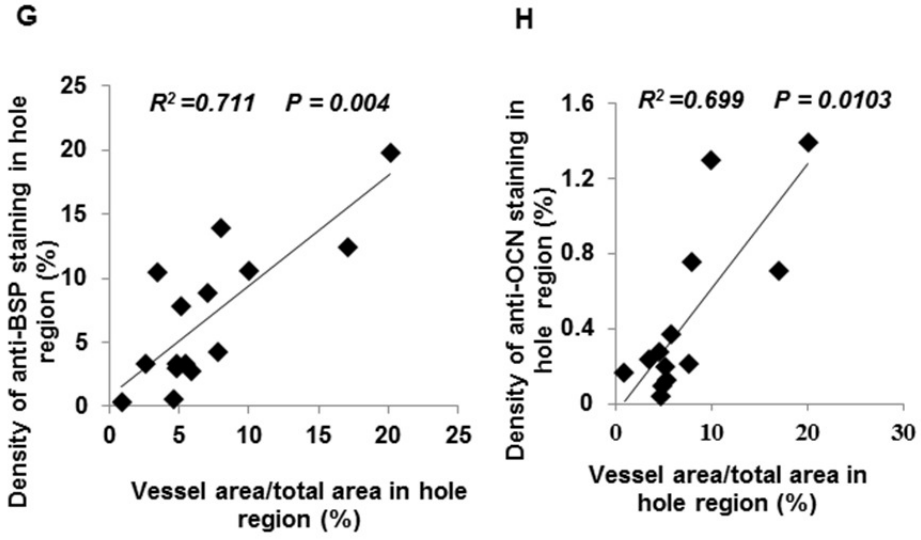

Figure 13 (continued)

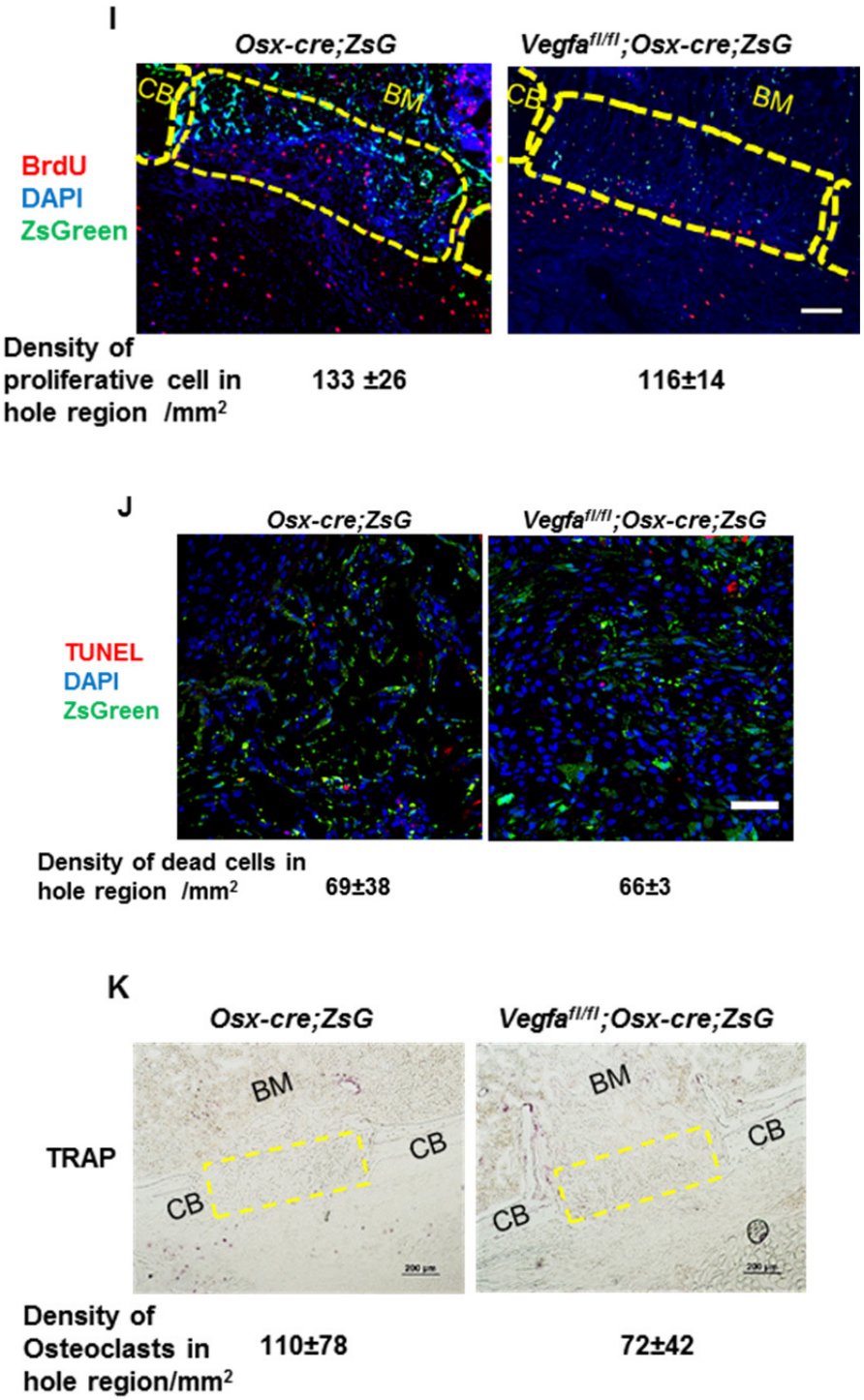

Figure 13 (continued). **Reduced angiogenesis and osteoblast differentiation in *Vegfa$^{fl/fl}$;Osx-cre; ZsG* mice at PSD7. (A)** Density of ZsG-positive cells in the hole region was of no difference between genotypes. **(B)** Low density of FSP-positive fibroblasts and low percent of FSP expressing ZsG+ osteolineage cells in hole region hole region of *Vegfa$^{fl/fl}$* mice compared with *Vegfa$^{fl/fl}$;Osx-cre* mice. Yellow cells, denoted by white arrow, represent fibroblasts differentiated from osteolineage cells. **(C, D)** Low Density of anti-BSP (C) or anti-OCN (D) stained area with or without normalized by total number of ZsG+ cells, in hole region of *Vegfa$^{fl/fl}$;Osx-cre;ZsG* mice compared with *Osx-cre;ZsG* mice. **(E)** Low density of blood vessels (113±34 /mm^2) and low percentage of vessel area (4.9±0.7%) in hole region of *Vegfa$^{fl/fl}$;Osx-cre;ZsG* compared with *Osx-cre;ZsG* mice (227±29/mm^2 and 126±25%). **(F)** Low Density of blood vessels in the hole region and adjacent area outside the hole of *Vegfa$^{fl/fl}$;Osx-cre;ZsG* compared with *Osx-cre;ZsG* mice. CB: cortical bone. **(G, H)** Strong correlation between blood vessel area and density of BSP (G) or OCN (H) staining in hole region. **(I, J)** Density of cells incorporating BrdU (I) and TUNEL-positive dead cells (J) in hole region was of no significance between *Vegfa$^{fl/fl}$;Osx-cre;ZsG* and *Osx-cre;ZsG*. **(K)** Low density of TRAP-positive osteoclasts observed in hole region of both *Vegfa$^{fl/fl}$;Osx-cre;ZsG* and *Osx-cre;ZsG* with no significant difference. Scale bar: 50 μm (B-E, J). 100μm (F, I), 200μm (K). N=4-6 (A-D, G, I, J). N=3-4 (K). *, *P<0.01,* **, *P<0.05. vs. Osx-cre;ZsG.*

High dosage fails but low dosage of recombinant VEGF enhances intramembranous bone formation in defects of *Vegfa$^{fl/fl}$;Osx-cre;ZsG* mice

To determine whether local delivery of recombinant VEGF in a tissue-engineered scaffold at the bone defect site could be used to stimulate the repair process, we first performed preliminary studies to examine the effects of inserting the scaffold, a collagen sponge, in the cortical bone defect. Maximal induction of mineralized bone formation was observed at PSD10 when most of the sponge was absorbed (data not shown). Therefore, PSD10 was chosen as the optimal time point for testing the effects of delivering exogenous VEGF in a collagen sponge on the repair process. In *Vegfa$^{fl/fl}$;Osx-cre;ZsG* mice, delivering 1μg VEGF failed but delivering 0.1μg VEGF enhanced the formation of mineralized bone in the injury compared with the control (PBS) group. However, the volume of newly formed bone in all groups of *Vegfa$^{fl/fl}$;Osx-cre;ZsG* mice was still below that of *Osx-cre;ZsG* control mice. In *Osx-cre;ZsG* mice, delivery of 0.1μg VEGF failed to improve bone repair in the defects compared with PBS controls (Figure 14A-C). These data indicate that local delivery of optimal amounts of VEGF enhances bone repair when VEGF levels are low at the repair site, but that VEGF in excess does not promote bone formation. In defects of *Vegfa$^{fl/fl}$;Osx-cre;ZsG* mice, delivery of 0.1μg VEGF enhanced collagen accumulation and BSP production (Figure 14D, E). However, the mineralization/collagen ratio and the total number of ZsG-positive bone forming cells did not change (Figure 14D, F), indicating that although 0.1μg VEGF restored induction of osteoid formation, it did not affect the delayed mineralization in *Vegfa$^{fl/fl}$;Osx-cre;ZsG* mice. The number of blood vessels in the hole region and the adjacent area outside the hole were increased in the 0.1μg VEGF treatment group of *Vegfa$^{fl/fl}$;Osx-cre;ZsG* mice,

but the vessel parameters were still lower than in *Osx-cre;ZsG* mice (Figure 15A). This suggests that a bolus delivery of VEGF may not satisfy the demand for VEGF during the entire repair process, since the exogenous VEGF would likely be metabolized in a relatively short period of time. Both 0.1μg and 1μg VEGF treatments increased the number of osteoclasts number in the hole defect region of *Vegfa*$^{fl/fl}$*;Osx-cre;ZsG* mice, but the number of osteoclasts was still much lower than in defects of *Osx-cre;ZsG* mice (Figure 15B). These results indicate that although VEGF is important for osteoclastogenesis, recruitment of osteoclasts does not appear to be a major factor in bone repair at this time point.

High dosage of VEGF inhibits intramembranous bone formation during cortical defect repair in wild type mice

Since delivery of a high dose (1μg) of VEGF failed to rescue compromised bone repair in *Vegfa*$^{fl/fl}$*;Osx-cre;ZsG* mice, we next studied effects of high dosage VEGF in *Osx-cre;ZsG* control mice. Less mineralized bone in the hole region of *Osx-cre;ZsG* mice was observed in the 1μg VEGF treatment group than in the PBS group at PSD7 (Figure 16A). Collagen accumulation, BSP levels and the number of blood vessels, were also reduced by VEGF treatment compared with PBS, but mineralization/collagen ratio was not altered (Figure 16B-D). A bolus of 1μg VEGF decreased the number of ZsG-positive osteoblastic cells in the injury hole, but this reduction was proportional to the decrease in the total number of cells (Figure 16E). Few osteoclasts were observed in both groups (Figure 16G), indicating that decreased bone formation in defects of mice treated with a high dose of locally delivered was not due to an increased number of osteoclasts.

Figure 14

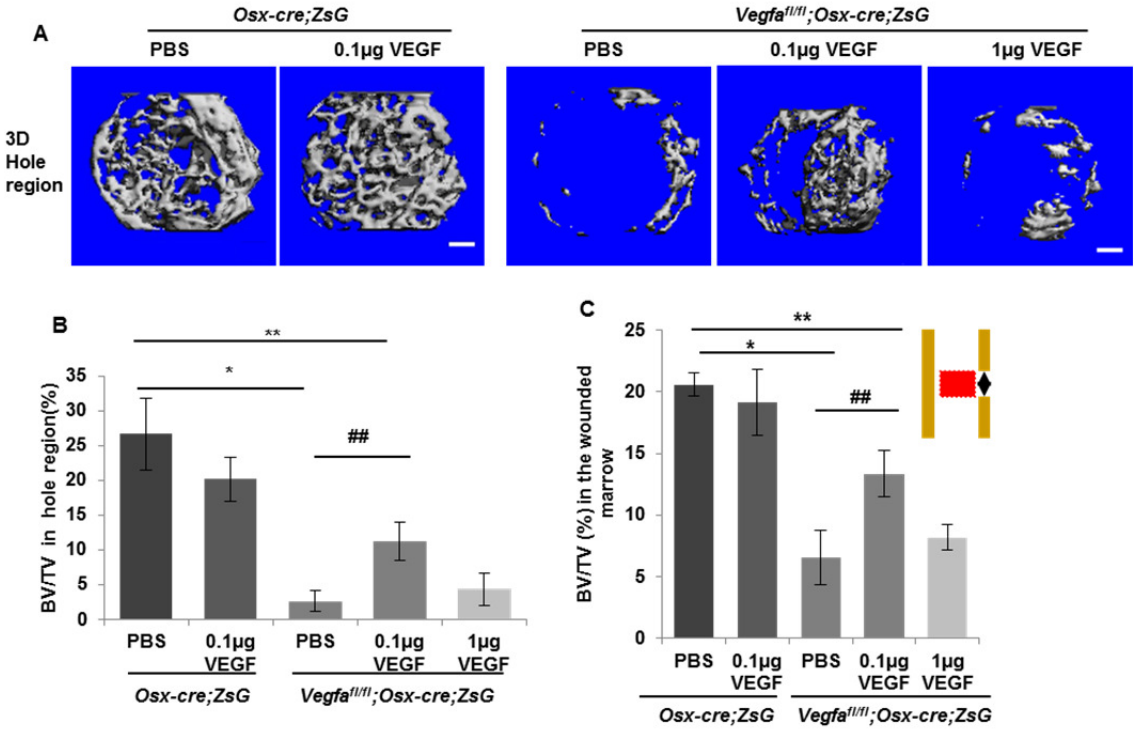
A
Osx-cre;ZsG
PBS
0.1μg VEGF
Vegfa fl/fl ;Osx-cre;ZsG
PBS
0.1μg VEGF
1μg VEGF
3D Hole region
B
BV/TV in hole region(%)
**
*
##
PBS
0.1μg VEGF
PBS
0.1μg VEGF
1μg VEGF
Osx-cre;ZsG
Vegfa fl/fl ;Osx-cre;ZsG
C
BV/TV (%) in the wounded marrow
**
*
##
PBS
0.1μg VEGF
PBS
0.1μg VEGF
1μg VEGF
Osx-cre;ZsG
Vegfa fl/fl ;Osx-cre;ZsG

Figure 14 (continued)

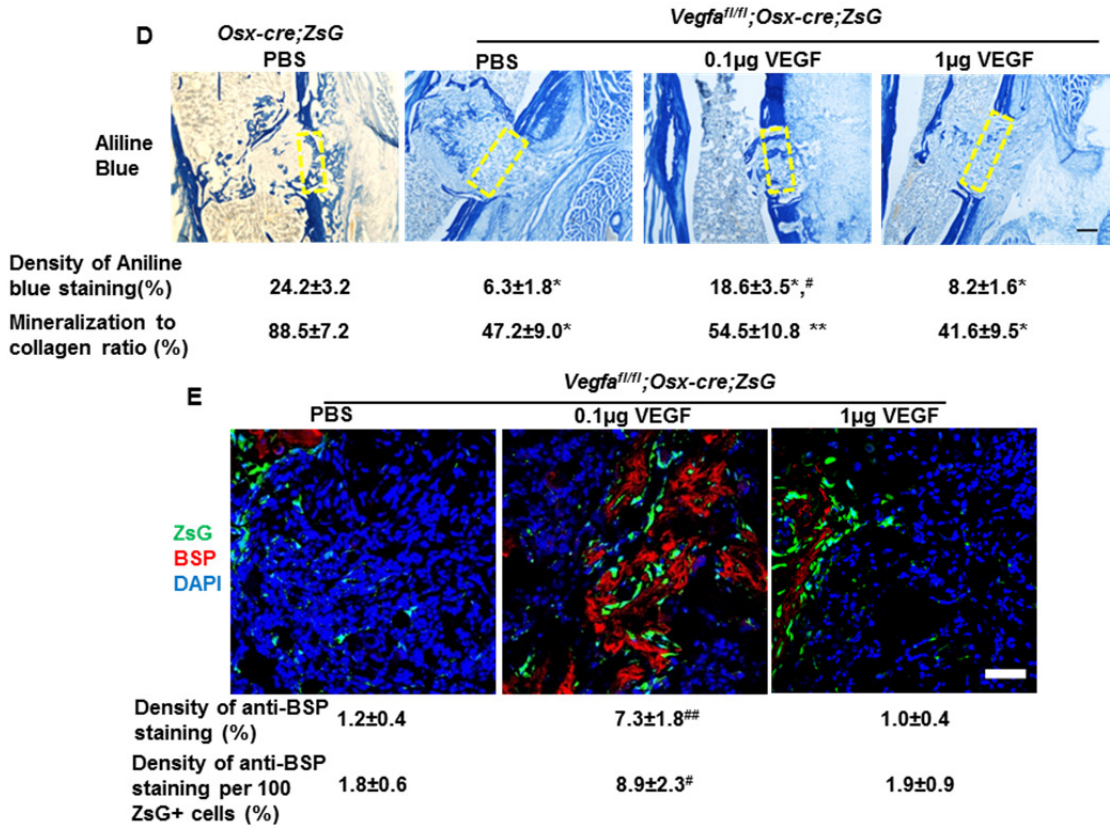

Figure 14 (continued). **1µg recombinant VEGF fails but 0.1µg VEGF enhances intramembranous bone formation in cortical defects of *Vegfa$^{fl/fl}$;Osx-cre;ZsG* mice at PSD10. (A)** 3D-reconstruction of mineralized bone formed in hole region of *Osx-cre;ZsG* mice treated with PBS or 0.1µg VEGF as well as *Vegfa$^{fl/fl}$;Osx-cre;ZsG* mice treated with PBS, 0.1 or 1µg VEGF. **(B, C)** BV/TV, based on µCT, of the mineralized bone formed in hole region (B) and wounded bone marrow (C). Red area: wounded bone marrow. **(D)** Aniline blue staining showing that 0.1µg VEGF increases the density of aniline blue staining in hole region of *Vegfa$^{fl/fl}$;Osx-cre;ZsG* mice, but fails to enhance the mineralization to collagen ratio. Yellow stippled rectangle: hole region. **(E)** 0.1µg VEGF enhanced the density of anti-BSP staining with or without normalization to total number of ZsG-positive cells in hole region of *Vegfa$^{fl/fl}$;Osx-cre;ZsG* mice. **(F)** The density of ZsG-positive cells and total cell number in hole region of *Vegfa$^{fl/fl}$;Osx-cre;ZsG* (CKO) mice were not significantly altered by VEGF treatment. Scale bars: 100µm (A), 200 µm (D), 50 µm (E). N=5-6. *, $^{\#}$, *P<0.01*; **, $^{\#\#}$, *P<0.05*. *,* *vs. Osx-cre;ZsG+PBS.* $^{\#, \#\#}$ *vs. Vegfa$^{fl/fl}$;Osx-cre;ZsG +PBS.*

Figure 15

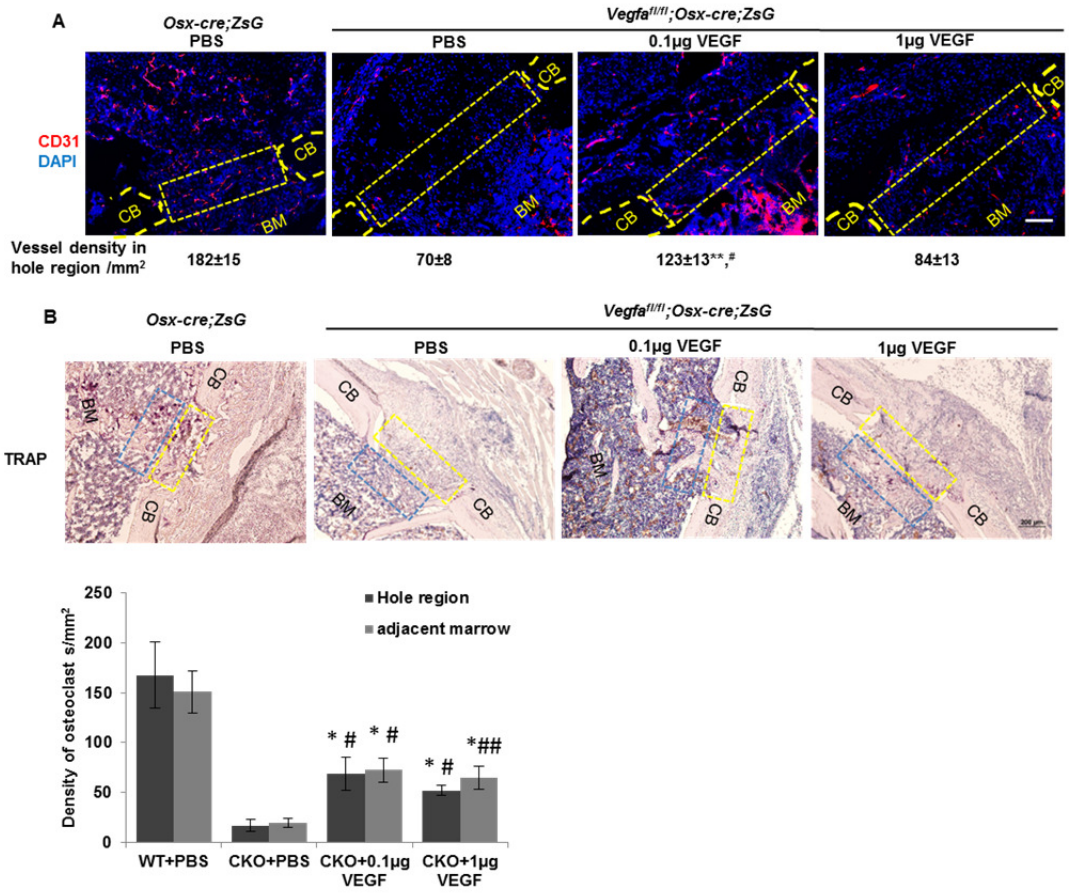
A
Osx-cre;ZsG
PBS
Vegfa fl/fl ;Osx-cre;ZsG
PBS
0.1μg VEGF
1μg VEGF
CD31
DAPI
CB
BM
Vessel density in hole region /mm2
182±15
70±8
123±13**,#
84±13
B
Osx-cre;ZsG
PBS
Vegfa fl/fl ;Osx-cre;ZsG
PBS
0.1μg VEGF
1μg VEGF
TRAP
Density of osteoclast s/mm2
Hole region
adjacent marrow
WT+PBS
CKO+PBS
CKO+0.1μg VEGF
CKO+1μg VEGF

Figure 15 (continued). **Blood vessel formation and osteoclast recruitments in defects of *Vegfa$^{fl/fl}$;Osx-cre;ZsG* mice at PSD10**. **(A)** Enhanced density (123 ± 13/mm^2) of blood vessels (based on anti-CD31 staining) in hone region of *Vegfa$^{fl/fl}$;Osx-cre;ZsG* mice treated with 0.1μg VEGF compared with PBS (70 ± 8/mm^2) or 1μg VEGF (84 ± 13/mm^2). **(B)** Density of TRAP-positive osteoclasts in hole region and adjacent area in injured BM. Scale bars: 100μm (A), 200μm (B). N=5-6. Yellow stippled rectangles: hole region (A, B); blue stippled rectangles: adjacent bone marrow regions (B). CB: cortical bone. WT: *Osx-cre;ZsG* mice. CKO*: Vegfa$^{fl/fl}$;Osx-cre* mice. *, $^{\#}$, *P<0.01*; **, $^{\#\#}$, *P<0.05*. * *vs. Osx-cre;ZsG+PBS.* $^{\#}$ vs. *Vegfa$^{fl/fl}$;Osx-cre;ZsG+PBS.*

Figure 16

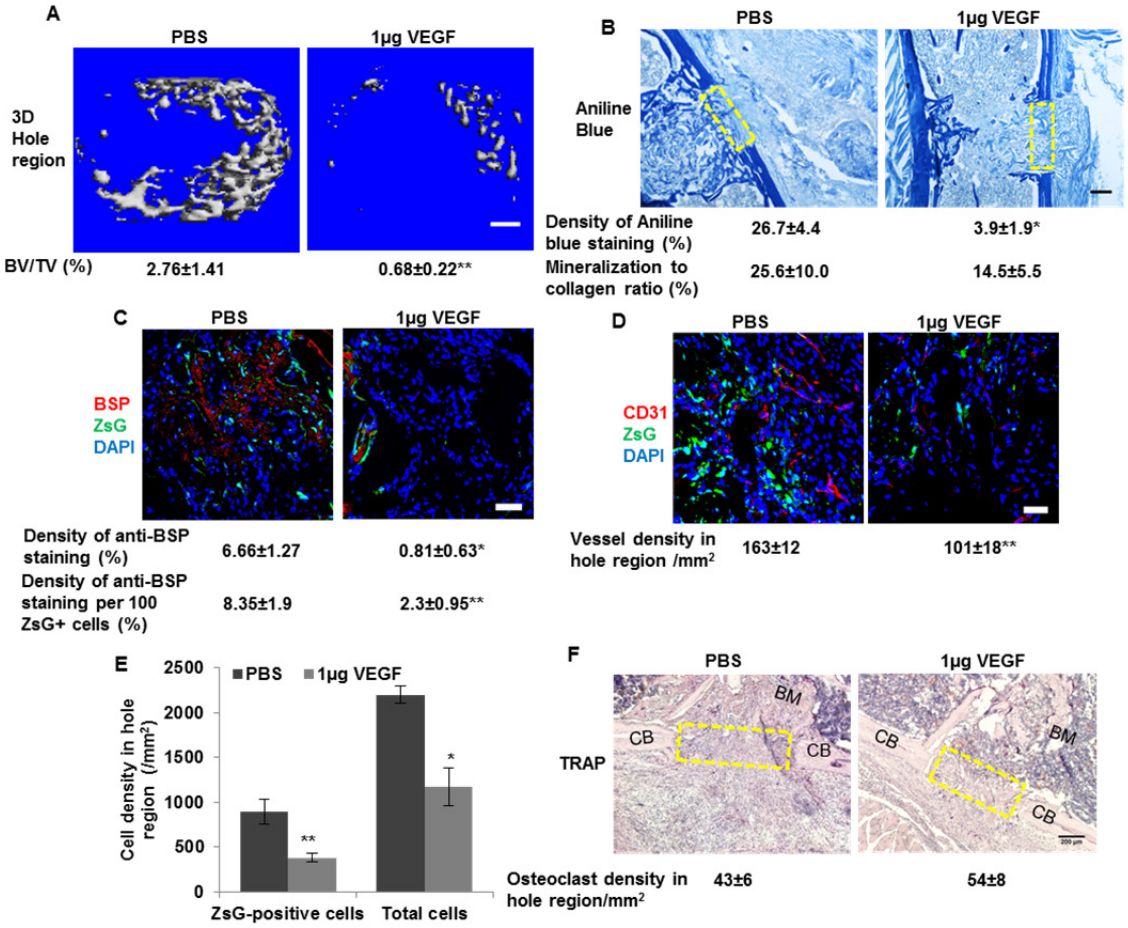
A
PBS
1μg VEGF
3D Hole region
BV/TV (%)
2.76±1.41
0.68±0.22**
B
PBS
1μg VEGF
Aniline Blue
Density of Aniline blue staining (%)
26.7±4.4
3.9±1.9*
Mineralization to collagen ratio (%)
25.6±10.0
14.5±5.5
C
PBS
1μg VEGF
BSP
ZsG
DAPI
Density of anti-BSP staining (%)
6.66±1.27
0.81±0.63*
Density of anti-BSP staining per 100 ZsG+ cells (%)
8.35±1.9
2.3±0.95**
D
PBS
1μg VEGF
CD31
ZsG
DAPI
Vessel density in hole region /mm²
163±12
101±18**
E
PBS
1μg VEGF
Cell density in hole region (/mm²)
2500
2000
1500
1000
500
0
**
*
ZsG-positive cells
Total cells
F
PBS
1μg VEGF
TRAP
BM
CB
CB
CB
BM
CB
Osteoclast density in hole region/mm²
43±6
54±8

Figure 16 (continued). **High-dose VEGF inhibits mineralized bone formation in defects of *Osx-cre;ZsG* mice at PSD7. (A)** Less mineralized bone formed in hole region in *Osx-cre;ZsG* mice treated with 1μg VEGF (0.68 ± 0.22 % in BV/TV) compared with PBS (2.76 ± 1.41%) by μCT. **(B)** Aniline blue staining shows that 1μg VEGF inhibits density of aniline blue staining in hole region of *Osx-cre;ZsG* mice compared with PBS, but does not alter mineralization to collagen ratio. **(C)** 1μg VEGF inhibits density of anti-BSP staining with or without normalization to total number of ZsG-positive cells in hole region of *Osx-cre;ZsG* mice. **(D)** Low density (101 ± 18 /mm^2) of blood vessels (determined by anti-CD31 staining) in hole region of *Osx-cre;ZsG* mice treated with 1μg VEGF compared with PBS treatment (163 ± 12/mm^2). **(E)** Reduced density of ZsG-positive cells and total cells in hole region of *Osx-cre;ZsG* mice with VEGF treatment compared with PBS treatment. **(F)** No difference in low density of TRAP-positive osteoclasts in hole region of mice treated with VEGF or PBS. Yellow stippled rectangles: hole regions (B, F). CB: cortical bone. Scale bars: 100 μm (A, F), 200μm (B), 50 μm (C, D). N=4-5. *, $P<0.01$; **, $P<0.05$.

Postnatal deletion of *Vegfa* in osteolinage cells causes delayed bone repair mediated by intramembranous ossification

It can be argued that the compromised bone repair in *Vegfa* CKO mice might not be a direct consequence of disrupted VEGF production by osterix-expressing cells, but instead the result of VEGF-dependent changes in osteolineage cells during development that are carried over into the postnatal period in mice. To address this possibility and allow assessment of bone repair when VEGF expression is disrupted in the osteoblastic lineage postnatally, doxycycline was administrated to a group of pregnant mothers and their offspring to block *Osx-Cre* expression (see Methods). Doxycycline was then withdrawn to let Cre recombinase become active in Osx-positive cells. Without doxycycline treatment, *Vegfa$^{fl/fl}$;Osx-cre* mice showed a decrease in body weight and body size compared with *Vegfa$^{fl/fl}$* mice; however, this difference was abolished in 8-week old mice continuously treated with doxycycline (Figure 17A). In addition, the absence of ZsG signal in hind limbs of *Vegfa$^{fl/fl}$;Osx-cre;ZsG* mice given doxycycline validated the efficient inhibition of Cre expression, while strong ZsG signals in bones of 8-week old *Osx-cre;Vegfa$^{fl/fl}$;ZsG* mice with doxycycline withdrawn at 4-weeks demonstrated that Cre recombinase was successfully induced in the absence of doxycycline (Figure 17B). In 9-week old mice with doxycycline withdrawn at 4 weeks, body weight was not significantly different between *Vegfa CKO* and *Vegfa$^{fl/fl}$ mice,* and no reduction of newly formed mineralized bone in the injury region was observed in *Vegfa CKO* mice at PSD7 compared with controls (Figure 18A-D). In mice of the same age and similar body weight, but with doxycycline withdrawn one week after birth, the volume of newly formed mineralized bone in the hole region was decreased in

Vegfa$^{fl/fl}$*;Osx-cre* mice compared with controls (Figure 17C). Trabecular number was decreased while trabecular separation was increased (Figure 17C). Collagen accumulation as well as mineralization/collagen ratio were also decreased (Figure 17D). These data are almost identical to the findings based on the use of mice that had not been treated with doxycycline during development.

Figure 17

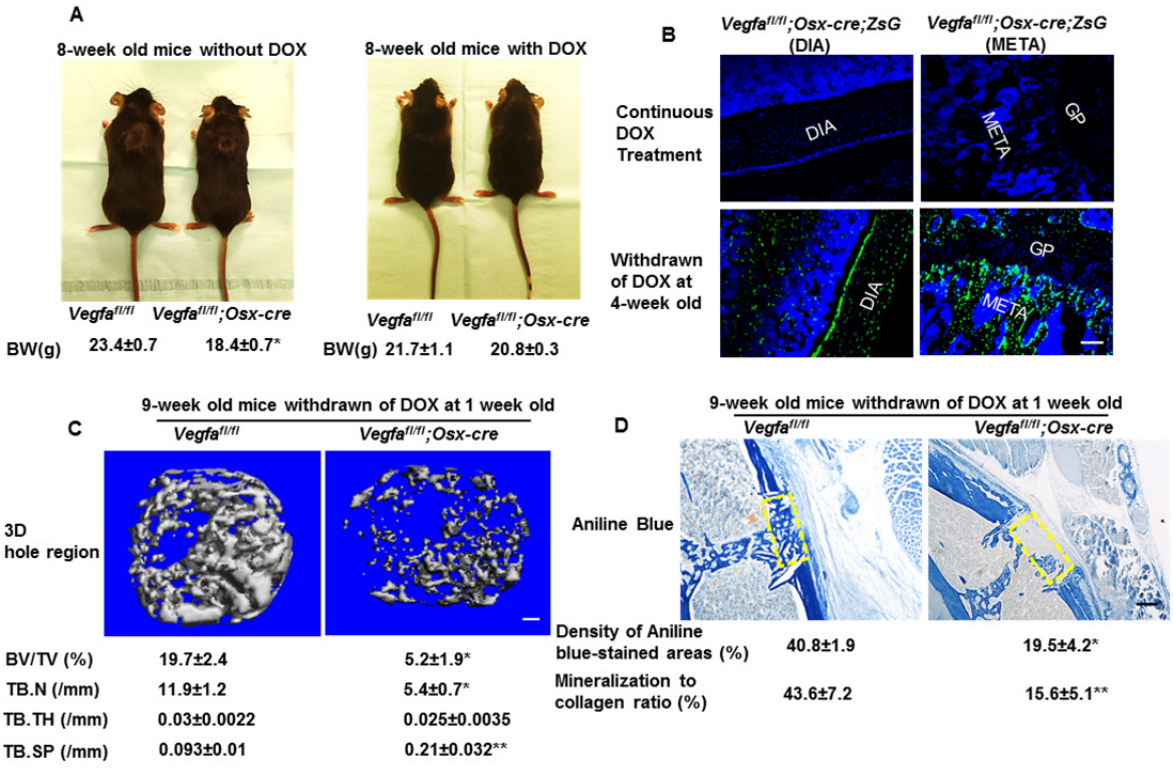

Figure 17 (continued). **Delayed intramembranous bone formation in cortical defects when *Vegfa* is deleted in osteolineage cells postnatally. (A)** Reduced body size and weight in 8-week old *Vegfa*$^{fl/fl}$*;Osx-cre* mice compared with *Vegfa*$^{fl/fl}$ mice without doxycycline (DOX) treatment (N=8-10); this reduction was eliminated in DOX-treated mice (N=4-6). **(B)** Absence of Cre-activated ZsG in diaphysis (DIA) and metaphysis (META) of 8-week old *Vegfa*$^{fl/fl}$*;Osx-cre;ZsG* mice continuously fed with DOX; ZsG induced in mice with DOX withdrawn at 4 weeks. GP: growth plate. **(C)** μCT analysis of mineralized bone formed in hole region of 9-week old mice with DOX withdrawn at one week shows reduced bone volume and trabecular thickness, increased trabecular separation in hole region of *Vegfa*$^{fl/fl}$*;Osx-cre* compared with of *Vegfa*$^{fl/fl}$ mice. **(D)** Reduced density of aniline blue staining (19.5 ± 4.2%) and decreased mineralization to collagen ratio (15.6 ± 5.1%) in hole region of 9-week old *Vegfa*$^{fl/fl}$*;Osx-cre* mice with DOX withdrawn at one week, compared with of *Vegfa*$^{fl/fl}$ mice (40.8 ± 1.9 and 43.6 ± 7.2%). Yellow stippled rectangle: hole region (D). Scale bars: 100μm (B, C), 200μm (D). N=6-10 (C-D). *, $P<0.01$; **, $P<0.05$.

Figure 18

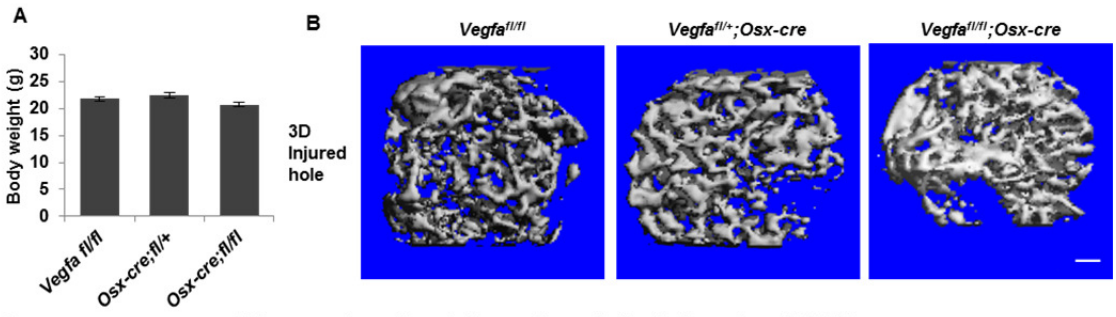

C **µCT parameters of newly formed bone in the hole region at PSD7**

	Vegfa$^{fl/fl}$	*Vegfa*$^{fl/+}$*;Osx-cre*	*Vegfa*$^{fl/fl}$*;Osx-cre*
BV (mm^3)	0.023±0.0084	0.024±0.0026	0.018±0.005
BV/TV (%)	19.21±7.33	19.32±2.13	17.06±4.81
TB.N (/mm)	10.41±3.21	13.21±1.55	12.12±2.28
TB.TH (mm)	0.028±0.0034	0.027±0.001	0.025±0.001
TB.SP (mm)	0.19±0.08	0.084±0.015	0.105±0.027

D **µCT parameters of newly formed bone in marrow space at PSD7**

	Vegfa$^{fl/fl}$	*Vegfa*$^{fl/+}$*;Osx-cre*	*Vegfa*$^{fl/fl}$*;Osx-cre*
BV (mm^3)	0.093±0.012	0.13±0.015**	0.13±0.006**
BV/TV (%)	25.25±3.06	30.04±1.81	29.21±1.22
TB.N (/mm)	9.85±2.44	13.66±1.81	12.38±1.6
TB.TH (mm)	0.033±0.0007	0.034±0.0006	0.035±0.0011
TB.SP (mm)	0.13±0.027	0.079±0.016	0.087±0.015

Figure 18. **Bone repair is not changed in defects of 9 weeks old *Vegfa*$^{fl/fl}$*;Osx-cre* withdrawn of doxycycline at 4 weeks old. (A)** Body weight between 9 weeks old *Vegfa*$^{fl/fl}$ and *Vegfa*$^{fl/fl}$*;Osx-cre* withdrawn of DOX at 4 weeks old. N=5-7. **(B)** 3D reconstruction of mineralized bone formed in hole region by µCT. Scale bar: 100µm. **(C, D)** µCT analysis of the mineralized bone formed in the hole region (C) and injured bone marrow (D). N=5-7. **, $P<0.05$. *vs. Vegfa*$^{fl/fl}$

Targeting *Vegfa* expression in osteoblasts and hypertrophic chondrocytes impairs cartilage turnover in periosteal callus

Endochondral bone formation was observed in the injured periosteum (PO), particularly distal to the injury hole in the tibial defect. Safranin O staining in the PO about 2 mm distal to the hole was selected for quantitative assessments of the cartilage. At PSD7, the relative amount of cartilage in *Vegfa* CKO mice was similar to that of controls. At PSD10, control mice showed decreased amounts of cartilage while *Vegfa* CKO mice showed an increase. At PSD14, there was almost no cartilage left in controls while a substantial amount of cartilage remained in the *Vegfa* CKO mice (Figure 19A, B). These data indicate a delay of cartilage removal in PO of *Vegfa* CKO mice. In addition, the higher percentage of cartilage in *Vegfa CKO* mice also suggests that cartilage formation in the injured periosteum is enhanced when VEGF levels are reduced. Compared with $Vegfa^{fl/fl}$ mice, the number of blood vessels and osteoclasts were significantly reduced in the injured periosteum of *Vegfa* CKO mice at PSD10 (Figure 19C, D), suggesting a delay in blood vessel invasion and osteoclast/chondroclast recruitment. Although the thickness of the periosteal callus was almost the same in *Vegfa* CKO and $Vegfa^{fl/fl}$ mice at PSD14, the immature bony tissue in the PO of *Vegfa* CKO mice as compared with the mature woven bone in $Vegfa^{fl/fl}$ mice (Figure 20A), further suggests delayed endochondral bone formation. *Osx-cre;*$Vegfa^{fl/fl}$*;ZsG* mice also showed increased amounts of safranin O-positive cartilage and increased numbers of Sox9-positive chondrocytes in the PO compared with *Osx-Cre;ZsG* mice at PSD10, which is consistent with the possibility that VEGF acts as an inhibitor of chondrogenesis during the repair process (Figure 20B, C). Only few cells co-expressing ZsG and Sox9 were

observed, indicating that increased numbers of chondrocytes in *Osx-cre;Vegfa$^{fl/fl}$;ZsG* mice are not due to trans-differentiation from osteoblastic lineage cells (Figure 20C). Since BMP2 is important for periosteal cartilage formation in cortical defect healing and fracture repair (Minear et al., 2010b; Tsuji et al., 2006), we stained for BMP2 and found reduced levels of staining in *Vegfa$^{fl/fl}$;Osx-cre;ZsG* compared with *Osx-cre;ZsG* mice (Figure 20D). Thus, increased amounts of cartilage in the defect of *Vegfa* CKO mice are unlikely to be a consequence of increased BMP2 levels.

Figure 19

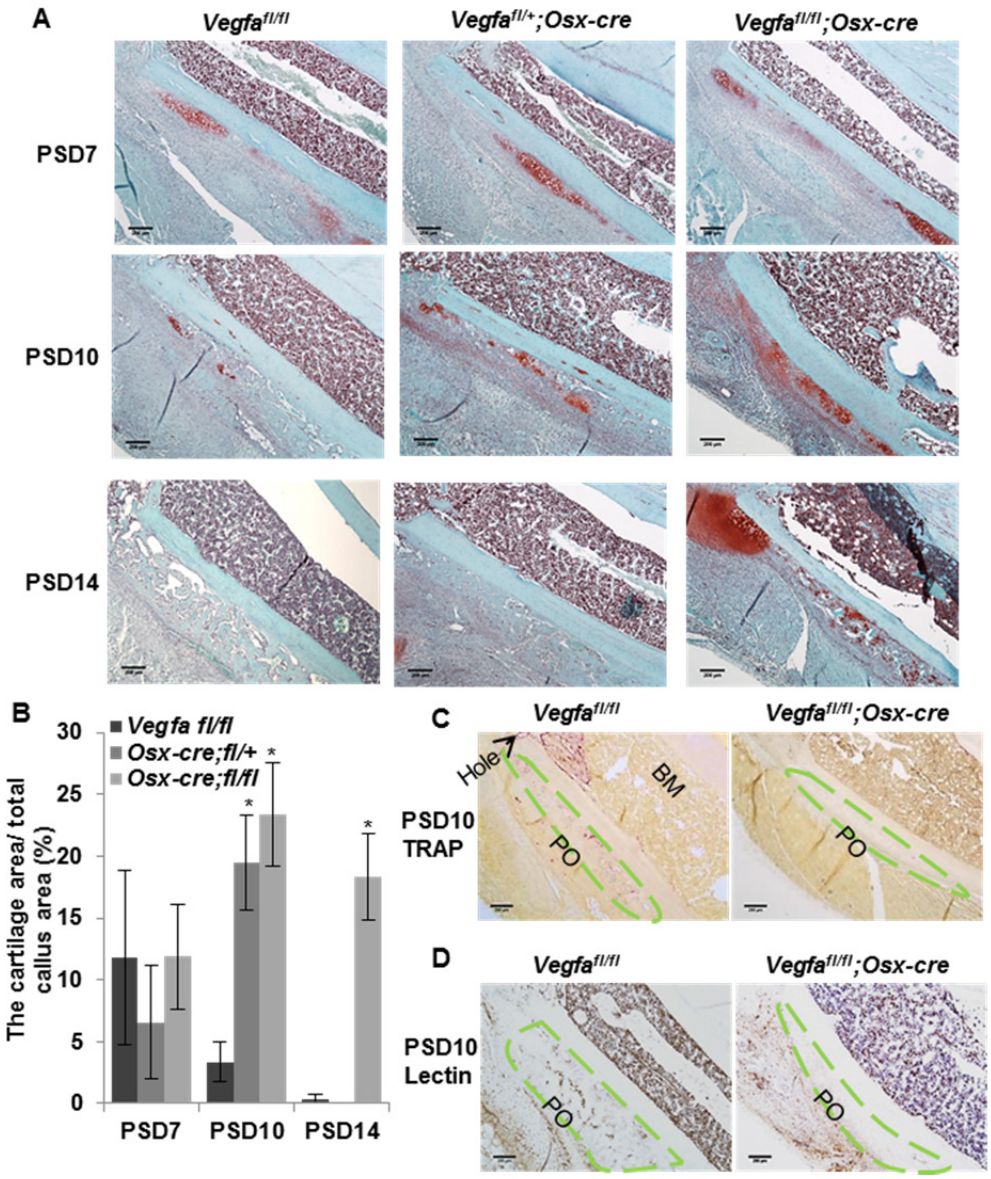
A
Vegfa fl/fl
Vegfa fl/+;Osx-cre
Vegfa fl/fl;Osx-cre
PSD7
PSD10
PSD14
B
Vegfa fl/fl
Osx-cre;fl/+
Osx-cre;fl/fl
The cartilage area/ total callus area (%)
30
25
20
15
10
5
0
PSD7
PSD10
PSD14
C
Vegfa fl/fl
Vegfa fl/fl;Osx-cre
PSD10 TRAP
Hole
BM
PO
PO
D
Vegfa fl/fl
Vegfa fl/fl;Osx-cre
PSD10 Lectin
PO
PO

Figure 19 (continued). **Deletion of *Vegfa* in osteoblasts and hypertrophic chondrocytes impairs cartilage resorption in injured periosteum**. **(A, B)** Safranin O- staining on sections from *Vegfa*$^{fl/fl}$, *Vegfa*$^{fl/+}$*;Osx-cre* and *Vegfa*$^{fl/fl}$*;Osx-cre* mice at PSD 7, 10 and 14 to show periosteal cartilage (A), and percent of cartilage in periosteum about 2mm distal to the injured hole was calculated (B). In *Vegfa*$^{fl/fl}$ mice, periosteal cartilage was gradually resorbed from PSD7 to PSD10, however, this resorption was delayed and cartilage formation was even promoted in periosteum of *Vegfa*$^{fl/fl}$*;Osx-cre* mice. N=4-8. **(C, D)** TRAP-positive osteoclasts/chondroclasts and lectin-positive vascular endothelial cells was greatly decreased in periosteum (PO) of *Vegfa*$^{fl/fl}$*;Osx-cre* mice compared with *Vegfa*$^{fl/fl}$ mice. Green frame shows the injured periosteum. N=3-4. Scale bar: 200μm (A, C, D). *, $P<0.01$; *vs. Vegfa*$^{fl/fl}$.

Figure 20

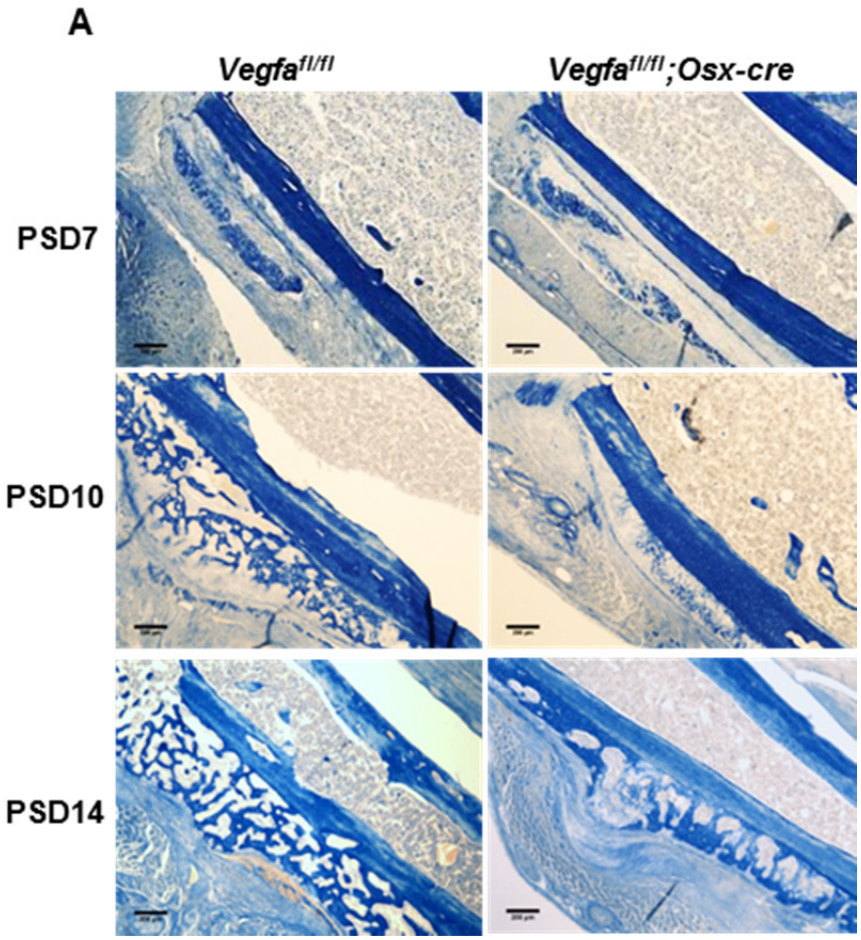

Figure 20 (continued)

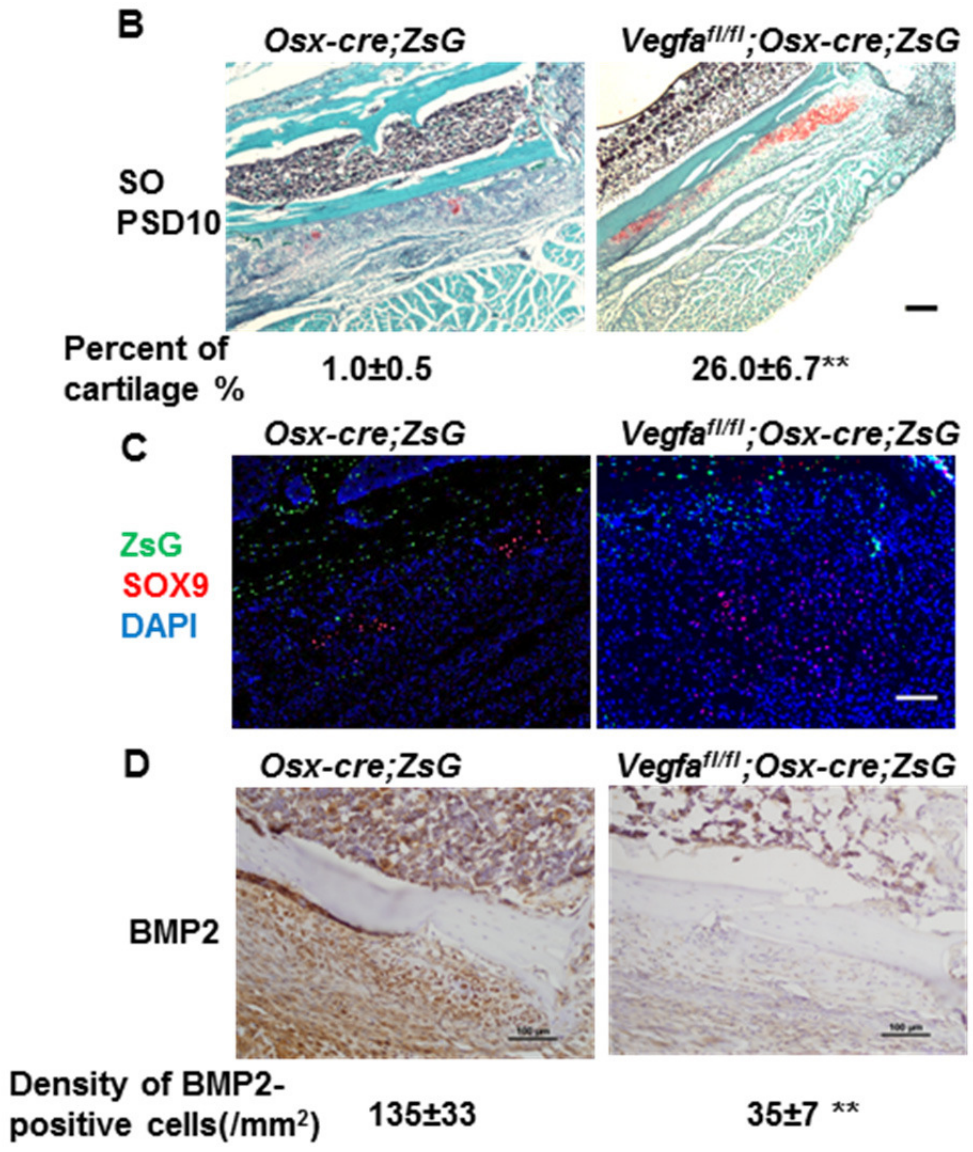

Figure 20 (continued). **Delayed replacement of cartilaginous callus by bony callus in the wounded periosteum of *Vegfa*$^{fl/fl}$*;Osx-cre* mice. (A)** Aniline blue staining on sections from mice at PSD7, 10 and 14 to show bony callus in periosteum. N=4-8. **(B)** SO staining on sections from *Osx-cre;ZsG* and *Vegfa*$^{fl/fl}$*;Osx-cre;ZsG* mice at PSD10. Percent of cartilage out of periosteum about 2mm distal to the injured hole was calculated. Increase of cartilage percentage in *Vegfa*$^{fl/fl}$*;Osx-cre;ZsG* mice compared with *Osx-cre;ZsG* mice N=3-5. **(C, D)** More SOX9-positve chondrocytes (C, N=3-4) and decrease of BMP2-positive cells (D, N=5-6) in injured periosteum of *Vegfa*$^{fl/fl}$*;Osx-cre;ZsG* mice than in *Osx-cre;ZsG* mice. N=3-4. Scale bar: 200μm (A, B), 100μm (C, D). **, $P<0.05$.

Deletion of *Vegfa* in osteoblastic cells reduces callus remodeling

In wild type mice, woven bone formed in the periosteum was gradually resorbed and remodeled into a new layer of bone outside the original cortical bone. At the edge of the newly formed bone, a new ossification center, containing immature chondrocytes, proliferative chondrocytes, hypertrophic chondrocytes as well as bony trabeculae, was observed in periosteal callus of *Osx-cre* mice and *Vegfa*$^{fl/fl}$ *mice* at PSD28 (data not shown), reflecting a strong regenerative activity. In contrast, this process was greatly reduced in both homozygous and heterozygous *Vegfa* knockout mice (Figure 21A, B). The callus thickness (distance between the new layer of bone and the original cortical bone), normalized to the total volume of the corresponding tibial segment, together with volume at callus, also normalized to total tibial segment volume, was reduced in *Vegfa* CKO mice (Figure 21C, D). Osteoclasts were accumulated on the surface of the newly formed bony layer in *Vegfa*$^{fl/fl}$ *mice,* while only few osteoclasts were found in *Vegfa* CKO mice (Figure 21E).

Figure 21

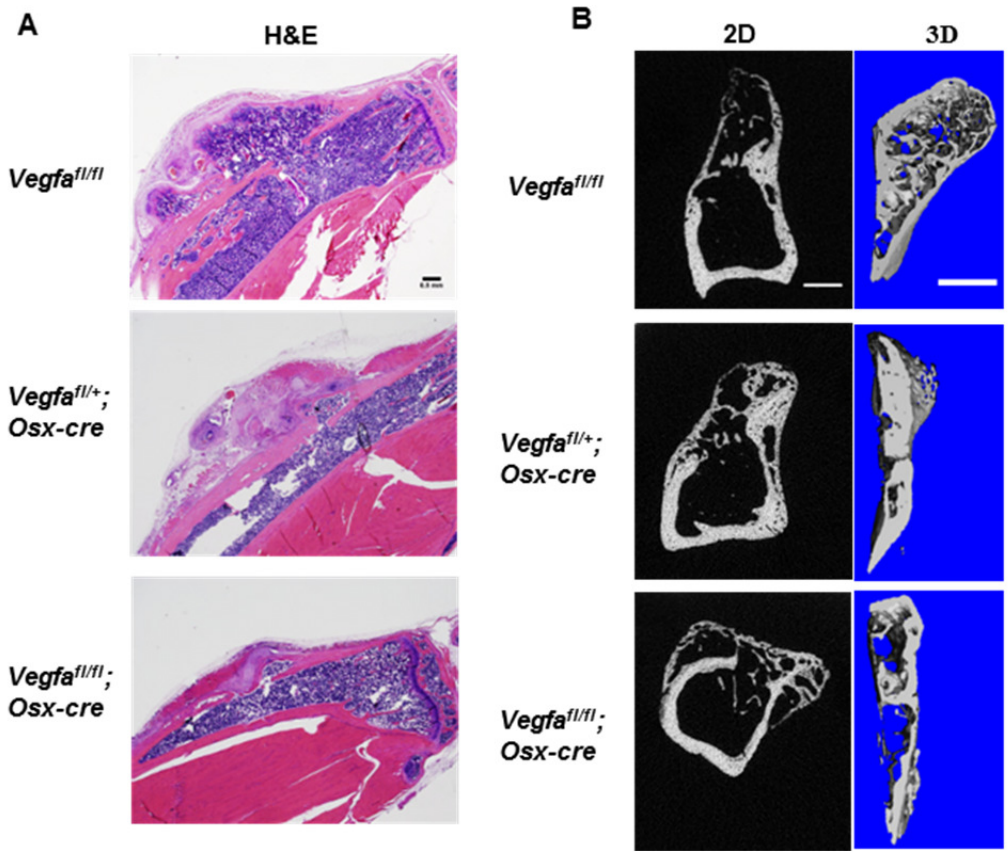
A
H&E
Vegfa fl/fl
Vegfa fl/+; Osx-cre
Vegfa fl/fl; Osx-cre
B
2D
3D
Vegfa fl/fl
Vegfa fl/+; Osx-cre
Vegfa fl/fl; Osx-cre

Figure 21 (continued)

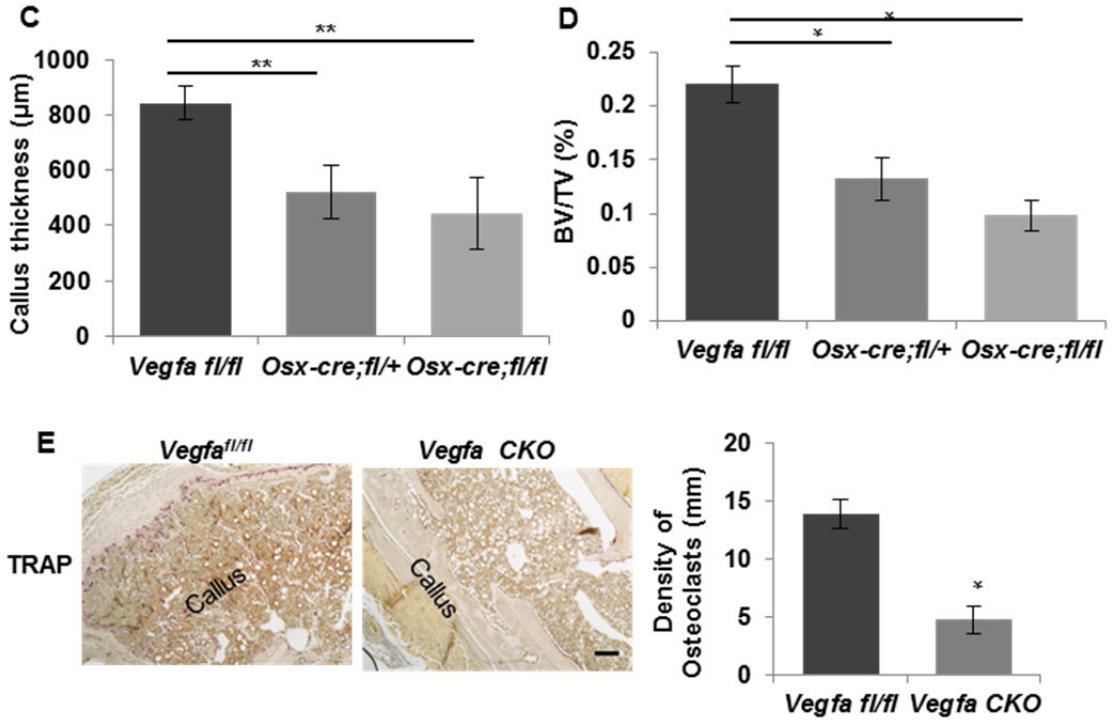

Figure 21 (continued). **Deletion of *Vegfa* in osteoblastic cells reduces callus remodeling at PSD28. (A)** H&E staining on sections from *Vegfa*$^{fl/fl}$, *Vegfa*$^{fl/+}$*;Osx-cre* and *Vegfa*$^{fl/fl}$*;Osx-cre* mice showing periosteal callus remodeling at PSD28. **(B)** Left panel showed the 2D image of sagittal sections of injured tibia. The right panel displayed 3D reconstruction of the periosteal callus. **(C)** Decreased of callus thickness, calculated as the distance from the edge of periosteal callus to the injured cortical bone normalized by the total volume of the corresponding tibial segment, in *Vegfa*$^{fl/fl}$*;Osx-cre* compared with *Vegfa*$^{fl/fl}$ mice N=5-6. **(D)** Decrease of BV/TV, calculated as total callus bone volume normalized by total volume of the corresponding tibial segment, in *Vegfa*$^{fl/fl}$*;Osx-cre* compared with *Vegfa*$^{fl/fl}$ mice N=5-6. **(E)** Low density of TRAP-osteoclasts, represented as the number of osteoclasts normalized by the total length of callus bone, in *Vegfa*$^{fl/fl}$*;Osx-cre* compared with *Vegfa*$^{fl/fl}$ mice. N=4. Scale bar: 500µm (A, B), 200µm (E). *, $P<0.01$; **, $P<0.05$.

Discussion

In the present study, we discovered that an appropriate dosage of paracrine VEGF from osteoblastic cells is critical for the angiogenesis-osteogenesis coupling during bone repair and either too little or too much VEGF may interrupt this coupling process and cause the compromised bone healing. The documented functions of osteoblast-derived VEGF in healing of small bone defects may also provide the biological basis for the application of VEGF in other bone regenerative processes.

Bone repair is initiated by the inflammatory reaction with ordered infiltration of neutrophils and then macrophages. Osteoblastic cells regulate the release of neutrophils to the circulation under the inflammatory stimuli through CXCL12-CXCR4 axis (Eash et al., 2010). Previously VEGF was reported to induce neutrophil chemotaxis and increase sinusoid permeability in the bone marrow (Ancelin et al., 2004; Lim et al., 2014), supporting our finding that osteoblast-generated VEGF facilitates entry of neutrophils into the circulation following bone injury, adding to the regulatory machineries of neutrophils by osteoblastic cells. Following neutrophil infiltration, a decrease of macrophage recruitment and blood vessel invasion was observed in defects of *Vegfa*$^{fl/fl}$*;Osx-cre* mice, but we do not know which comes first since both macrophages and endothelial cells respond to VEGF. It was reported that macrophage infiltration preceded angiogenesis in wound healing and tumor progression since deletion of macrophages led to significant reduction of angiogenesis (He and Marneros, 2013; Lin et al., 2006). Therefore, except for the direct targeting on endothelial cells, the pro-angiogenic effect of osteoblast-derived VEGF may also be mediated by macrophages

since VEGF is a chemotactic factor for macrophage/monocytes (Barleon et al., 1996; Clauss et al., 1990; Leek et al., 2000), and macrophages in the regenerative phase release angiogenic factors to initiate angiogenesis and repair described in the previous studies (Sunderkotter et al., 1991; Tonnesen et al., 2000; Wu et al., 2013).

Bone repair and regeneration was inhibited by reducing VEGF level with sFlt1 or VEGF neutralizing antibodies in previous studies (Street et al., 2002; Wang et al., 2011a), which is consistent with our data. In humans, VEGF levels are decreased in mesenchymal progenitors with age caused by osteoporosis (Efimenko et al., 2011; Pufe et al., 2003; Wilson et al., 2010). Therefore, our data gave one explanation for mechanisms of age/osteoporosis related defective bone healing and suggested VEGF supplement as a potential therapeutic strategy. However, consequences of exogenous VEGF application exhibited certain extent of variation. VEGF enhanced bone healing and regeneration in many models but also failed in certain studies using ex vivo gene therapy or recombinant VEGF (Eckardt et al., 2003; Kaipel et al., 2012; Peng et al., 2002; Schonmeyr et al., 2010). Different from large bone repair defect, only low amount VEGF was needed in the our model of small bone defect healing, where exogenous VEGF didn't help regenerate bone when VEGF level is adequate and excess VEGF even exhibits detrimental effects through binding VEGFR2 on osteoblasts and inhibiting osteoblast functions. It is also possible that excess VEGF inhibits pericyte functions through VEGFR2 mediated inhibition of PDGFR (Greenberg et al., 2008), which is important molecule for pericyte maturation, and further leads to formation of immature blood vessels. These data demonstrated the complexity of VEGF in the pathology and therapeutic strategies. When using VEGF modulation to treat bone defect repair and other

strategies for bone regeneration, the amount of VEGF should be carefully considered to avoid beyond physiological dosage.

In the rescue assay of *Vegfa*$^{fl/fl}$*;Osx-cre* mice, osteoinduction was totally rescued by low dose of VEGF, suggesting the necessary of paracrine VEGF. However, osteoblast mineralization, which is a relative later incidence in bone defect repair, was only partially restored. In this case, a bolus addition of VEGF may not satisfy the demand for VEGF in the whole process of repair, especially in the late mineralization stage. That may explain the failure of fully restore of osteoblast mineralization. Slow-release VEGF loaded in specific scaffolds, which restore VEGF level continuously may better improve defect repair in this scenario (Geng et al., 2011; Silva and Mooney, 2010). In addition, intracellular VEGF, which is not secreted but potentially binds nuclear envelop proteins and enters into nuclei to participate transcription regulation (Gerber et al., 2002; Lee et al., 2007; Liu et al., 2012), may be another possibility for the failure of exogenous VEGF to fully rescue the comprised repair. Modified permeable VEGF fused to a nuclear localization signal may help to determine the role of intracellular VEGF in bone repair in the future.

To our surprise, 9-week old of *Vegfa*$^{fl/fl}$*;Osx-cre* mice withdrawn of doxycycline from week 4 exhibited normal bone repair. In these mice, osteoblast precursors and their descendants, which expressed osterix before week 4 or shortly after that, are not targets of Cre and therefore still generate VEGF. The paracrine VEGF secreted by these cells may be enough to support bone repair even VEGF is deleted in the newly formed Osx-positive cells. Currently, whether bone forming cells in defects of our model come from

mesenchymal progenitors which migrate in, proliferate and differentiate, or adjacent pre-osteoblasts or even later stage of osteoblasts, which already overtook Osx-positive stage, migrated in to directly form bone is not completely understood. If first assumption is the only repair machinery, we would conclude that optimal amount of paracrine VEGF is enough to support bone repair even intracellular VEGF in newly differentiated osteoblasts is lacking. But in any case that the second assumption exists, we could not exclude the intracellular VEGF. By using *Vegfa*$^{fl/fl}$*;Osx-cre* mice with DOX withdrawn at a earlier time, osteolineage cells expressing VEGF normally were replaced gradually by newly formed cells in which VEGF was deleted so that the total extracellular VEGF was insufficient to support the normal bone healing. These data indirectly highlighted the importance of paracrine VEGF from osteoblasts during bone repair.

The delayed infiltration of blood vessels and osteoclasts in the injured periosteum and delayed cartilage turnover in *Vegfa*$^{fl/fl}$*;Osx-cre* mice, was consistent with the major phenotypes of *VEGF*$^{120/120}$ (mice expressing only VEGF120 isoform) and mice treated with sFlt1 during bone development (Gerber et al., 1999; Zelzer et al., 2002), indicating essential roles of VEGF from osteoblastic cells or hypertrophic chondrocytes in periosteal response after bone injure could recapitulate their functions during endochondral bone formation during development. Besides delay of cartilage resorption, an increase of cartilage formation was observed in periosteum of *Vegfa CKO* mice, which was consistent with previous studies showing that inhibition of VEGF signaling in early skeletal progenitors may facilitate the fate of determination from bone to cartilage forming cells (Chan et al., 2015). In addition, soluble Flt1 gene therapy was shown to improve BMP4-induced chondrogenic differentiation of muscle-derived stem cells

(MDSCs) in vitro and also promote articular cartilage repair regeneration(Kubo et al., 2009; Matsumoto et al., 2009), indicating that blocking VEGF could be a potential approach to improve cartilage healing. At PSD28, large amount of osteoclasts residing along the new bone layer indicated the active bone remodeling. Osteogenic factors released from pre-osteoclasts or bone matrix after bone resorption, such as TGF-β, IGF, PDGF-BB, coordinate formation of blood vessels and bones (Crane and Cao, 2014; Tang et al., 2009; Xie et al., 2014). VEGF was also known to bind VEGFR1 in osteoclasts and regulate their differentiation and activation (Aldridge et al., 2005; Liu et al., 2012). Therefore at the remodeling stage, reduction of VEGF in bone cells may cause decrease of osteoclast recruitment, less release of osteogenic signals from resorbed bone matrix, and subsequent reduction of callus bone volume.

In summary, our data revealed that osteoblast-derived VEGF is important for various stages of bone defect repair. First, VEGF is indispensable to initiate macrophage related angiogenesis response to bone trauma. This is consistence with previous studies that VEGF stimulate monocyte/macrophage infiltration and activation, further indicating VEGF maybe also important in inflammation driven disorders such as atherosclerosis and arthritis. Secondly, during IO-mediated repair, an optimal amount of paracrine VEGF from osteoblasts is required for angiogenesis-osteogenesis coupling. Third, VEGF either from osteoblasts or hypertrophic chondrocytes is important for the recruitment of blood vessel and osteoclasts, mediation of cartilage resorption and replacement by bone during endochondral ossification-mediated bone repair. Lastly, during bone remodeling phase, VEGF is important for the remodeling or regenerative capability through regulating

osteoclasts. These findings add to understanding of VEGF functions and may provide a basis for novel strategies based on VEGF modulation to improve bone defect repair.

Chapter III

VEGFR2 deficiency in osteoblast precursors and their progeny enhances osteoblast maturation and mineralization during bone repair

Introduction

Osteoblast-derived VEGF plays an essential role in angiogenesis-osteogenesis coupling, as well as coordination of bone resorption and bone formation (Liu et al., 2012; Wang et al., 2007). Most functions of VEGF are mediated by paracrine effects through targeting on adjacent endothelial cells and osteoclasts. In early osteoblastic cells, VEGF also controls osteoblastogenesis and adipogenesis in an intracrine mechanism that is resistant to effects of extracellular VEGF (Liu et al., 2012). Whether osteoblast-generated VEGF binds to VEGF receptors in a cell autonomous manner and to what extents that autocrine VEGF regulates osteoblast functions during bone healing is currently not well established.

VEGFR2, the main VEGF receptor, is predominantly expressed in endothelial cells to mediate the mitogenic and angiogenic effects in the response to VEGF (Koch et al., 2011). In addition to endothelial cells, it is also expressed and functional in other cells types, including pericytes, lymphocytes and osteoclasts (Aldridge et al., 2005). Depending on different species and collection methods, VEGFR expression is variable in osteoblastic cells, which makes it difficult to study autocrine effects of osteoblast-derived VEGF (Clarkin and Gerstenfeld, 2013). VEGF receptors, including VEGFR1 and VEGFR2, were previously detected in primary human osteoblasts, and exogenous VEGF is capable to promote the migration, proliferation and differentiation of human osteoblasts (Mayr-Wohlfart et al., 2002). However, primary murine mesenchymal progenitors and osteoblasts fail to respond to exogenous VEGF in some studies (Eckardt et al., 2003; Liu et al., 2012), arguing for the active functions of VEGF receptors in mice.

Studies of mice with deletion of *Vegfr1* or *Vegfr2* in osteoblastic cells show that these mice exhibit reduced bone density two weeks after birth (Liu et al., 2012). Reduced numbers of osteoprogenitor cells was also observed in the bone marrow from these mice (Liu et al., 2012), further indicating that both VEGFR1 and VEGFR2 are important for the postnatal bone formation. However, the autocrine effects of VEGF mediated by VEGFR2 during bone repair are not clear.

In the Chapter II, we demonstrate that paracrine VEGF from osteoblastic cells is important for healing of cortical defects. To further dissect the autocrine effects of osteoblast-derived VEGF on osteoblastic differentiation and bone formation during bone repair, we generated conditional knockout mice by deleting the major VEGF receptor, VEGFR2, in osteoblast lineage cells using osterix-cre mice, and examined the consequences of cortical defect healing in these mice.

Materials and Methods

Mouse Strains

Osx-GFP::Cre (Rodda and McMahon, 2006) and *CAG-loxP-stop-loxP-ZsGreen* (Ai6) mouse lines were purchased from Jackson Laboratory. *Flk1(Vegfr2) floxed* mice were provided by Genentech. To generate $Flk1^{fl/fl}$*;Osx-cre* mice, hemizygous *Osx-cre* transgenic mice were crossed with $Flk1^{fl/fl}$ mice to produce heterozygous $Flk1^{fl/+}$ offspring carrying a *Cre* allele. These mice were then crossed with $Flk1^{fl/fl}$ mice generating the following three genotypes: $Flk1^{fl/fl}$*;Osx-cre* (*Vegfr2 CKO* mice), $Flk1^{fl/+}$*;Osx-cre* and $Flk1^{fl/fl}$ mice. To trace the osterix-positive cells and their progeny, a cre-activating reporter, ZsGreen, was introduced into *Osx-cre,* $Flk1^{fl/+}$*;Osx-cre and* $Flk1^{fl/fl}$*;Osx-cre* mice.

Tibial monocortical defect model

The tibial monocortical defect, used as a simplified stable facture model, was described in Chapter II. Mice at post-surgery day (PSD) 7, 10, and 14 were collected for analysis.

µCT analysis

µCT 35 system (Scanco Medical) with a spatial resolution of 7µm was used to analyze the injured tibiae.

Histology and histomorphorphometry

At the time of euthanasia, injured tibiae were dissected, fixed, decalcified and embedded in paraffin or optimal cutting temperature (OCT) compound. 8µm thick longitudinal sections using the injured hole as landmark were cut, and stained with H&E,

aniline blue, TRAP or safranin O. 6-8 tissues sections from each mouse, stained with aniline blue, were used to determine the amount of newly formed osseous tissues in the hole region, and sections stained with safranin O were used for the calculation of cartilage area in the extracortical area as described in Chapter II.

Immunofluorescence

Standard protocol for immunofluorescence was used as described in Chapter II. The following primary antibodies were used: anti- BSP (1:50, Santa Cruz), anti-osteocalcin (1:50, Santa Cruz), and anti-ALP (1:50, Santa Cruz). For TUNEL staining, dead cells were detected using in situ cell death detection kit, TMR Red (Roche).

In vitro osteoblastic differentiation and mineralization assay

Isolation and culture of primary osteoblasts from tibia and femur of 8- to 12-week-old mice were as described in Chapter II. Osteoblastic cells were seeded in 12-well plates containing complete culture medium. Upon reaching 70-80% confluent, cell were switched to osteogenic medium (10% FBS, 10mM β-glycerophosphate, and 50μg/mL ascorbic acid with 50ng/ml BMP2). Culture medium was replaced every 2 days. Von Kossa assay was used to measure the mineralization after 21 days of culture.

Statistical Analysis

The data are presented as mean ± standard error, and were subjected to unpaired 2-tailed Student's *t*-test. *P* values less than 0.05 were considered significant.

Results

Deficiency of *Vegfr2* in osteoblastic cells enhances mineralized bone formation in defects at PSD7

In *Flk1*$^{fl/fl}$*;Osx-cre* mice, formation of mineralized bone in the hole region as well as in the injured bone marrow was increased compared with controls at PSD7 (Figure 22A, B). For the mineralized bone formed in the hole region of *Flk1*$^{fl/fl}$*;Osx-cre* mice, trabecular number as well as trabecular thickness was increased, and trabecular separation was decreased compared with of controls (Figure 22A).

Deficiency of *Vegfr2* in osteoblastic cells enhances osteoblast maturation and mineralization in healing of cortical defect

At PSD7, collagen accumulation, represented by the density of aniline blue stained area, and BSP levels in the hole region, which are two important bone matrix proteins secreted by osteoblasts in their early differentiation stage, were not significantly different between *Flk1*$^{fl/fl}$*;Osx-cre* and *Flk1*$^{fl/fl}$ mice (Figure 23A, C). However, levels of OCN, which is a mature osteoblast marker, and alkaline phosphatase (ALP), an important indicators of mineralization, were increased by 4.7 and 3.0-folds, respectively, in the hole region of *Flk1*$^{fl/fl}$*;Osx-cre* mice compared with *Flk1*$^{fl/fl}$ mice (Figure 23D, E). In addition, the mineralization to collagen ratio was also greatly increased in *Flk1*$^{fl/fl}$*;Osx-cre* compared with *Flk1*$^{fl/+}$*;Osx-cre* and *Flk1*$^{fl/fl}$ mice (Figure 23B), indicating the enhanced osteoblast mineralization when *Vegfr2* is removed from osteoblastic cells. In addition, osteoblasts isolated from *Flk1*$^{fl/fl}$*;Osx-cre* mice showed increased mineralization in the stimulation of BMP2 compared with cells from *Flk1*$^{fl/fl}$ mice (Figure 23F), further

supporting the enhanced osteoblast maturation and mineralization in *Flk1$^{fl/fl}$;Osx-cre* mice under certain conditions during bone repair, such as elevation of BMPs.

Figure 22

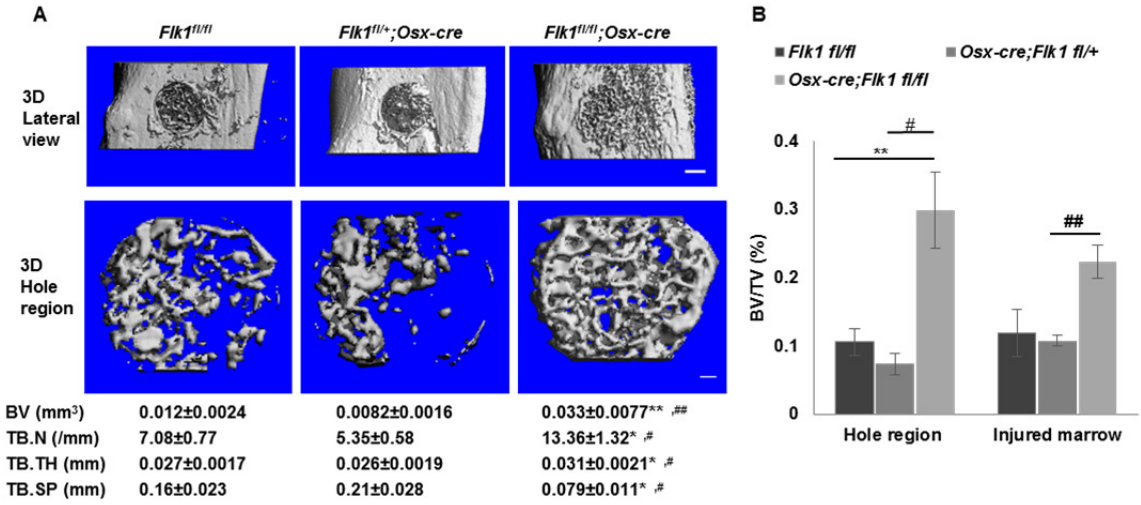

Figure 22. **Deficiency of *Vegfr2* in osteoblastic cells enhances mineralized bone formation in defects at PSD7. (A)** 3D-reconstruction of the injured tibia from lateral views (top panel, scale bar: 500μm) and mineralized bone formed in hole region (lower panel, scale bar: 100μm) by μCT. **(B)** μCT analysis of mineralized bone formed in the hole region and injure marrow and BV/TV was calculated. N=6-7 *, $^{\#}$ *P<0.01*; **, $^{\#\#}$, *P<0.05*. *,** *vs. Flk$^{fl/fl}$*. $^{\#,\#\#}$ *vs. Flk$^{fl/+}$;Osx-cre.*

Figure 23

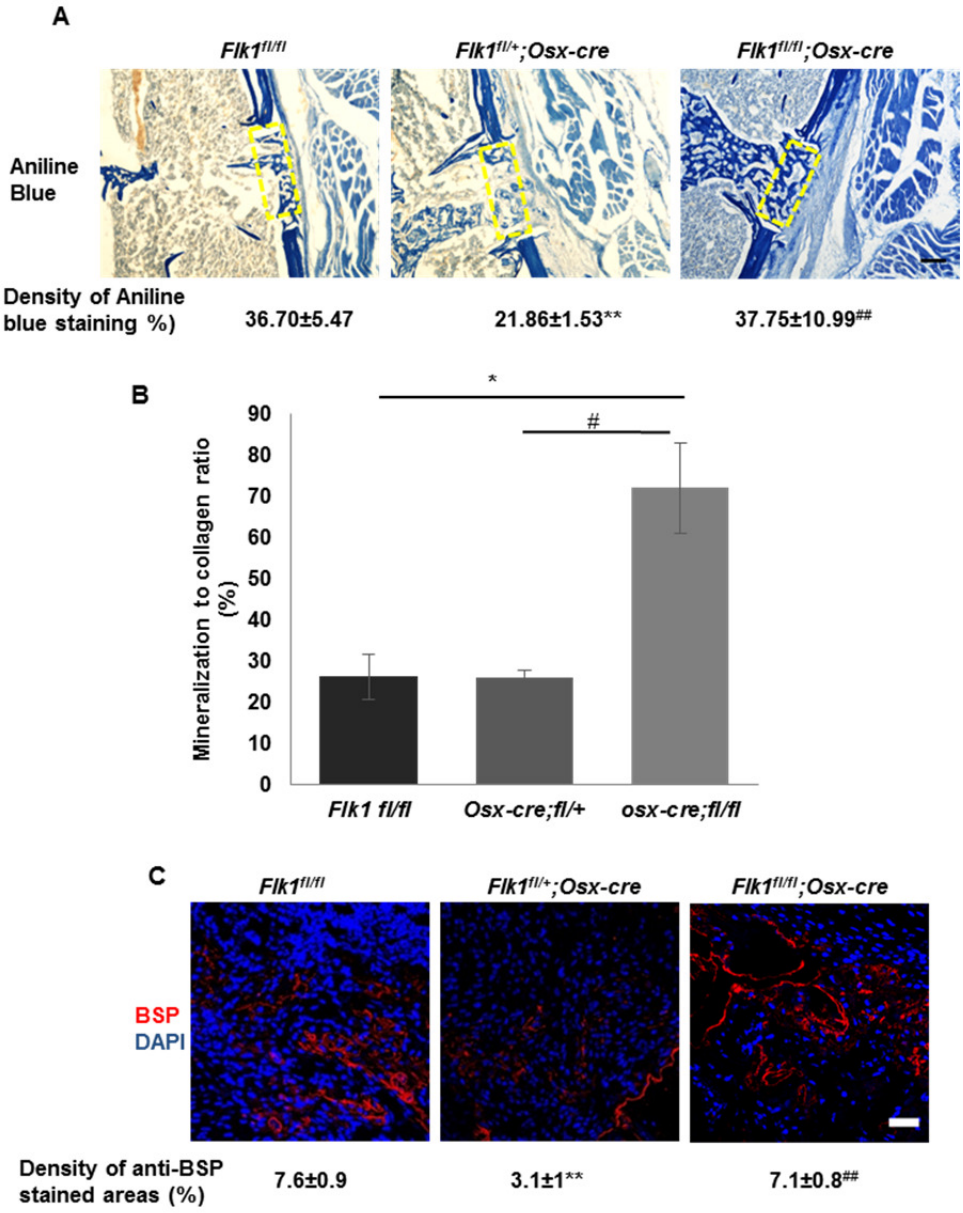
A
Flk1fl/fl
Flk1fl/+;Osx-cre
Flk1fl/fl;Osx-cre
Aniline Blue
Density of Aniline blue staining %)
36.70±5.47
21.86±1.53**
37.75±10.99##
B
*
#
Mineralization to collagen ratio (%)
90
80
70
60
50
40
30
20
10
0
Flk1 fl/fl
Osx-cre;fl/+
osx-cre;fl/fl
C
Flk1fl/fl
Flk1fl/+;Osx-cre
Flk1fl/fl;Osx-cre
BSP
DAPI
Density of anti-BSP stained areas (%)
7.6±0.9
3.1±1**
7.1±0.8##

Figure 23 (continued)

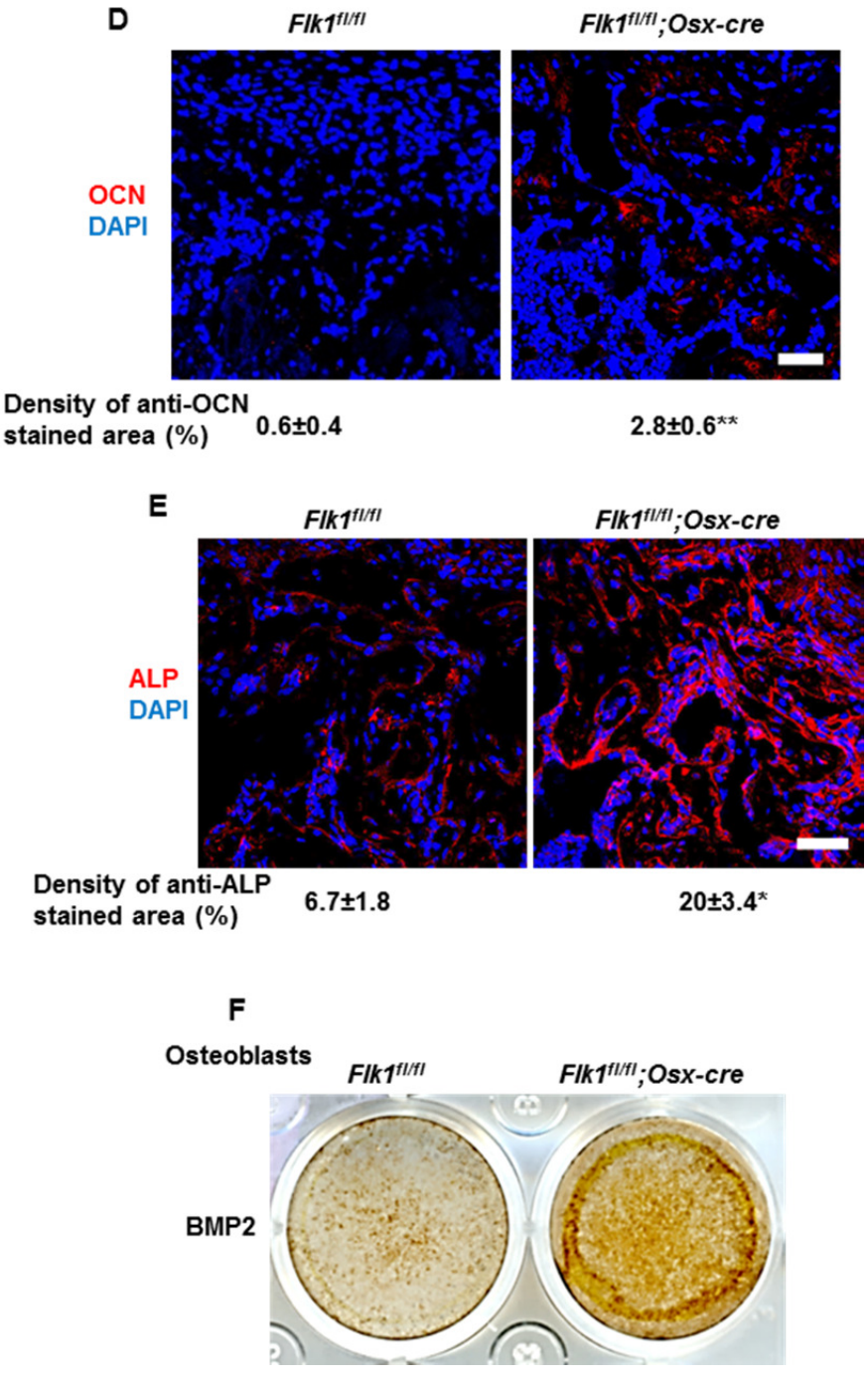

Figure 23 (continued). **Deficiency of *Vegfr2* in osteoblastic cells enhances osteoblast maturation and mineralization in cortical defect healing at PSD7. (A)** Aniline blue staining to show collagen accumulation. Percent of aniline blue-positive area was calculated in the hole region. **(B)** Mineralization to collagen ratio was increased in *Flk1$^{fl/fl}$;Osx-cre* mice. **(C)** Low percentage of anti-BSP staining in hole region of *Flk1 $^{fl/+}$;Osx-cre* mice compared with *Flk1$^{fl/fl}$;Osx-cre and Flk1$^{fl/fl}$* mice at PSD7. **(D, E)** High percentage of anti-OCN (D) and anti-ALP (E) staining in the hole region of *Flk1$^{fl/fl}$;Osx-cre* compared with *Flk1$^{fl/fl}$* mice. **(F)** Von Kossa staining of osteoblasts isolated from *Flk1$^{fl/fl}$* and *Flk1$^{fl/fl}$;Osx-cre* mice after 21 days of culture in the mineralization medium containing 50ng/ml BMP2. Scale bar: 200μm (A), 50μm (C, D, E). N=6-7 *, $^{\#}$ *P<0.01*; **, $^{\#\#}$, *P<0.05*. *, ** *vs. Flk1$^{fl/fl}$*. $^{\#, \#\#}$ *vs. Flk1$^{fl/+}$;Osx-cre.*

Deletion of *Vegfr2* in osteoblastic cells does not alter the numbers of blood vessels, dead cells or osteoblastic cells in the hole region during cortical defect healing

It is possible that absence of VEGFR2 in osteoblasts would promote angiogenesis by providing more VEGF available for endothelial cells. To test this, we stained sections with anti-CD31, and found that the number of blood vessels was practically the same between *Flk1$^{fl/fl}$;Osx-cre* mice and controls, suggesting that the enhanced formation of mineralized bone in hole region of *Flk1$^{fl/fl}$;Osx-cre* mice was probably not due to the increased angiogenesis (Figure 24A). VEGFR2-mediated signaling is important for the cell survival. TUNEL staining *in situ* showed no difference for the number of dead cells in the hole region of *Flk1$^{fl/fl}$;Osx-cre* and *Flk1$^{fl/fl}$* mice (Figure 24B), indicating that other factors may compensate for loss of VEGFR2-mediated pro-survival signaling *in vivo*. We introduced the cre-activating report, ZsGreen (ZsG), to *Osx-cre*, *Flk1$^{fl/fl}$;Osx-cre and Flk1$^{fl/+}$;Osx-cre* mice to trace the fate of osteoblast precursors and their progeny. No significant difference was observed for the number of ZsG-positive cells between *Flk1$^{fl/fl}$;Osx-cre;ZsG* mice and controls, suggesting that the enhanced formation of mineralized bone in the hole region of *Flk1$^{fl/fl}$;Osx-cre* mice may not likely due to the increased numbers of bone forming cells (Figure 24C).

Figure 24

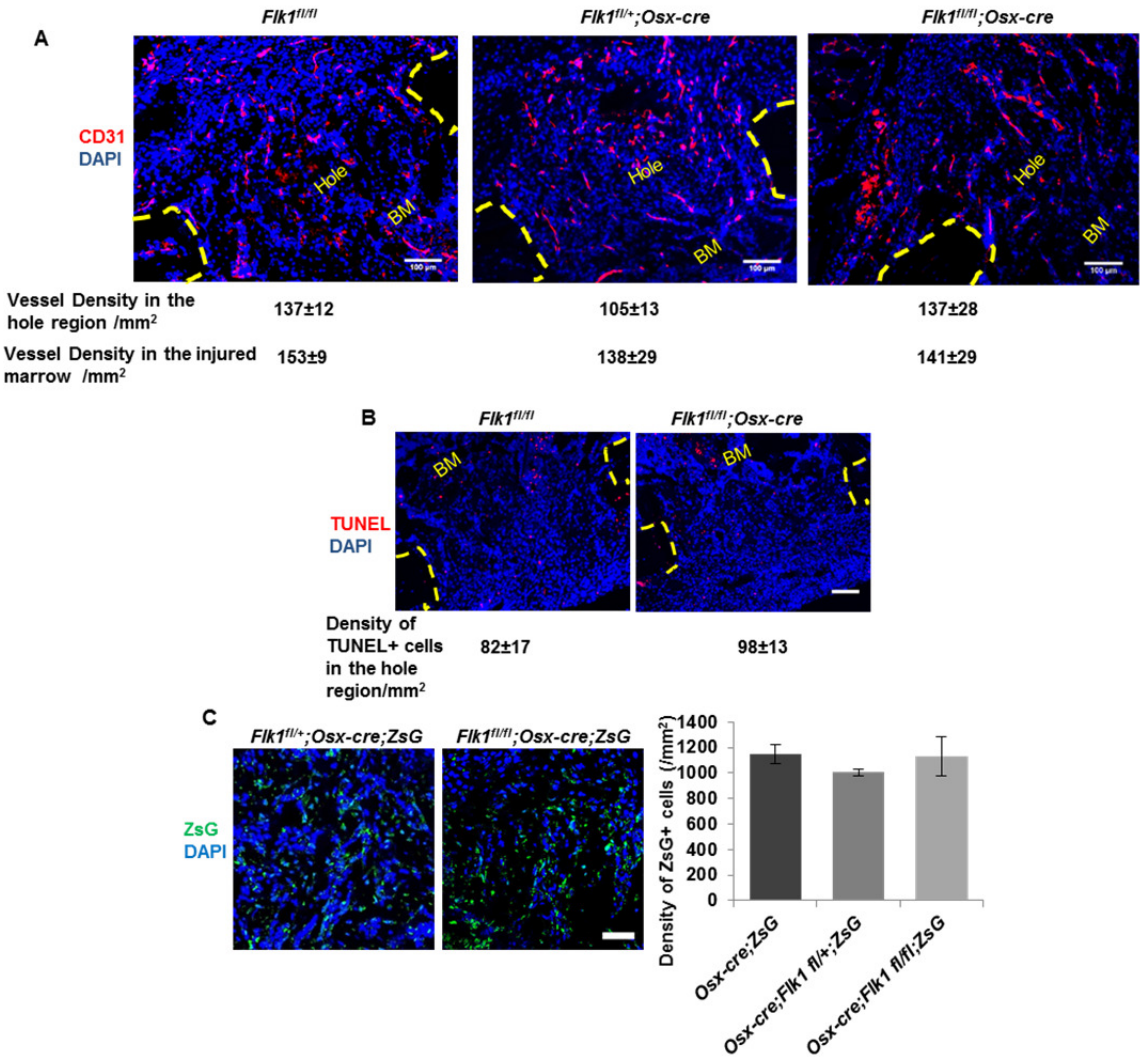
A
Flk1fl/fl
Flk1fl/+;Osx-cre
Flk1fl/fl;Osx-cre
CD31
DAPI
Hole
BM
Vessel Density in the hole region /mm2
137±12
105±13
137±28
Vessel Density in the injured marrow /mm2
153±9
138±29
141±29
B
Flk1fl/fl
Flk1fl/fl;Osx-cre
TUNEL
DAPI
BM
Density of TUNEL+ cells in the hole region/mm2
82±17
98±13
C
Flk1fl/+;Osx-cre;ZsG
Flk1fl/fl;Osx-cre;ZsG
ZsG
DAPI
Density of ZsG+ cells (/mm2)
1400
1200
1000
800
600
400
200
0
Osx-cre;ZsG
Osx-cre;Flk1 fl/+;ZsG
Osx-cre;Flk1 fl/fl;ZsG

Figure 24 (continued). **Deletion of *Vegfr2* in osteoblastic cells does not alter the number of blood vessels, dead cells or osteoblastic cells in the defect region. (A)** CD31 staining in the injured region. Density of blood vessel in hole region and adjacent injured marrow was calculated based on CD31 staining. N=4-7. **(B)** TUNEL staining in fields within injured hole to display dead cells. Number of TUNEL-positive cells was calculated in hole region. N=7. **(C)** Representative images showing ZsG-positive cells. The density of ZsG+ cells was calculated in hole region. N=6-7. Scale bar: 50μm (C), 100μm (A, B).

Endochondral bone formation in the injured periosteum is not altered in mice with deletion of *Vegfr2* in osteoblastic cells

At PSD10, Safranin O-stained cartilage was observed in the injured periosteum (PO) of both *Flk1$^{fl/fl}$;Osx-cre* and control mice, indicating the occurrence of endochondral ossification. Although the percentage of cartilage in PO of *Flk1$^{fl/fl}$;Osx-cre* mice was higher than that of *Flk1$^{fl/fl}$;Osx-cre* mice, statistical significance was lacking. At PSD14, there was almost none cartilage left in both mice, indicating that different from *Vegfa CKO* mice where there was a delay of cartilage resorption, cartilage turnover was not significantly altered in *Vegfr2 CKO* mice. No significant difference was observed for periosteal callus thickness between *Flk1$^{fl/fl}$;Osx-cre* and *Flk1$^{fl/fl}$* mice at PSD10 and PSD14 (Figure 25A, B), further indicating that EO-mediated periosteal responses were not altered when *Vegfr2* was removed from osteoblastic cells.

Figure 25

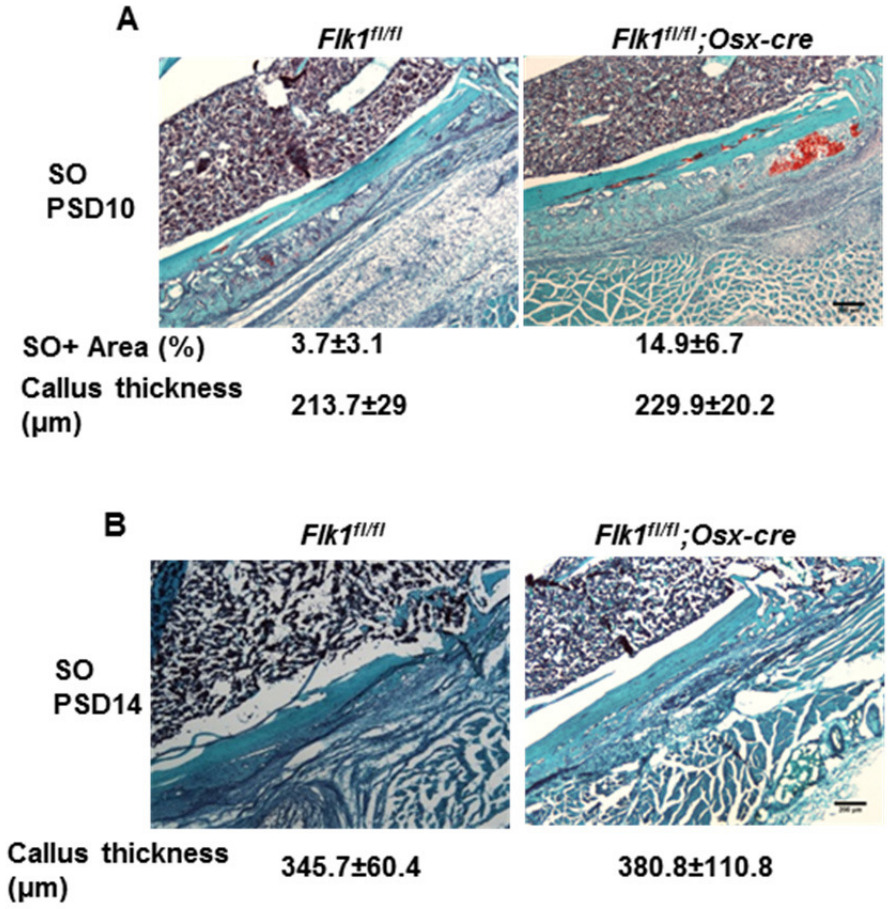

Figure 25. **Endochondral ossification mediated periosteal response is not altered when *Vegfr2* is removed from osteoblastic cells. (A, B)** Safranin O (SO) staining in the periosteum distal to hole region from mice at PSD10 (A) and PSD14 (B). Percent of SO-positive cartilage and callus thickness was calculated. N=3-5. Scale bar: 200μm.

Discussion

In the present study, we demonstrate that deletion of *Vegfr2* in osteoblast precursors and their progeny enhances osteoblast differentiation and mineralization during cortical defect healing. VEGFR2-mediated autocrine VEGF signaling might be a negative regulator for osteoblast differentiation in the context of bone healing, indirectly highlighting the importance of paracrine VEGF, and also providing a mechanism for the inhibitory effects of excess VEGF in healing of a small bone defect.

The enhanced formation of mineralized bone in defects of *Flk1$^{fl/fl}$;Osx-cre* mice during bone healing, which is different from the phenotypes of skeletal development in the same strain, indicated that bone repair has its own characteristics compared with bone development, such as existence of bone marrow niche, abundant inflammatory cells and cytokines. The inflammatory cells in the initial stage of bone injury, interact with mesenchymal progenitors and endothelial cells closely, and release many factors that are not induced during bone development, such as PIGF (Maes et al., 2006).

In endothelial cells, activation of VEGFR2 recruits the inhibitory smad, Smad7, through PI3K pathway to decrease the activation of Smad2/3 (Yamauchi et al., 2004). It may be also applied on osteoblasts, as osteoblasts isolated from *Flk1$^{fl/fl}$;Osx-cre* mice exhibit increased mineralization *in vitro* when stimulated with Smad transducing factors, BMP2. In addition, VEGF inhibits activation of PDGFR through VEGFR2 in various cells (Greenberg et al., 2008; Pennock and Kazlauskas, 2012). Since PDGF plays an important role in bone formation and regeneration (Caplan and Correa, 2011), it is also possible that deletion of *Vegfr2* enhances PDGFR signaling in osteoblasts.

Since the progeny of osterix-positive osteoblast precursors include pericytes (Chen et al., 2014), *Vegfr2* is also potentially deleted from pericytes. VEGFR2 in pericytes is considered as a negative regulator for pericyte function (Greenberg et al., 2008). Thus, reduced VEGFR2 in pericytes may cause improvement of their functions and vessels maturation. In addition to osteoblastic cells and pericytes, descendants of osteoblast precursors also include, but are not limited to, adipocytes and bone marrow stromal cells (Ono et al., 2014). The rare existence of adipose tissues in the injured sites makes the contribution of VEGFR2 in adipocyte less possible.

In our models, some ZsG-positive osteolineage cells, located in the perisinusoidal area, were found to express VEGFR2 (data not shown). These cells could be osterix-positive bone marrow stromal cells, which overlap with a population of mesenchymal progenitors. However, VEGFR2 expression was seldom observed in the mature osteoblastic cells located in the newly formed trabeculae within the defects. This is consistent with previous findings that expression of VEGF receptors in murine mesenchymal progenitor cells was decreased with osteogenic differentiation (Deckers et al., 2000). These data further suggest that VEGFR2 in mesenchymal progenitor cells may act as a negative regulator for osteoblastogenesis.

In the injured periosteum, *Vegfr2* deletion from osteoblastic cells failed to influence the endochondral bone formation. The osteochondroprogenitors could differentiate to chondrocytes or osteoblasts in the injured periosteum. In this area, VEGFR2 expression is mainly located in the vasculature (data not shown). It is possible that osteochondroprogenitor cells do not express VEGFR2, and therefore removal of

VEGFR2 would not influence their differentiation and functions in the periosteal response to injuries.

In summary, our data revealed a novel function of autocrine VEGF from osteoblasts, which may act as a negative regulator for osteoblast differentiation and bone formation during bone repair. The autocrine effects of VEGF on bone forming progenitor cells, together with the paracrine and intracrine pathways, add to the complexity of VEGF application. Understanding of VEGFR2 signaling in osteolineage cells with different stages of differentiation may help to develop strategies of VEGFR2 modulation to promote bone regeneration.

Chapter IV

Soluble VEGFR1 reverses BMP2 inhibition of intramembranous ossification during healing of cortical defects

Introduction

BMP2 plays a pivotal role in bone development and postnatal bone repair, and is widely used in many bone regenerative procedures (Rosen, 2009). Currently, recombinant BMP2 (rBMP2) and rBMP7 are the only FDA-approved growth factors in use for spinal infusion, treatment of non-union fractures, and bone grafting.

Human and animal studies using rBMP2 showed a large variation in individual responses (Boyne et al., 1997; Howell et al., 1997). Various factors, including BMP2 concentrations, carrier properties, interaction with other growth factors and hormones, influence the effects of rBMP2 in bone regeneration (Groeneveld and Burger, 2000). The osteoinduction property of BMP2 depends on osteogenic or chondrogenic differentiation of skeletal stem cells. These cells are heterogeneous cell populations and include mesenchymal progenitors in perisinusoid, trabecular and endosteal locations, as well as osteochondroprogenitors in the periosteum and skeletal muscles (Chan et al., 2015; Ono et al., 2014; Wosczyna et al., 2012). Skeletal stem cells in different locations respond in their own ways to rBMP2 (Colnot, 2009). BMPs have been reported to promote osteogenic or chondrogenic differentiation of bone marrow-derived mesenchymal progenitors *in vitro* (Taipaleenmaki et al., 2008), but they seldom induce cartilage formation in the intramedullary space *in vivo***,** suggesting that bone marrow contains cartilage-inhibiting factors. In contrast, osteochondroprogenitors in periosteum and muscle interstitium respond strongly to rBMP2, and this can cause unwanted ectopic ossification (Yamamoto et al., 1998; Zhang et al., 2005).

BMP2 exhibits redundant functions with other BMPs, such as BMP4 and BMP7, and is indispensable during skeletal development. It is also required for cartilaginous callus formation during postnatal bone repair (Tsuji et al., 2006). Studies of mice with *BMP2* deleted in chondrocytes or osteoblasts showed that only chondrocyte-derived BMP2 is a prerequisite for fracture healing (Mi et al., 2013). Using a cortical defect model, Wang *et al*. also found that BMP2 produced by periosteal progenitor cells is essential for healing of bone defect (Wang et al., 2011b). These data underscore the importance of BMP2 in chondrogenesis, by skeletal progenitors in the periosteum and surrounding muscles during bone repair. However in the intramedullary space, recombinant BMP2 inhibits osteogenic differentiation and intramembranous bone formation during cortical defect healing (Minear et al., 2010b).

A number of growth factors, including VEGF, FGF2 and TGF-β1, have been reported to influence BMP-induced bone formation. VEGF is frequently used together with BMPs in bone regenerative procedures. Low ratios of VEGF to BMP2/4 have synergistic effects on bone regeneration, while higher ratios have detrimental effects (Peng et al., 2002; Peng et al., 2005). Another angiogenic factor, FGF2, also has synergistic effects with BMPs on osteoblast differentiation at low concentrations (Fujimura et al., 2002; Hanada et al., 1997), but high doses of FGF2 have inhibitory effects (Fujimura et al., 2002; Wang and Aspenberg, 1993).

Conversion of vascular endothelial cells to mesenchymal stem-like cells contributes to ectopic ossification in patients with fibrodysplasia ossificans progressiva (FOP) and in a mouse model of FOP (Medici et al., 2010), indicating that endothelial cells may represent a potential reservoir of bone forming cells. In cultured endothelial

cells, VEGF inhibits endothelial to mesenchymal transition (EndMT) induced by BMP4 (Medici et al., 2010). The inhibitory effect of VEGF on EndMT plays a critical role in the development of cardiac valves (Chang et al., 2004; Dor et al., 2001). Thus, it is possible that blocking of extracellular VEGF activity, by adding the decoy receptor sFlt1, may facilitate EndMT induced by BMP2 during healing of bone defects.

In Chapter II, high levels of VEGF were shown to inhibit intramembranous bone formation in the intramedullary space. This is similar to the inhibitory effects of delivering rBMP2 on healing of cortical defects. Considering BMP2 induces VEGF in osteoblastic cells, we hypothesize that the inhibitory effects of BMP2 on intramembranous bone formation during healing of cortical defects may be mediated by extracellular VEGF.

Materials and Methods

Mouse Strains

VE-cadherin-cre (Alva et al., 2006) and *CAG-loxP-stop-loxP-tdTomato* (Ai14) mouse lines were from Jackson Laboratory. To generate *VE-cadherin-cre;tdTomato* mice, hemizygous *VE-cadherin-cre* transgenic mice were crossed with homozygous *tdTomato mice*.

Tibial monocortical defect model

The tibial cortical defect used as a simplified stable facture model, was described previously (Kim et al., 2007; Minear et al., 2010a; Minear et al., 2010b). Skeletal mature *VE-cadherin-cre;tdTomato* mice (9-12 weeks old male) were used for all studies. A monocortical osseous hole (1 mm diameter) was created on the anterior surface of the tibia crest using a round burr attached to a dental drill. The soft tissue wound was closed by suturing the muscle and skin layers separately. Injured tibiae were collected at post-surgery day 10 (PSD10).

Delivery of recombinant rBMP2 and sFlt1.

Absorbable collagen hemostatic sponges (Avitene) were cut to the dimensions of the injured region. Sponges were soaked in 1µl of human recombinant BMP2 (R&D System) or murine recombinant sFlt1 (R&D System) with concentration of 1µg/µl or for 30 min at 4 Cº. In the co-delivery of BMP2 and sFlt1, sponges were soaked in 1µl of mixed protein with concentration of 0.95µg/µl for each. After the injury was made, the loaded sponge was inserted into the defects, followed by a single stitch of the cut muscle flap to cover the wound.

μCT analysis

Injured tibiae were analyzed using a μCT35 system (Scanco Medical) with a spatial resolution of 7μm. Sagittal images of injured tibiae were used to perform three-dimensional (3-D) histomorphometric analysis. We defined the region of interest to cover hole region between the interrupted cortical bone ends, injured bone marrow, and periosteal callus outside the hole, separately. Any remaining old bone fragments during drilling were excluded from the region of interest. We used a total of 120 consecutive images (about 0.84mm in length) to present most of the injured region and periosteal callus for 3-D reconstruction and analysis.

Histology and histomorphorphometry

Fixed samples were decalcified and embedded in paraffin or optimal cutting temperature (OCT) compound (Tissue-TEK). 8μm thick longitudinal sections using the hole region as landmark were cut, and stained with aniline blue, safranin O or tartrate-resistant acid phosphatase (TRAP). 6-8 tissues sections from each mouse were stained with aniline blue or safranin O to determine the amount of newly formed osseous tissues or cartilage using a method described in the previous Chapters.

Immunofluorescence

Immunofluorescence staining for anti-BSP was performed using a standard protocol as described in the previous Chapters.

Statistics

The data are presented as mean ± standard error and were subjected to unpaired 2-tailed Student's *t*-test. *P* values less than 0.05 were considered significant.

Results

Recombinant BMP2 inhibits intramembranous bone formation in the intramedullary space and this can be reversed by soluble VEGFR1 (sFlt1)

The cortical defect model is a simplified stable fracture model. Ten days after surgery (PSD10), trabecular bone formed in the hole region and wounded marrow space as described in the previous Chapters. Compared with PBS, delivery of rBMP2 in the injury region inhibited formation of mineralized bone. In the hole region, bone volume as well as trabecular number was decreased, and trabecular separation was increased (Figure 26A, B). Co-delivery of sFlt1 and rBMP2 not only reversed the inhibitory effects of rBMP2 on mineralized bone formation in the intramedullary space, but also enhanced bone regeneration in the hole region compared with PBS or sFlt1 alone (Figure 26A-C). Because the penetration of the drill into the marrow space showed some variation, mineralized bone formation in the wounded marrow space in mice with co-delivery of rBMP2 and sFlt1 failed to show an increase compared with the PBS and sFlt1 groups (Figure 26C).

Figure 26

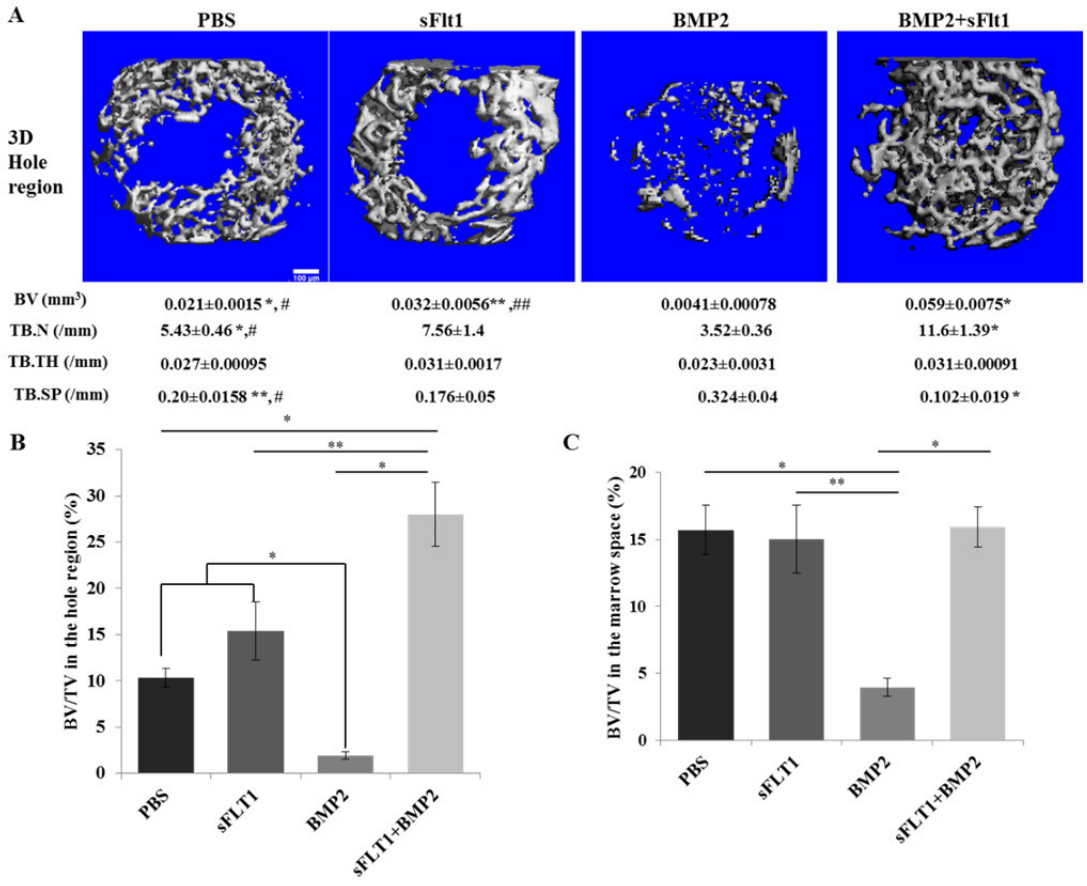

Figure 26. **BMP2 inhibits mineralized bone formation in hole region and wounded marrow and this can be reversed by sFlt1. (A)** 3D-reconstruction of mineralized bone formed in hole region by μCT. Scale bar: 100μm. **(B, C)** μCT analysis of BV/TV for mineralized bone formed in hole region (B) and wounded marrow space (C). N=4-6. *, $^{\#}$ *P<0.01*; **, $^{\#\#}$, *P<0.05*. *, ** *vs. BMP2* (A). $^{\#}$, $^{\#\#}$ *vs. BMP2+sFlt1* (A).

Recombinant BMP2 enhances endochondral ossification in injured periosteum, and this is not affected by co-delivery of sFlt1

At PSD10, μCT showed that mineralized bone in the periosteal area was significantly enhanced by rBMP2, with or without sFlt1, compared with PBS or sFlt1 alone (Figure 27A, B). This indicates that BMP2 acts as an inducer of periosteal callus formation. This was further demonstrated by the enhanced callus thickness in the BMP2 treatment group (Figure 27D). Safranin-O staining showed a large amount of cartilage in the periosteal callus in mice treated with rBMP2. In contrast, only small amounts of cartilage were observed in PBS and sFlt1 groups (Figure 27C, E). Addition of sFlt1 showed little influence on mineralized bone and cartilage formation induced by rBMP2 in the injured periosteum. This indicates that sFlt1, when loaded on collagen sponges and inserted in the injured hole, may not diffuse into the periosteal area.

Recombinant BMP2 inhibits collagen accumulation and BSP production in the injured region which this is reversed by sFlt1

Compared with massive collagen accumulation and BSP production in groups treated with PBS or sFlt1 alone, collagen and BSP staining was significantly reduced in groups treated with rBMP2. This reduction could be reversed by co-delivery of sFlt1 and rBMP2 (Figure 28A, B, D). The mineralization to collagen ratio was also decreased by rBMP2 treatment (Figure 28C), indicating that rBMP2 not only decreases the osteoinduction, but also inhibits the process of mineralization. Co-delivery of sFlt1 and rBMP2 completely reversed the inhibitory effects of rBMP2 on osteoinduction and matrix mineralization. In addition, the total cell numbers in the injury hole was not

significantly different between groups, indicating that reduction of bone matrix proteins by rBMP2 treatment was not due to a decrease in cell number (Figure 28D).

Figure 27

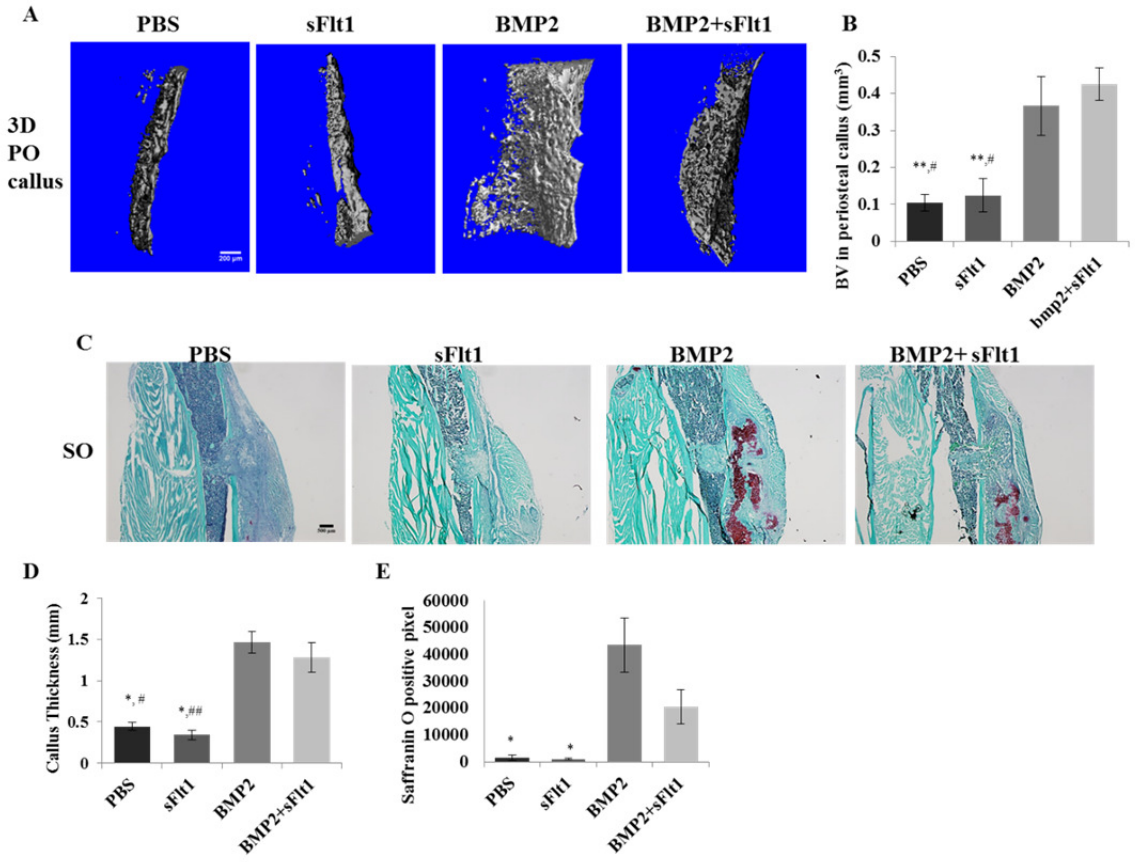

Figure 27 (continued). **BMP2 enhances endochondral ossification in injured periosteum and this is not affected by delivery of sFlt1. (A)** 3D-reconstruction of the periosteal callus by μCT. Increased mineralized bone after treatment with BMP2, with or without sFlt1. Scale bar: 200μm. **(B)** μCT analysis of BV/TV for mineralized bone formed in injured periosteum. N=6. **(C)** Safranin O staining showing cartilage accumulation in injured periosteum following BMP2 treatment, with or without sFlt1. Scale bar: 500μm. **(D)** Callus thickness reflects periosteal response to bone injury. N=4-6. (E) Increased safranin O-stained areas in periosteum (PO) from mice treated with rBMP2, but no significant difference between groups receiving BMP2 with or without sFlt1. N=4-6. *, $^{\#}$ *P<0.01*; **, $^{\#\#}$, *P<0.05*. *,** *vs. BMP2*. $^{\#,\ \#\#}$ *vs. BMP2+sFlt1*.

Figure 28

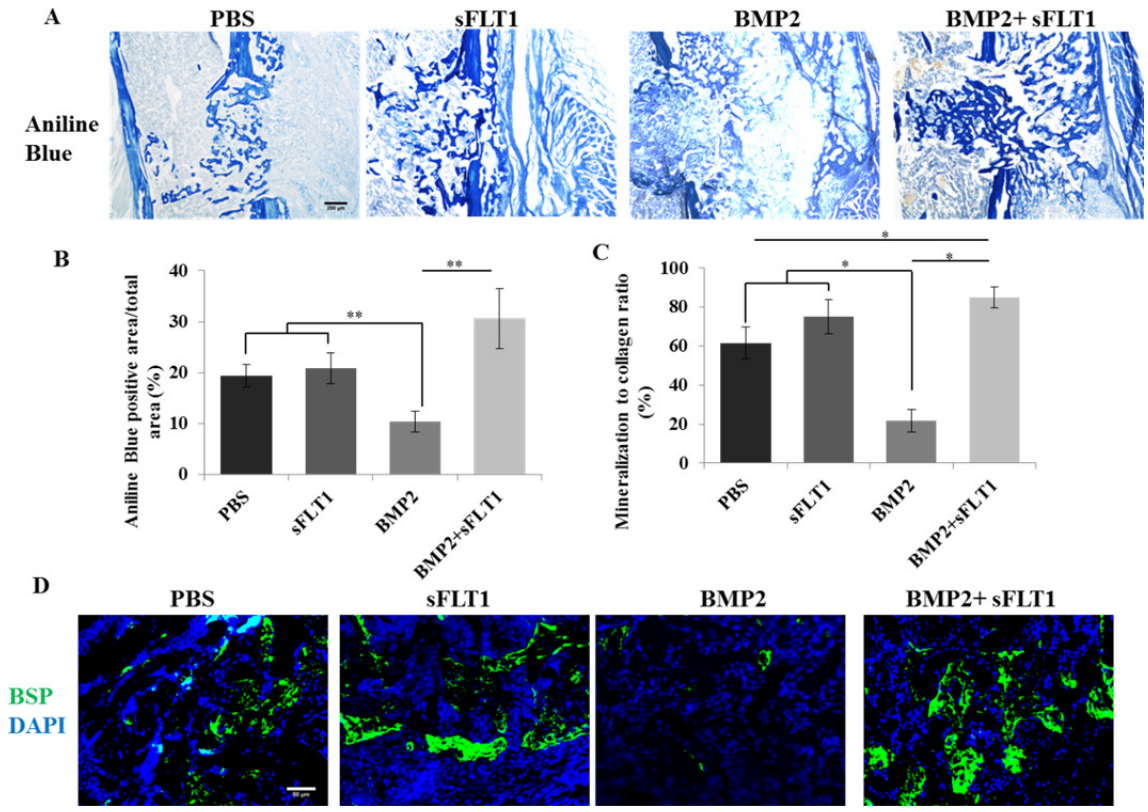

Figure 28. **Recombinant BMP2 inhibits collagen accumulation and BSP production in the cortical hole region and this can be reversed by sFlt1. (A)** Aniline blue stained area representing collagen accumulation, is reduced in hole region of mice treated with rBMP2. Scale bar: 200µm. **(B)** Relative amounts of aniline blue-stained areas in hole regions were compared in different groups. N=4-7. **(C)** Decreased mineralization to collagen ratio in hole region of mice treated with rBMP2. N=4-6. **(D)** Decreased anti-BSP staining in hole region of mice treated with BMP2 compared with other groups. Scale bar: 50µm. *, *P<0.01*; **, *P<0.05*.

The effects of rBMP2 and sFlt1 on healing of cortical defects are unlikely due to changes in angiogenesis or recruitment of osteoclasts

The number of blood vessels, calculated based on tdTomato expression in endothelial cells, was not different in the hole regions of the different groups (Figure 29A). This indicates that decreased bone formation in mice treated with BMP2 is not due to changes in angiogenesis. Adding sFlt1 failed to inhibit blood vessel formation in the hole region at PSD10 (Figure 29A). This differs from systemic application of sFlt1, which resulted in inhibition on both mineralized bone and blood vessel formation in bone defects (Street et al., 2002). In the current model, adding a bolus of sFlt1in the injury region, may not be sufficient to inhibit VEGF-mediated angiogenesis during the repair process. Alternatively, other angiogenic factors may compensate for the inhibition of VEGF. In addition, the number of TRAP positive osteoclasts in the hole region did not differ between groups (Figure 30A, B). In the periosteal callus, osteoclast numbers in mice treated with rBMP2 (with or without sFlt1) were increased compared with mice treated with PBS or sFlt1 alone (Figure 30A, B). This indicates that the inhibited intramembranous bone formation in intramedullary space and increased periosteal callus in mice treated with rBMP2 are unlikely due to alterations in osteoclast recruitment.

Figure 29

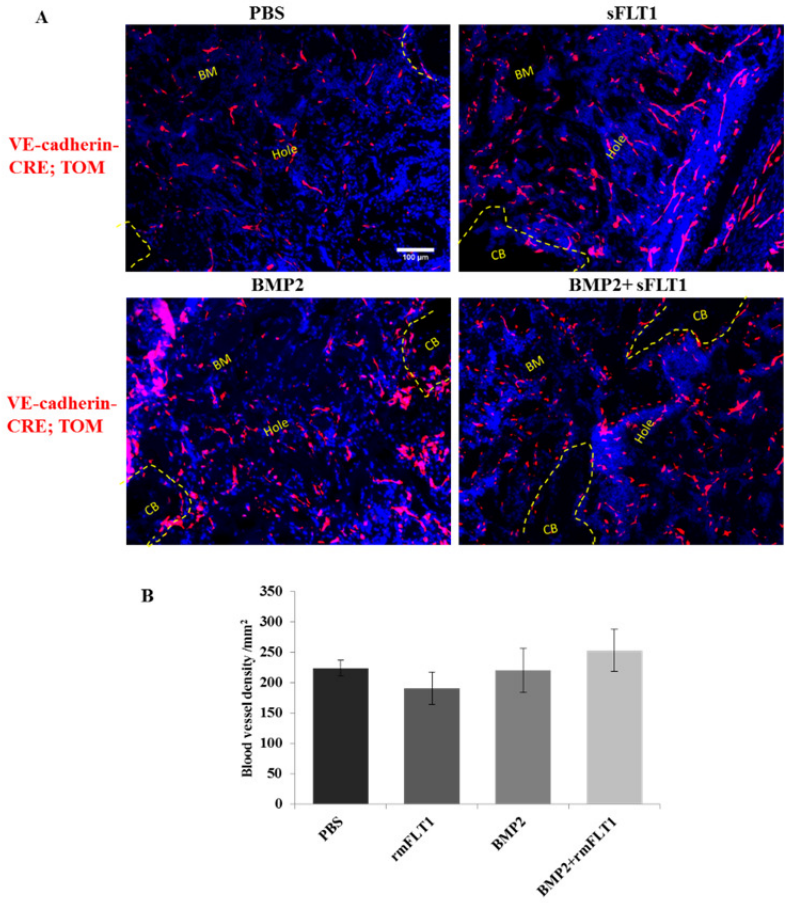

Figure 29. **The number of blood vessels in hole regions exhibit no significant differences between different groups at PSD10. (A)** Representative image showing tdTomato-positive cells, representing endothelial cells and their progeny, in the injury hole of *VE-cadherin-cre;tdTomato* mice. Scale bar: 100μm. **(B)** Density of blood vessels in hole region, calculated based on tdTomato-positive endothelial cells, was not much different in various groups. N=4-6.

Figure 30

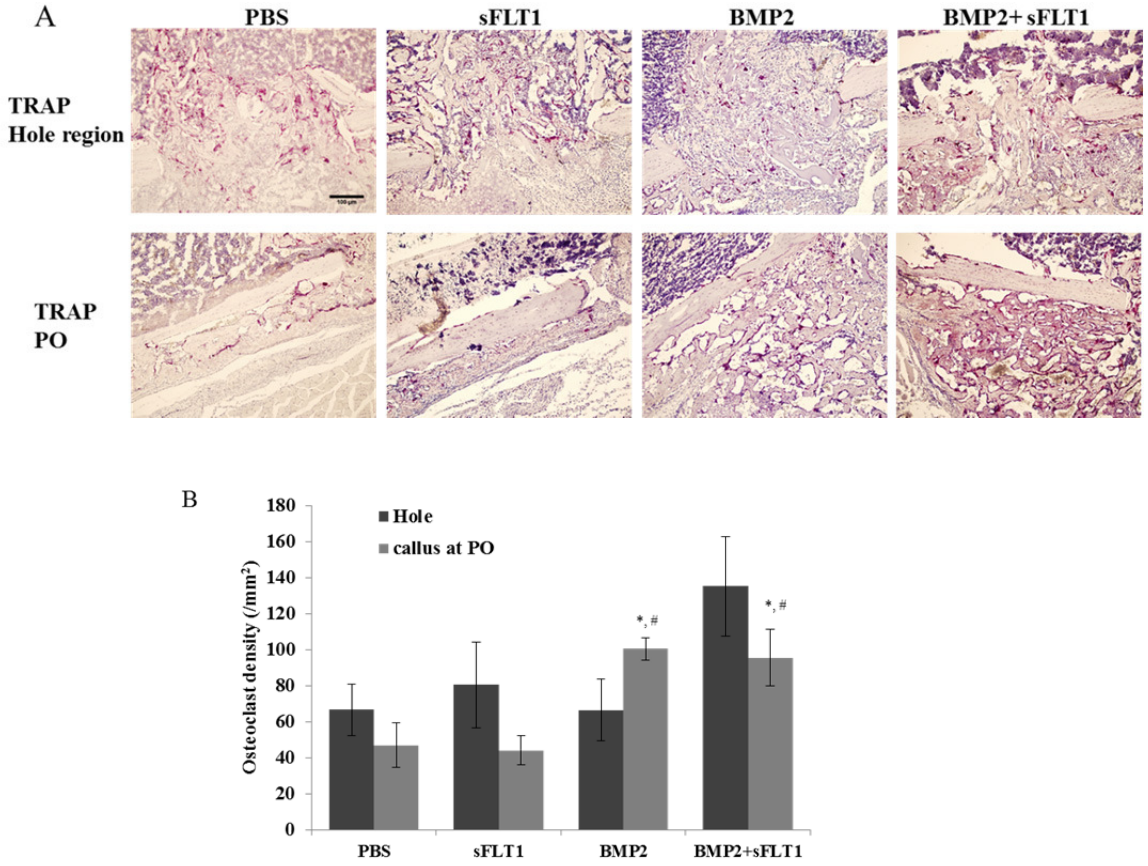

Figure 30. **The effects of rBMP2 and sFLT1 on healing of cortical defects are not likely due to alterations in osteoclast recruitment. (A)** TRAP-positive osteoclasts (stained red) in the injury hole (top panel) and wounded periosteum distal to the hole (lower panel). Scale bar: 100μm. **(B)** Density of osteoclasts (numbers of osteoclasts/area in hole region or periosteal callus) in hole regions and callus areas at periosteum (PO). N=4-6 *, $^{\#}$ *P<0.01*; *, *vs. PBS.* $^{\#}$, *vs. sFLT1*.

Co-delivery of rBMP2 and sFlt1 promotes expression of the osteoblast marker, bone sialoprotein, in endothelial lineage cells

Recombinant BMP2 and sFlt1 are considered promoters of endothelial to mesenchymal transition. When used alone, rBMP2 and sFlt1 seldom induce BSP expression in endothelial cells. However, in the injury sites from mice with co-delivery of these two factors, some tdTomato-positive endothelial cells were also positive for BSP (Figure 31), suggesting these bone matrix producing cells may have an endothelial origin.

Figure 31

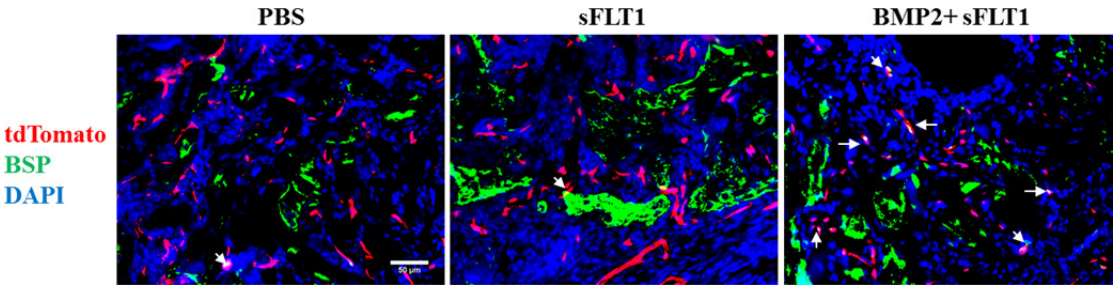

Figure 31. **Co-delivery of rBMP2 and sFlt1 promotes expression of the osteoblast marker, bone sialoprotein, in endothelial lineage cells.** More yellow cells (white arrows), expressing cre-activated reporter, *tdTomato,* and the bone matrix protein BSP, were observed in hole regions of mice with co-delivery of rBMP2 and sFlt1 compared with delivery of PBS or sFlt1 alone. Scale bar: 50μm. N=4-6

Discussion

In the current cortical defect model, rBMP2 exhibits a different regenerative capacity in different repair locations. It enhances the differentiation of osteochondroprogenitors to chondrocytes in the periosteum, while it inhibits the osteogenic differentiation of osteoprogenitors in the endosteum and bone marrow space. This inhibition of intramembranous bone formation by rBMP2 during bone healing may be mediated by excess VEGF, as it could be completely reversed by co-delivery of sFlt1.

The inhibitory effects of BMP2 on intramembranous ossification-mediated bone repair have been reported to be mediated by Wnt inhibition (Minear et al., 2010b). A feedback loop between BMP and Wnt signaling during bone development, shows that BMP signaling negatively regulates bone mass through inhibition of Wnt by sclerostin, an antagonist of both Wnt and BMP2 signaling (Kamiya et al., 2008). This BMP/Wnt feedback is also observed in postnatal bone formation and bone repair (Baker et al., 1999; Fuentealba et al., 2007). As Wnt signaling is a prerequisite for bone formation (Rodda and McMahon, 2006), inhibition of Wnt by BMP2 decreases osteogenic differentiation of osteoprogenitor cells, and causes reduced bone formation in the intramedullary space. In injured periosteum, inhibition of Wnt in osteochondroprogenitor cells causes a lineage switch from osteogenic to chondrogenic differentiation by increasing Sox9 expression and inducing cartilage formation (ten Berge et al., 2008)

BMP2 is a strong inducer of VEGF expression in osteolineage cells, so it is possible that VEGF levels may be enhanced in bone injury regions by exogenous rBMP2 (Deckers et al., 2002). In chapter II, we found that too much VEGF inhibits bone repair in

the injured marrow space of wild type mice. If rBMP2 induces VEGF expression beyond physiological levels during healing of the small defects, excess VEGF may inhibit bone repair. In chapter III, we found that VEGFR2 in osteoblasts may be a negative regulator of osteoblast mineralization and maturation. Thus, increased levels of VEGF, induced by rBMP2, may bind to VEGFR2 in osteolineage cells as well as to mesenchymal progenitors and inhibit their osteogenic differentiation.

The combination of BMP2 and VEGF has frequently been used in strategies aimed at promoting bone regeneration, but the outcomes have been variable. Administration of sFlt1 inhibits BMP2-induced ectopic bone formation but promotes cartilage accumulation, while VEGF promotes BMP2-induced ectopic bone formation and accelerates cartilage resorption by promoting blood vessel invasion (Peng et al., 2005). The VEGF to BMP ratio appears to be important for the effects of BMPs in bone repair. A low ratio (1:5) induces better bone regeneration than a high ratio (5:1) (Peng et al., 2005), indicating that high-dose VEGF may decrease the regenerative potential of BMP2. The interaction between VEGF and BMP4 shows similar patterns. In a critical-sized defect model, only a low VEGF to BMP4 ratio (1:5) promotes bone regeneration; high ratios inhibit bone regeneration (Peng et al., 2002). In addition, high doses of VEGF inhibit BMP2 expression and high doses of VEGF inhibit osteoblastic differentiation of MSCs *in vitro and in vivo* (Song et al., 2011). Li et al. also observed that co-expression of VEGF and BMP4 in muscle-derived stem cell reduces their bone forming potential (Li et al., 2009). These findings support the conclusion that that too much VEGF is detrimental for the ability of BMPs to induce osteogenesis.

The combination of BMP2 and sFlt1 promoted the production of bone matrix proteins in endothelial lineage cells during bone healing, raising the possibility that co-delivery of the two factors may increase the numbers of bone forming cells with an endothelial origin. Thus, the functional interactions between VEGF and BMP2 complicate the use of VEGF in the context of bone repair. VEGF is not only regulated by BMP2, but it also modulates the signaling transduction of BMP2. It is possible that the individual variations in BMP2 signaling may therefore be partially attributed to variations in VEGF levels at regenerative sites in bone. In cases where abundant osteochondroprogenitors exist and chondrogenesis is favored, adding BMP2 could be beneficial, and inhibition of VEGF by neutralizing antibodies or sFlt1 may enhance cartilage regeneration induced by BMP2. In contrast, in conditions where intramembranous ossification is favored, BMP2 may have detrimental effects on bone regeneration, and decreased levels of extracellular VEGF may stimulate the osteogenic effects of BMP2.

Chapter 5

Conclusions and Perspective

In this Dissertation study, mouse genetics and lineage-tracing strategies were used to obtain insights into VEGF-dependent mechanisms controlling osteoblast differentiation and bone formation during bone repair. The results demonstrate that VEGF controls several steps and processes during the repair of small bone defects. They also provide a biological framework for the development of improved procedures, based on VEGF, to stimulate bone repair and regeneration.

Osteoblast-derived VEGF is important for neutrophil release, macrophage infiltration and angiogenic response during the inflammatory phase of bone repair.

VEGF, produced by osterix-positive osteoblast precursors and their descendants, regulates neutrophil release into the circulation during the initial stage of acute inflammation at a site of injured bone. During the resolution phase when macrophages are recruited to phagocytose dead or aging neutrophils and initiate the repair cascade, VEGF is also critical for macrophage infiltration and early angiogenic responses. The ability of VEGF to promote monocyte/macrophage infiltration, differentiation and/or activation indicates that VEGF may also be important in inflammation driven disorders, such as atherosclerosis and rheumatoid arthritis.

During healing of bone defects, an optimal level of osteoblast-derived VEGF is required for intramembranous ossification in the intramedullary space; too little or too much VEGF leads to impaired bone repair.

In genetically engineered mice with *Vegfa* deleted in osteoblastic cells, bone repair was compromised. The finding highlights the importance of osteoblast-derived VEGF in the support of normal bone healing. In humans, VEGF levels are decreased in

mesenchymal progenitor cells with age or in osteoporosis. Therefore, the data provide a mechanism that may contribute to age/osteoporosis related defective bone healing, and they suggest that VEGF supplementation in osteoblasts may have therapeutic effects. In contrast to large bone defects, only small amounts of VEGF are needed for the healing of small bone defects. In these cases, addition of exogenous VEGF does not stimulate bone regeneration if endogenous VEGF levels are adequate; in fact, excess VEGF may have inhibitory effects. Therefore, when recombinant VEGF is used to bone defects or promote bone regeneration, VEGF dosage should be carefully considered to avoid levels that are beyond the physiological range. The optimal level of VEGF may depend on the specific type of repair. The tibial monocortical defect model examined here is different from most clinical situations. To determine an optimal physiological range of VEGF levels that are required for bone repair, mouse surgical models that better resemble clinical situations, such as bone fracture models or distraction osteogenesis, need to be studied.

Osteoblast-derived VEGF has paracrine, autocrine and intracrine effects. The maintenance of angiogenesis-osteogenesis coupling by VEGF in intra-osseous bone repair is primarily mediated by paracrine effects.

During the initial inflammation after bone injury, angiogenic factors such as VEGF, produced by osteoblasts, act on adjacent endothelial cells to stimulate vasculogenesis and angiogenesis in a paracrine manner. The increased vascularity brings in bone-forming progenitor cells nutrients, oxygen and minerals. In addition, vascular cells release various osteogenic factors, including BMP2, that promote osteoblast

differentiation and mineralization. VEGF, mainly produced by osteoblastic cells, is essential in these processes. Significant reduction of VEGF levels interrupts communication between bone and blood vessels, and impairs intramembranous ossification-mediated bone repair (Figure 32).

In addition to the paracrine effects on blood vessels, osteoblast-derived VEGF affects osteoblast function directly through autocrine and intracrine effects. Expression of VEGF receptors is quite variable in murine osteoblasts, but removal of *Vegfr2* from Osterix-positive precursor cells and their descendants enhances osteoblast maturation and mineralization. This indicates that VEGFR2, albeit expressed at low levels, is functional in osteoblast lineage cells, including CXCL12-positive bone marrow stromal cells, early osteoblast precursors, pre-osteoblasts, mature osteoblasts and osteocytes. The broad range of cellular targets of Osterix-cre-mediated *Vegfr2* deletion limits the interpretation of specific roles of VEGFR2 in osteoblast differentiation. Nonetheless, the enhanced bone repair in defects of *Vegfr2*$^{fl/fl}$*;Osx-cre* mice indirectly highlights the importance of paracrine VEGF signaling in bone repair, and provides a potential mechanism for the inhibitory effects of excess VEGF on intramembranous bone formation during bone repair.

Figure 32

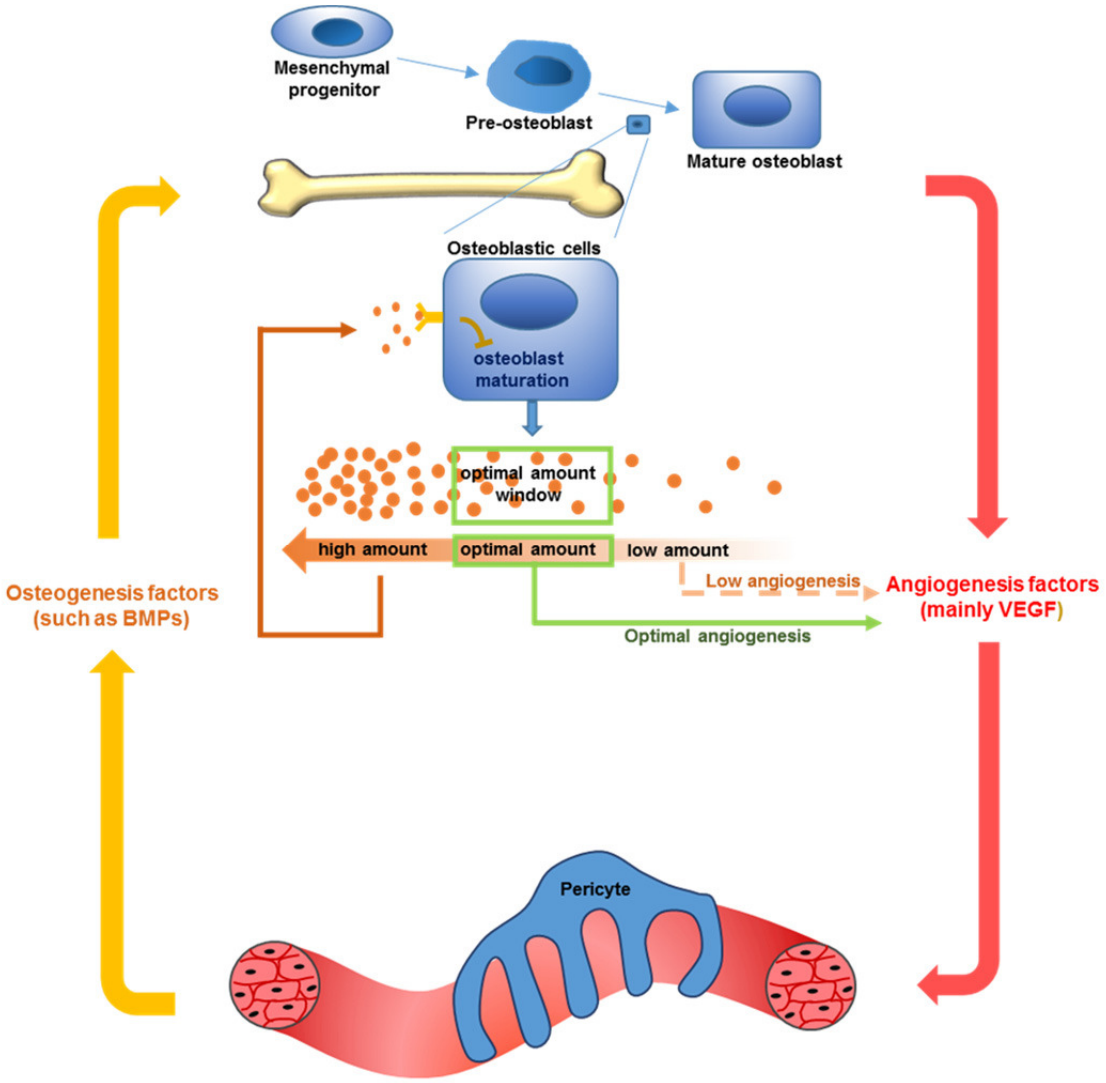
Mesenchymal progenitor
Pre-osteoblast
Mature osteoblast
Osteoblastic cells
osteoblast maturation
optimal amount window
high amount
optimal amount
low amount
Low angiogenesis
Optimal angiogenesis
Osteogenesis factors (such as BMPs)
Angiogenesis factors (mainly VEGF)
Pericyte

Figure 32 (continued). **Schematic diagram illustrating the roles of osteoblast-derived VEGF in healing of bone defects**. During postnatal bone healing, bone cells and blood vessels are in close communication. Stimulated by hypoxia in the inflammation phase, osteoblasts release angiogenic factors, including VEGF, and induce proliferation and migration of endothelial cells. Increased vasculogenesis and angiogenesis bring bone-forming progenitor cells, nutrients, oxygen and minerals necessary for mineralization. In addition, the newly formed vasculature releases osteogenic factors, such as BMP2, promoting osteoblast differentiation and mineralization. In the bone healing process, the levels of VEGF have an optimal range. Reduced VEGF levels decreases communication between bone and blood vessels, and causes compromised bone healing; whereas VEGF levels beyond physiological range have detrimental effects on bone repair po ssibly by inhibiting osteoblast maturation and mineralization via VEGFR2 signaling in osteoblasts.

The roles of osteoblast- or hypertrophic chondrocyte-derived VEGF in periosteal cartilage turnover and remodeling recapitulate VEGF functions in endochondral bone formation during development.

Periosteal thickening during bone repair recapitulates key processes of endochondral ossification during development. This includes cartilage formation, vascular invasion, osteoclastogenesis, proteolytic enzyme activities and cartilage resorption. In addition to delayed degradation of cartilage in the wounded periosteum, *Vegfa* CKO mice also showed strong induction of chondrogenesis, indicating that VEGF might be involved in lineage determination of periosteal progenitor cells towards chondrocytes instead of osteoblasts. Lack of VEGF in hypertrophic chondrocytes in *Vegfa* CKO mice may cause delayed infiltration of blood vessels and osteoclasts. This is consistent with the major phenotypes of $VEGF^{120/120}$ mice (expressing only VEGF120 isoform) and mice treated with sFlt1 systemically during bone development.

Inhibition of VEGF by sFlt1 reverses the inhibitory effect of BMP2 on intramembranous ossification-mediated bone repair during cortical defect healing.

In the current cortical defect model, rBMP2 has different regenerative effects in different repair locations. In the periosteum, it enhances the differentiation of osteochondroprogenitor cells to chondrocytes, while it inhibits osteogenic differentiation of mesenchymal progenitors in the endosteum and bone marrow. In this dissertation study, we found that blocking extracellular VEGF by sFlt1 reverses the inhibitory effects of BMP2 on intramembranous ossification in the intramedullary space during healing of cortical defects. In clinical applications for bone regeneration, rBMP2 shows large

variations in different individuals. This variation may be explained, at least in part, by differences in VEGF levels at bone regenerative sites.

In summary, our data reveal that VEGF, particularly VEGF produced by osteoblast lineage cells, is important during various stages of bone defect repair. The new insights into the details of VEGF functions, in an environment rich in growth factors, skeletal stem cells and bone matrix proteins, may provide a basis for therapeutic strategies based on VEGF modulation to improve bone repair and regeneration. Previous studies and the current dissertation study suggest that VEGF levels in osteoblasts decrease with age. This reduction may well be related to defects in bone repair. If correct, the targeted supplementation of appropriate amounts of VEGF at repair sites may be of substantial clinical value in the treatment of patients with defective bone healing.

Bibliography

Abedi H, Zachary I (1997). Vascular endothelial growth factor stimulates tyrosine phosphorylation and recruitment to new focal adhesions of focal adhesion kinase and paxillin in endothelial cells. *Journal of Biological Chemistry* 272(24)*:*15442-15451.

Ai-Aql ZS, Alagl AS, Graves DT, Gerstenfeld LC, Einhorn TA (2008). Molecular mechanisms controlling bone formation during fracture healing and distraction osteogenesis. *J Dent Res* 87(2)*:*107-118.

Albanese A, Licata ME, Polizzi B, Campisi G (2013). Platelet-rich plasma (PRP) in dental and oral surgery: from the wound healing to bone regeneration. *Immun Ageing* 10:23

Aldridge SE, Lennard TWJ, Williams JR, Birch MA (2005). Vascular endothelial growth factor receptors in osteoclast differentiation and function. *Biochem Bioph Res Co* 335(3)*:*793-798.

Alva JA, Zovein AC, Monvoisin A, Murphy T, Salazar A, Harvey NL *et al.* (2006). VE-Cadherin-Cre-recombinase transgenic mouse: a tool for lineage analysis and gene deletion in endothelial cells. *Developmental dynamics : an official publication of the American Association of Anatomists* 235(3)*:*759-767.

Ancelin M, Chollet-Martin S, Herve MA, Legrand C, El Benna J, Perrot-Applanat M (2004). Vascular endothelial growth factor VEGF189 induces human neutrophil chemotaxis in extravascular tissue via an autocrine amplification mechanism. *Lab Invest* 84(4)*:*502-512.

Baker JC, Beddington RSP, Harland RM (1999). Wnt signaling in Xenopus embryos inhibits Bmp4 expression and activates neural development. *Gene Dev* 13(23)*:*3149-3159.

Bakker AD, Klein-Nulend J (2012). Osteoblast Isolation from Murine Calvaria and Long Bones. *Methods Mol Biol* 816:19-29.

Ball SG, Shuttleworth CA, Kielty CM (2007). Vascular endothelial growth factor can signal through platelet-derived growth factor receptors. *J Cell Biol* 177(3)*:*489-500.

Barleon B, Sozzani S, Zhou D, Weich HA, Mantovani A, Marme D (1996). Migration of human monocytes in response to vascular endothelial growth factor (VEGF) is mediated via the VEGF receptor flt-1. *Blood* 87(8)*:*3336-3343.

Barleon B, Siemeister G, MartinyBaron G, Weindel K, Herzog C, Marme D (1997). Vascular endothelial growth factor up-regulates its receptor fms-like tyrosine kinase 1

(FLT-1) and a soluble variant of FLT-1 in human vascular endothelial cells. *Cancer research* 57(23)*:*5421-5425.

Behr B, Leucht P, Longaker MT, Quarto N (2010). Fgf-9 is required for angiogenesis and osteogenesis in long bone repair. *P Natl Acad Sci USA* 107(26)*:*11853-11858.

Benjamin LE, Hemo I, Keshet E (1998). A plasticity window for blood vessel remodelling is defined by pericyte coverage of the preformed endothelial network and is regulated by PDGF-B and VEGF. *Development* 125(9)*:*1591-1598.

Bergers G, Song S, Meyer-Morse N, Bergsland E, Hanahan D (2003). Benefits of targeting both pericytes and endothelial cells in the tumor vasculature with kinase inhibitors. *The Journal of clinical investigation* 111(9)*:*1287-1295.

Bishop JA, Palanca AA, Bellino MJ, Lowenberg DW (2012). Assessment of Compromised Fracture Healing. *J Am Acad Orthop Sur* 20(5)*:*273-282.

Boyne PJ, Marx RE, Nevins M, Triplett G, Lazaro E, Lilly LC *et al.* (1997). A feasibility study evaluating rhBMP-2/absorbable collagen sponge for maxillary sinus floor augmentation. *Int J Periodont Rest* 17(1)*:*10-25.

Brancato SK, Albina JE (2011). Wound Macrophages as Key Regulators of Repair Origin, Phenotype, and Function. *Am J Pathol* 178(1)*:*19-25.

Bruder SP, Fink DJ, Caplan AI (1994). Mesenchymal Stem-Cells in in Bone-Development, Bone Repair, and Skeletal Regeneration Therapy. *J Cell Biochem* 56(3)*:*283-294.

Caplan AI, Correa D (2011). PDGF in Bone Formation and Regeneration: New Insights into a Novel Mechanism Involving MSCs. *J Orthop Res* 29(12)*:*1795-1803.

Carlevaro MF, Cermelli S, Cancedda R, Cancedda FD (2000). Vascular endothelial growth factor (VEGF) in cartilage neovascularization and chondrocyte differentiation: auto-paracrine role during endochondral bone formation. *Journal of cell science* 113(1)*:*59-69.

Carmeliet P, Moons L, Luttun A, Vincenti V, Compernolle V, De Mol M *et al.* (2001). Synergism between vascular endothelial growth factor and placental growth factor contributes to angiogenesis and plasma extravasation in pathological conditions. *Nat Med* 7(5)*:*575-583.

Chan CKF, Seo EY, Chen JY, Lo D, McArdle A, Sinha R *et al.* (2015). Identification and Specification of the Mouse Skeletal Stem Cell. *Cell* 160(1-2)*:*285-298.

Chang CP, Neilson JR, Bayle JH, Gestwicki JE, Kuo A, Stankunas K *et al.* (2004). A field of myocardial-endocardial NFAT signaling underlies heart valve morphogenesis. *Cell* 118(5)*:*649-663.

Chen JQ, Shi Y, Regan J, Karuppaiah K, Ornitz DM, Long FX (2014). Osx-Cre Targets Multiple Cell Types besides Osteoblast Lineage in Postnatal Mice. *Plos One* 9(1).

Chen L, He ZQ, Chen B, Yang MJ, Zhao YN, Sun WJ *et al.* (2010). Loading of VEGF to the heparin cross-linked demineralized bone matrix improves vascularization of the scaffold. *J Mater Sci-Mater M* 21(1)*:*309-317.

Choi IH, Chung CY, Cho TJ, Yoo WJ (2002). Angiogenesis and mineralization during distraction osteogenesis. *J Korean Med Sci* 17(4)*:*435-447.

Claesson-Welsh L (2008). VEGF-B taken to our hearts - Specific effect of VEGF-B in myocardial ischemia. *Arterioscl Throm Vas* 28(9)*:*1575-1576.

Clarkin CE, Gerstenfeld LC (2013). VEGF and bone cell signalling: an essential vessel for communication? *Cell Biochem Funct* 31(1)*:*1-11.

Clauss M, Gerlach M, Gerlach H, Brett J, Wang F, Familletti PC *et al.* (1990). Vascular-Permeability Factor - a Tumor-Derived Polypeptide That Induces Endothelial-Cell and Monocyte Procoagulant Activity, and Promotes Monocyte Migration. *J Exp Med* 172(6)*:*1535-1545.

Colnot C (2009). Skeletal Cell Fate Decisions Within Periosteum and Bone Marrow During Bone Regeneration. *J Bone Miner Res* 24(2)*:*274-282.

Conn G, Bayne ML, Soderman DD, Kwok PW, Sullivan KA, Palisi TM *et al.* (1990). Amino-Acid and Cdna Sequences of a Vascular Endothelial-Cell Mitogen That Is Homologous to Platelet-Derived Growth-Factor. *P Natl Acad Sci USA* 87(7)*:*2628-2632.

Costa N, Paramanathan S, Mac Donald D, Wierzbicki AS, Hampson G (2009). Factors regulating circulating vascular endothelial growth factor (VEGF): Association with bone mineral density (BMD) in post-menopausal osteoporosis. *Cytokine* 46(3)*:*376-381.

Coultas L, Chawengsaksophak K, Rossant J (2005). Endothelial cells and VEGF in vascular development. *Nature* 438(7070)*:*937-945.

Crane JL, Cao X (2014). Function of matrix IGF-1 in coupling bone resorption and formation. *J Mol Med* 92(2)*:*107-115.

Cross MJ, Dixelius J, Matsumoto T, Claesson-Welsh L (2003). VEGF-receptor signal transduction. *Trends in biochemical sciences* 28(9)*:*488-494.

Cu ZP, Zhang X, Li L, Wang QG, Yu XX, Feng T (2013). Acceleration of segmental bone regeneration in a rabbit model by strontium-doped calcium polyphosphate scaffold through stimulating VEGF and bFGF secretion from osteoblasts. *Mat Sci Eng C-Mater* 33(1)*:*274-281.

Deckers MML, Karperien M, van der Bent C, Yamashita T, Papapoulos SE, Lowik CWGM (2000). Expression of vascular endothelial growth factors and their receptors during osteoblast differentiation. *Endocrinology* 141(5)*:*1667-1674.

Deckers MML, van Bezooijen RL, van der Horst G, Hoogendam J, van der Bent C, Papapoulos SE *et al.* (2002). Bone morphogenetic proteins stimulate angiogenesis through osteoblast-derived vascular endothelial growth factor A. *Endocrinology* 143(4)*:*1545-1553.

Dimitriou R, Tsiridis E, Giannoudis PV (2005). Current concepts of molecular aspects of bone healing. *Injury* 36(12)*:*1392-1404.

Ding WG, Wei ZX, Liu JB (2011). Reduced local blood supply to the tibial metaphysis is associated with ovariectomy-induced osteoporosis in mice. *Connect Tissue Res* 52(1)*:*25-29.

Dor Y, Camenisch T, Itin A, Fishman GI, McDonald JA, Carmeliet P *et al.* (2001). A novel role for VEGF in endocardial cushion formation and its potential contribution to congenital heart defects. *Development* 128(9)*:*1531-1538.

Eash KJ, Greenbaum AM, Gopalan PK, Link DC (2010). CXCR2 and CXCR4 antagonistically regulate neutrophil trafficking from murine bone marrow. *J Clin Invest* 120(7)*:*2423-2431.

Eckardt H, Bundgaard KG, Christensen KS, Lind M, Hansen ES, Hvid I (2003). Effects of locally applied vascular endothelial growth factor (VEGF) and VEGF-inhibitor to the rabbit tibia during distraction osteogenesis. *J Orthop Res* 21(2)*:*335-340.

Efimenko A, Starostina E, Kalinina N, Stolzing A (2011). Angiogenic properties of aged adipose derived mesenchymal stem cells after hypoxic conditioning. *Journal of translational medicine* 9:10.

Emad B, Sherif el M, Basma GM, Wong RW, Bendeus M, Rabie AB (2006). Vascular endothelial growth factor augments the healing of demineralized bone matrix grafts. *International journal of surgery* 4(3)*:*160-166.

Ferguson C, Alpern E, Miclau T, Helms JA (1999). Does adult fracture repair recapitulate embryonic skeletal formation? *Mechanisms of development* 87(1-2)*:*57-66.

Ferrara N, DavisSmyth T (1997). The biology of vascular endothelial growth factor. *Endocr Rev* 18(1)*:*4-25.

Ferrara N, Gerber HP, LeCouter J (2003). The biology of VEGF and its receptors. *Nat Med* 9(6)*:*669-676.

Fuentealba LC, Eivers E, Ikeda A, Hurtado C, Kuroda H, Pera EM *et al.* (2007). Integrating patterning signals: Wnt/GSK3 regulates the duration of the BMP/Smad1 signal. *Cell* 131(5)*:*980-993.

Fujimura K, Bessho K, Okubo Y, Kusumoto K, Segami N, Iizuka T (2002). The effect of fibroblast growth factor-2 on the osteoinductive activity of recombinant human bone morphogenetic protein-2 in rat muscle. *Arch Oral Biol* 47(8)*:*577-584.

Fulton D, Gratton JP, McCabe TJ, Fontana J, Fujio Y, Walsh K *et al.* (1999). Regulation of endothelium-derived nitric oxide production by the protein kinase Akt. *Nature* 399(6736)*:*597-601.

Geng HQ, Song H, Qi J, Cui DX (2011). Sustained release of VEGF from PLGA nanoparticles embedded thermo-sensitive hydrogel in full-thickness porcine bladder acellular matrix. *Nanoscale Res Lett* 6(1):312.

Gerber HP, Vu TH, Ryan AM, Kowalski J, Werb Z, Ferrara N (1999). VEGF couples hypertrophic cartilage remodeling, ossification and angiogenesis during endochondral bone formation. *Nat Med* 5(6)*:*623-628.

Gerber HP, Malik AK, Solar GP, Sherman D, Liang XH, Meng G *et al.* (2002). VEGF regulates haematopoietic stem cell survival by an internal autocrine loop mechanism. *Nature* 417(6892)*:*954-958.

Goad DL, Rubin J, Wang H, Tashjian AH, Patterson C (1996). Enhanced expression of vascular endothelial growth factor in human SaOS-2 osteoblast-like cells and murine osteoblasts induced by insulin-like growth factor I. *Endocrinology* 137(6)*:*2262-2268.

Gomez-Barrena E, Rosset P, Lozano D, Stanovici J, Ermthaller C, Gerbhard F (2015). Bone fracture healing: Cell therapy in delayed unions and nonunions. *Bone* 70(93-101.

Greenberg JI, Shields DJ, Barillas SG, Acevedo LM, Murphy E, Huang JH *et al.* (2008). A role for VEGF as a negative regulator of pericyte function and vessel maturation. *Nature* 456(7223)*:*809-U101.

Groeneveld EHJ, Burger EH (2000). Bone morphogenetic proteins in human bone regeneration. *Eur J Endocrinol* 142(1)*:*9-21.

Hanada K, Dennis JE, Caplan AI (1997). Stimulatory effects of basic fibroblast growth factor and bone morphogenetic protein-2 on osteogenic differentiation of rat bone marrow-derived mesenchymal stem cells. *J Bone Miner Res* 12(10)*:*1606-1614.

Harada S, Nagy JA, Sullivan KA, Thomas KA, Endo N, Rodan GA *et al.* (1994). Induction of Vascular Endothelial Growth-Factor Expression by Prostaglandin E(2) and E(1) in Osteoblasts. *J Clin Invest* 93(6)*:*2490-2496.

Hattori K, Heissig B, Wu Y, Dias S, Tejada R, Ferris B *et al.* (2002). Placental growth factor reconstitutes hematopoiesis by recruiting VEGFR1(+) stem cells from bone-marrow microenvironment. *Nat Med* 8(8)*:*841-849.

He LZ, Marneros AG (2013). Macrophages Are Essential for the Early Wound Healing Response and the Formation of a Fibrovascular Scar. *Am J Pathol* 182(6)*:*2407-2417.

Henriksen K, Karsdal M, Delaisse JM, Engsig MT (2003). RANKL and vascular endothelial growth factor (VEGF) induce osteoclast chemotaxis through an ERK1/2-dependent mechanism. *Journal of Biological Chemistry* 278(49)*:*48745-48753.

Hoeben A, Landuyt B, Highley MS, Wildiers H, Van Oosterom AT, De Bruijn EA (2004). Vascular endothelial growth factor and angiogenesis. *Pharmacol Rev* 56(4)*:*549-580.

Howell TH, Fiorellini J, Jones A, Alder M, Nummikoski P, Lazaro M *et al.* (1997). A feasibility study evaluating rhBMP-2 absorbable collagen sponge device for local alveolar ridge preservation or augmentation. *Int J Periodont Rest* 17(2)*:*124-39.

Jaasma MJ, Jackson WM, Tang RY, Keaveny TM (2007). Adaptation of cellular mechanical behavior to mechanical loading for osteoblastic cells. *Journal of biomechanics* 40(9)*:*1938-1945.

Jacobsen KA, Al-Aql ZS, Wan C, Fitch JL, Stapleton SN, Mason ZD *et al.* (2008). Bone formation during distraction osteogenesis is dependent on both VEGFR1 and VEGFR2 signaling. *J Bone Miner Res* 23(5)*:*596-609.

Jiang S, Haider HK, Ahmed RPH, Idris NM, Salim A, Ashraf M (2008). Transcriptional profiling of young and old mesenchymal stem cells in response to oxygen deprivation and reparability of the infarcted myocardium. *J Mol Cell Cardiol* 44(3)*:*582-596.

Jinnin M, Medici D, Park L, Limaye N, Liu Y, Boscolo E *et al.* (2008). Suppressed NFAT-dependent VEGFR1 expression and constitutive VEGFR2 signaling in infantile hemangioma. *Nat Med* 14(11)*:*1236-1246.

Joukov V, Pajusola K, Kaipainen A, Chilov D, Lahtinen I, Kukk E *et al.* (1996). A novel vascular endothelial growth factor, VEGF-C, is a ligand for the Flt4 (VEGFR-3) and KDR (VEGFR-2) receptor tyrosine kinases. *The EMBO journal* 15(7)*:*1751.

Jung YD, Liu W, Reinmuth N, Ahmad SA, Fan F, Gallick GE *et al.* (2001). Vascular endothelial growth factor is upregulated by interleukin-1 beta in human vascular smooth muscle cells via the P38 mitogen-activated protein kinase pathway. *Angiogenesis* 4(2)*:*155-162.

Kaigler D, Silva EA, Mooney DJ (2013). Guided Bone Regeneration Using Injectable Vascular Endothelial Growth Factor Delivery Gel. *J Periodontol* 84(2)*:*230-238.

Kaipel M, Schutzenberger S, Schultz A, Ferguson J, Slezak P, Morton TJ *et al.* (2012). BMP-2 but not VEGF or PDGF in fibrin matrix supports bone healing in a delayed-union rat model. *J Orthop Res* 30(10)*:*1563-1569.

Kamiya N, Ye L, Kobayashi T, Mochida Y, Yamauchi M, Kronenberg HM *et al.* (2008). BMP signaling negatively regulates bone mass through sclerostin by inhibiting the canonical Wnt pathway. *Development* 135(22)*:*3801-3811.

Kawao N, Tamura Y, Okumoto K, Yano M, Okada K, Matsuo O *et al.* (2013). Plasminogen plays a crucial role in bone repair. *J Bone Miner Res* 28(7)*:*1561-1574.

Kim JB, Leucht P, Lam K, Luppen C, Ten Berge D, Nusse R *et al.* (2007). Bone regeneration is regulated by Wnt signaling. *J Bone Miner Res* 22(12)*:*1913-1923.

Koch S, Tugues S, Li X, Gualandi L, Claesson-Welsh L (2011). Signal transduction by vascular endothelial growth factor receptors. *Biochem J* 437(2)*:*169-183.

Kodama H, Yamasaki A, Nose M, Niida S, Ohgame Y, Abe M *et al.* (1991). Congenital Osteoclast Deficiency in Osteopetrotic (Op/Op) Mice Is Cured by Injections of Macrophage Colony-Stimulating Factor. *J Exp Med* 173(1)*:*269-272.

Krock BL, Skuli N, Simon MC (2011). Hypoxia-induced angiogenesis: good and evil. *Genes & cancer* 2(12)*:*1117-1133.

Kubo S, Cooper GM, Matsumoto T, Phillippi JA, Corsi KA, Usas A *et al.* (2009). Blocking Vascular Endothelial Growth Factor With Soluble Flt-1 Improves the Chondrogenic Potential of Mouse Skeletal Muscle-Derived Stem Cells. *Arthritis Rheum* 60(1)*:*155-165.

Lamalice L, Houle F, Jourdan G, Huot J (2004). Phosphorylation of tyrosine 1214 on VEGFR2 is required for VEGF-induced activation of Cdc42 upstream of SAPK2/p38. *Oncogene* 23(2)*:*434-445.

Lee S, Chen TT, Barber CL, Jordan MC, Murdock J, Desai S *et al.* (2007). Autocrine VEGF signaling is required for vascular homeostasis. *Cell* 130(4)*:*691-703.

Leek RD, Hunt NC, Landers RJ, Lewis CE, Royds JA, Harris AL (2000). Macrophage infiltration is associated with VEGF and EGFR expression in breast cancer. *J Pathol* 190(4)*:*430-436.

Li GH, Corsi-Payne K, Zheng B, Usas A, Peng HR, Huard J (2009). The Dose of Growth Factors Influences the Synergistic Effect of Vascular Endothelial Growth Factor on Bone Morphogenetic Protein 4-Induced Ectopic Bone Formation. *Tissue Eng Pt A* 15(8)*:*2123-2133.

Lim SR, Zhang Y, Zhang DF, Chen F, Hosaka K, Feng NH *et al.* (2014). VEGFR2-Mediated Vascular Dilation as a Mechanism of VEGF-Induced Anemia and Bone Marrow Cell Mobilization. *Cell Rep* 9(2)*:*569-580.

Lin EY, Li JF, Gnatovskiy L, Deng Y, Zhu L, Grzesik DA *et al.* (2006). Macrophages regulate the angiogenic switch in a mouse model of breast cancer. *Cancer research* 66(23)*:*11238-11246.

Liu D, Jia HY, Holmes DIR, Stannard A, Zachary I (2003). Vascular endothelial growth factor-regulated gene expression in endothelial cells - KDR-mediated induction of Egr3 and the related nuclear receptors Nur77, Nurr1, and Nor1. *Arterioscl Throm Vas* 23(11)*:*2002-2007.

Liu D, Evans I, Britton G, Zachary I (2008). The zinc-finger transcription factor, early growth response 3, mediates VEGF-induced angiogenesis. *Oncogene* 27(21)*:*2989-2998.

Liu YQ, Berendsen AD, Jia SD, Lotinun S, Baron R, Ferrara N *et al.* (2012). Intracellular VEGF regulates the balance between osteoblast and adipocyte differentiation. *J Clin Invest* 122(9)*:*3101-3113.

Maeda T, Kawane T, Horiuchi N (2003). Statins augment vascular endothelial growth factor expression in osteoblastic cells vial inhibition of protein prenylation. *Endocrinology* 144(2)*:*681-692.

Maes C, Stockmans I, Moermans K, Van Looveren R, Smets N, Carmeliet P *et al.* (2004). Soluble VEGF isoforms are essential for establishing epiphyseal vascularization and regulating chondrocyte development and survival. *The Journal of clinical investigation* 113(2)*:*188-199.

Maes C, Coenegrachts L, Stockmans I, Daci E, Luttun A, Petryk A *et al.* (2006). Placental growth factor mediates mesenchymal cell development, cartilage turnover, and bone remodeling during fracture repair. *J Clin Invest* 116(5)*:*1230-1242.

Maes C, Kobayashi T, Selig MK, Torrekens S, Roth SI, Mackem S *et al.* (2010). Osteoblast Precursors, but Not Mature Osteoblasts, Move into Developing and Fractured Bones along with Invading Blood Vessels. *Dev Cell* 19(2)*:*329-344.

Maharaj ASR, D'Amore PA (2007). Roles for VEGF in the adult. *Microvasc Res* 74(2-3)*:*100-113.

Makinen T, Veikkola T, Mustjoki S, Karpanen T, Catimel B, Nice EC *et al.* (2001). Isolated lymphatic endothelial cells transduce growth, survival and migratory signals via the VEGF-C/D receptor VEGFR-3. *Embo Journal* 20(17)*:*4762-4773.

Marsell R, Einhorn TA (2011). The biology of fracture healing. *Injury* 42(6)*:*551-555.

Maru Y, Yamaguchi S, Shibuya M (1998). Flt-1, a receptor for vascular endothelial growth factor, has transforming and morphogenic potentials. *Oncogene* 16(20)*:*2585-2595.

Matsubara H, Hogan DE, Morgan EF, Mortlock DP, Einhorn TA, Gerstenfeld LC (2012). Vascular tissues are a primary source of BMP2 expression during bone formation induced by distraction osteogenesis. *Bone* 51(1)*:*168-180.

Matsumoto T, Cooper GM, Gharaibeh B, Meszaros LB, Li G, Usas A *et al.* (2008). Blocking VEGF as a potential approach to improve cartilage healing after osteoarthritis. *Journal of musculoskeletal & neuronal interactions* 8(4)*:*316-317.

Matsumoto T, Cooper GM, Gharaibeh B, Meszaros LB, Li GG, Usas A *et al.* (2009). Cartilage Repair in a Rat Model of Osteoarthritis Through Intraarticular Transplantation of Muscle-Derived Stem Cells Expressing Bone Morphogenetic Protein 4 and Soluble Flt-1. *Arthritis Rheum* 60(5)*:*1390-1405.

Maxwell PH, Wiesener MS, Chang GW, Clifford SC, Vaux EC, Cockman ME *et al.* (1999). The tumour suppressor protein VHL targets hypoxia-inducible factors for oxygen-dependent proteolysis. *Nature* 399(6733)*:*271-275.

Mayr-Wohlfart U, Waltenberger J, Hausser H, Kessler S, Gunther KP, Dehio C *et al.* (2002). Vascular endothelial growth factor stimulates chemotactic migration of primary human osteoblasts. *Bone* 30(3)*:*472-477.

Medici D, Shore EM, Lounev VY, Kaplan FS, Kalluri R, Olsen BR (2010). Conversion of vascular endothelial cells into multipotent stem-like cells. *Nat Med* 16(12)*:*1400-U1480.

Mi M, Jin HT, Wang BL, Yukata K, Sheu TJ, Ke QH *et al.* (2013). Chondrocyte BMP2 signaling plays an essential role in bone fracture healing. *Gene* 512(2)*:*211-218.

Minear S, Leucht P, Jiang J, Liu B, Zeng A, Fuerer C *et al.* (2010a). Wnt Proteins Promote Bone Regeneration. *Sci Transl Med* 2(29).

Minear S, Leucht P, Miller S, Helms JA (2010b). rBMP Represses Wnt Signaling and Influences Skeletal Progenitor Cell Fate Specification During Bone Repair. *J Bone Miner Res* 25(6)*:*1196-1207.

Muller YA, Li B, Christinger HW, Wells JA, Cunningham BC, DeVos AM (1997). Vascular endothelial growth factor: Crystal structure and functional mapping of the kinase domain receptor binding site. *Proceedings of the National Academy of Sciences of the United States of America* 94(14)*:*7192-7197.

Nakagawa M, Kaneda T, Arakawa T, Morita S, Sato T, Yomada T *et al.* (2000). Vascular endothelial growth factor (VEGF) directly enhances osteoclastic bone resorption and survival of mature osteoclasts. *Febs Lett* 473(2)*:*161-164.

Nakai T, Yoshimura Y, Deyama Y, Suzuki K, Iida J (2009). Mechanical stress up-regulates RANKL expression via the VEGF autocrine pathway in osteoblastic MC3T3-E1 cells. *Mol Med Rep* 2(2)*:*229-234.

Neufeld G, Cohen T, Gengrinovitch S, Poltorak Z (1999). Vascular endothelial growth factor (VEGF) and its receptors. *Faseb J* 13(1)*:*9-22.

Niida S, Kaku M, Amano H, Yoshida H, Kataoka H, Nishikawa S *et al.* (1999). Vascular endothelial growth factor can substitute for macrophage colony-stimulating factor in the support of osteoclastic bone resorption. *J Exp Med* 190(2)*:*293-298.

Olofsson B, Korpelainen E, Pepper MS, Mandriota SJ, Aase K, Kumar V *et al.* (1998). Vascular endothelial growth factor B (VEGF-B) binds to VEGF receptor-1 and regulates plasminogen activator activity in endothelial cells. *Proceedings of the National Academy of Sciences of the United States of America* 95(20)*:*11709-11714.

Olsson AK, Dimberg A, Kreuger J, Claesson-Welsh L (2006). VEGF receptor signalling - in control of vascular function. *Nat Rev Mol Cell Bio* 7(5)*:*359-371.

Ono N, Ono W, Nagasawa T, Kronenberg HM (2014). A subset of chondrogenic cells provides early mesenchymal progenitors in growing bones. *Nature cell biology* 16(12)*:*1157-1167.

Park JE, Chen HH, Winer J, Houck KA, Ferrara N (1994). Placenta growth factor. Potentiation of vascular endothelial growth factor bioactivity, in vitro and in vivo, and high affinity binding to Flt-1 but not to Flk-1/KDR. *The Journal of biological chemistry* 269(41)*:*25646-25654.

Peng HR, Wright V, Usas A, Gearhart B, Shen HC, Cummins J *et al.* (2002). Synergistic enhancement of bone formation and healing by stem cell-expressed VEGF and bone morphogenetic protein-4. *J Clin Invest* 110(6)*:*751-759.

Peng HR, Usas A, Olshanski A, Ho AM, Gearhart B, Cooper GM *et al.* (2005). VEGF improves, whereas sFlt1 inhibits, BMP2-induced bone formation and bone healing through modulation of angiogenesis. *J Bone Miner Res* 20(11)*:*2017-2027.

Pennock S, Kazlauskas A (2012). Vascular Endothelial Growth Factor A Competitively Inhibits Platelet-Derived Growth Factor (PDGF)-Dependent Activation of PDGF Receptor and Subsequent Signaling Events and Cellular Responses. *Mol Cell Biol* 32(10)*:*1955-1966.

Pepper MS, Wasi S, Ferrara N, Orci L, Montesano R (1994). In-Vitro Angiogenic and Proteolytic Properties of Bovine Lymphatic Endothelial-Cells. *Exp Cell Res* 210(2)*:*298-305.

Pfander D, Swoboda B, Cramer T (2006). The role of HIF-1alpha in maintaining cartilage homeostasis and during the pathogenesis of osteoarthritis. *Arthritis research & therapy* 8(1)*:*104.

Phillips GD, Stone AM, Jones BD, Schultz JC, Whitehead RA, Knighton DR (1994). Vascular endothelial growth factor (rhVEGF165) stimulates direct angiogenesis in the rabbit cornea. *In vivo* 8(6)*:*961-965.

Pola R, Aprahamian TR, Bosch-Marce M, Curry C, Gaetani E, Flex A *et al.* (2004). Age-dependent VEGF expression and intraneural neovascularization during regeneration of peripheral nerves. *Neurobiol Aging* 25(10)*:*1361-1368.

Pufe T, Scholz-Ahrens KE, Franke ATM, Petersen W, Mentlein R, Varoga D *et al.* (2003). The role of vascular endothelial growth factor in glucocorticoid-induced bone loss: evaluation in a minipig model. *Bone* 33(6)*:*869-876.

Rankin EB, Wu C, Khatri R, Wilson TLS, Andersen R, Araldi E *et al.* (2012). The HIF Signaling Pathway in Osteoblasts Directly Modulates Erythropoiesis through the Production of EPO. *Cell* 149(1)*:*63-74.

Rodda SJ, McMahon AP (2006). Distinct roles for Hedgehog and canonical Wnt signaling in specification, differentiation and maintenance of osteoblast progenitors. *Development* 133(16)*:*3231-3244.

Rosen V (2009). BMP2 signaling in bone development and repair. *Cytokine Growth F R* 20(5-6)*:*475-480.

Saadeh PB, Mehrara BJ, Steinbrech DS, Spector JA, Greenwald JA, Chim GS *et al.* (2000). Mechanisms of fibroblast growth factor-2 modulation of vascular endothelial growth factor expression by osteoblastic cells. *Endocrinology* 141(6)*:*2075-2083.

Schipani E, Maes C, Carmeliet G, Semenza GL (2009). Regulation of Osteogenesis-Angiogenesis Coupling by HIFs and VEGF. *J Bone Miner Res* 24(8)*:*1347-1353.

Schonmeyr BH, Soares M, Avraham T, Clavin NW, Gewalli F, Mehrara BJ (2010). Vascular Endothelial Growth Factor Inhibits Bone Morphogenetic Protein 2 Expression in Rat Mesenchymal Stem Cells. *Tissue Eng Pt A* 16(2)*:*653-662.

Schweighofer B, Testori J, Sturtzel C, Sattler S, Mayer H, Wagner O *et al.* (2009). The VEGF-induced transcriptional response comprises gene clusters at the crossroad of angiogenesis and inflammation. *Thromb Haemostasis* 102(3)*:*544-554.

Senel K, Baykal T, Seferoglu B, Altas EU, Baygutalp F, Ugur M *et al.* (2013). Circulating vascular endothelial growth factor concentrations in patients with postmenopausal osteoporosis. *Arch Med Sci* 9(4)*:*709-712.

Silva EA, Mooney DJ (2010). Effects of VEGF temporal and spatial presentation on angiogenesis. *Biomaterials* 31(6)*:*1235-1241.

Simon AM, Manigrasso MB, O'Connor JP (2002). Cyclo-oxygenase 2 function is essential for bone fracture healing. *J Bone Miner Res* 17(6)*:*963-976.

Sleeman JP (2006). The relationship between tumors and the lymphatics: What more is there to know? *Lymphology* 39(2)*:*62-68.

Song XB, Liu SH, Qu X, Hu YW, Zhang XY, Wang T *et al.* (2011). BMP2 and VEGF promote angiogenesis but retard terminal differentiation of osteoblasts in bone regeneration by up-regulating Id1. *Acta Bioch Bioph Sin* 43(10)*:*796-804.

Spector JA, Mehrara BJ, Greenwald JA, Saadeh PB, Steinbrech DS, Bouletreau PJ *et al.* (2001). Osteoblast expression of vascular endothelial growth factor is modulated by the extracellular microenvironment. *Am J Physiol-Cell Ph* 280(1)*:*C72-C80.

Steinbrech DS, Mehrara BJ, Saadeh PB, Greenwald JA, Spector JA, Gittes GK *et al.* (2000). VEGF expression in an osteoblast-like cell line is regulated by a hypoxia response mechanism. *Am J Physiol-Cell Ph* 278(4)*:*C853-C860.

Street J, Winter D, Wang JH, Wakai A, McGuinness A, Redmond HP (2000). Is human fracture hematoma inherently angiogenic? *Clinical orthopaedics and related research* 378)*:*224-237.

Street J, Bao M, deGuzman L, Bunting S, Peale FV, Ferrara N *et al.* (2002). Vascular endothelial growth factor stimulates bone repair by promoting angiogenesis and bone turnover. *Proceedings of the National Academy of Sciences of the United States of America* 99(15)*:*9656-9661.

Sunderkotter C, Goebeler M, Schulzeosthoff K, Bhardwaj R, Sorg C (1991). Macrophage-Derived Angiogenesis Factors. *Pharmacol Therapeut* 51(2)*:*195-216.

Swift ME, Kleinman HK, DiPietro LA (1999). Impaired wound repair and delayed angiogenesis in aged mice. *Lab Invest* 79(12)*:*1479-1487.

Taipaleenmaki H, Suomi S, Hentunen T, Laitala-Leinonen T, Saamanen AM (2008). Impact of stromal cell composition on BMP-induced chondrogenic differentiation of mouse bone marrow derived mesenchymal cells. *Experimental cell research* 314(13)*:*2400-2410.

Takahashi T, Ueno H, Shibuya M (1999). VEGF activates protein kinase C-dependent, but Ras-independent Raf-MEK-MAP kinase pathway for DNA synthesis in primary endothelial cells. *Oncogene* 18(13)*:*2221-2230.

Tang WJ, Yang F, Li Y, de Crombrugghe B, Jiao HL, Xiao GZ *et al.* (2012). Transcriptional Regulation of Vascular Endothelial Growth Factor (VEGF) by Osteoblast-specific Transcription Factor Osterix (Osx) in Osteoblasts. *Journal of Biological Chemistry* 287(3)*:*1671-1678.

Tang Y, Wu X, Lei W, Pang L, Wan C, Shi Z *et al.* (2009). TGF-beta1-induced migration of bone mesenchymal stem cells couples bone resorption with formation. *Nat Med* 15(7)*:*757-765.

Tarkka T, Sipola A, Jamsa T, Soini Y, Yla-Herttuala S, Tuukkanen J *et al.* (2003). Adenoviral VEGF-A gene transfer induces angiogenesis and promotes bone formation in healing osseous tissues. *The journal of gene medicine* 5(7)*:*560-566.

ten Berge D, Brugmann SA, Helms JA, Nusse R (2008). Wnt and FGF signals interact to coordinate growth with cell fate specification during limb development. *Development* 135(19)*:*3247-3257.

Thi MM, Iacobas DA, Iacobas S, Spray DC (2007). Fluid shear stress upregulates vascular endothelial growth factor gene expression in osteoblasts. *Ann Ny Acad Sci* 1117:73-81.

Thi MM, Suadicani SO, Spray DC (2010). Fluid Flow-induced Soluble Vascular Endothelial Growth Factor Isoforms Regulate Actin Adaptation in Osteoblasts. *Journal of Biological Chemistry* 285(40)*:*30931-30941.

Tonnesen MG, Feng XD, Clark RAF (2000). Angiogenesis in wound healing. *J Invest Derm Symp P* 5(1)*:*40-46.

Tsartsalis AN, Dokos C, Kaiafa GD, Tsartsalis DN, Kattamis A, Hatzitolios AI *et al.* (2012). Statins, bone formation and osteoporosis: hope or hype? *Horm-Int J Endocrino* 11(2)*:*126-139.

Tsuji K, Bandyopadhyay A, Harfe BD, Cox K, Kakar S, Gerstenfeld L *et al.* (2006). BMP2 activity, although dispensable for bone formation, is required for the initiation of fracture healing. *Nat Genet* 38(12)*:*1424-1429.

Tzeng HE, Tsai CH, Chang ZL, Su CM, Wang SW, Hwang WL *et al.* (2013). Interleukin-6 induces vascular endothelial growth factor expression and promotes angiogenesis through apoptosis signal-regulating kinase 1 in human osteosarcoma. *Biochem Pharmacol* 85(4)*:*531-540.

Ukai T, Shiraishi C, Moriyama H, Yoshimoto M, Hara Y (2003). Expression of receptor activator of NF-kappaB ligand, osteoprotegerin and interleukin-1 beta in mechanical force-induced bone resorption. *Bone* 32(5)*:*S155-S155.

Wang CJ, Huang KE, Sun YC, Yang YJ, Ko JY, Weng LH *et al.* (2011a). VEGF Modulates Angiogenesis and Osteogenesis in Shockwave-Promoted Fracture Healing in Rabbits. *J Surg Res* 171(1)*:*114-119.

Wang DS, Yamazaki K, Nohtomi K, Shizume K, Ohsumi K, Shibuya M *et al.* (1996). Increase of vascular endothelial growth factor mRNA expression by 1,25-dihydroxyvitamin D-3 in human osteoblast-like cells. *J Bone Miner Res* 11(4)*:*472-479.

Wang JS, Aspenberg P (1993). Basic Fibroblast Growth-Factor and Bone Induction in Rats. *Acta Orthop Scand* 64(5)*:*557-561.

Wang Q, Huang CL, Xue M, Zhang XP (2011b). Expression of endogenous BMP-2 in periosteal progenitor cells is essential for bone healing. *Bone* 48(3)*:*524-532.

Wang Y, Wan C, Deng LF, Liu XM, Cao XM, Gilbert SR *et al.* (2007). The hypoxia-inducible factor a pathway couples angiogenesis to osteogenesis during skeletal development. *J Clin Invest* 117(6)*:*1616-1626.

Wilson A, Shehadeh LA, Yu H, Webster KA (2010). Age-related molecular genetic changes of murine bone marrow mesenchymal stem cells. *Bmc Genomics* 11:229

Wosczyna MN, Biswas AA, Cogswell CA, Goldhamer DJ (2012). Multipotent progenitors resident in the skeletal muscle interstitium exhibit robust BMP-dependent osteogenic activity and mediate heterotopic ossification. *J Bone Miner Res* 27(5)*:*1004-1017.

Wu AC, Raggatt LJ, Alexander KA, Pettit AR (2013). Unraveling macrophage contributions to bone repair. *BoneKEy reports* 2:373.

Wu JY, Purton LE, Rodda SJ, Chen M, Weinstein LS, McMahon AP *et al.* (2008). Osteoblastic regulation of B lymphopoiesis is mediated by G(s)alpha-dependent signaling pathways. *P Natl Acad Sci USA* 105(44)*:*16976-16981.

Xie H, Cui Z, Wang L, Xia ZY, Hu Y, Xian LL *et al.* (2014). PDGF-BB secreted by preosteoclasts induces angiogenesis during coupling with osteogenesis. *Nat Med* 20(11)*:*1270-1278.

Yamamoto M, Tabata Y, Ikada Y (1998). Ectopic bone formation induced by biodegradable hydrogels incorporating bone morphogenetic protein. *J Biomat Sci-Polym E* 9(5)*:*439-458.

Yamauchi K, Nishimura Y, Shigematsu S, Takeuchi Y, Nakamura J, Aizawa T *et al.* (2004). Vascular endothelial cell growth factor attenuates actions of transforming growth factor-beta in human endothelial cells. *Journal of Biological Chemistry* 279(53)*:*55104-55108.

Yang QL, McHugh KP, Patntirapong S, Gu XS, Wunderlich L, Hauschka PV (2008). VEGF enhancement of osteoclast survival and bone resorption involves VEGF receptor-2 signaling and beta(3)-integrin. *Matrix Biol* 27(7)*:*589-599.

Yasui N, Sato M, Ochi T, Kimura T, Kawahata H, Kitamura Y *et al.* (1997). Three modes of ossification during distraction osteogenesis in the rat. *J Bone Joint Surg Br* 79B(5)*:*824-830.

Yeh LCC, Lee JC (1999). Osteogenic protein-1 increases gene expression of vascular endothelial growth factor in primary cultures of fetal rat calvaria cells. *Mol Cell Endocrinol* 153(1-2)*:*113-124.

Yonemura Y, Endo Y, Tabata K, Kawamura T, Yun HY, Bandou E *et al.* (2005). Role of VEGF-C and VEGF-D in lymphangiogenesis in gastric cancer. *International journal of clinical oncology* 10(5)*:*318-327.

Zelzer E, Glotzer DJ, Hartmann C, Thomas D, Fukai N, Soker S *et al.* (2001). Tissue specific regulation of VEGF expression during bone development requires Cbfa1/Runx2. *Mechanisms of development* 106(1-2)*:*97-106.

Zelzer E, McLean W, Ng YS, Fulkai N, Reginato AM, Lovejoy S *et al.* (2002). Skeletal defects in VEGF(120/120) mice reveal multiple roles for VEGF in skeletogenesis. *Development* 129(8)*:*1893-1904.

Zelzer E, Mamluk R, Ferrara N, Johnson RS, Schipani E, Olsen BR (2004). VEGFA is necessary for chondrocyte survival during bone development. *Development* 131(9):2161-2171.

Zelzer E, Olsen BR (2005). Multiple roles of vascular endothelial growth factor (VEGF) in skeletal development, growth, and repair. *Curr Top Dev Biol* 65:169-87.

Zhang XP, Xie C, Lin ASP, Ito H, Awad H, Lieberman JR *et al.* (2005). Periosteal progenitor cell fate in segmental cortical bone graft transplantations: Implications for functional tissue engineering. *J Bone Miner Res* 20(12):2124-2137.